

Air Force Institute of Technology

**AFIT Scholar**

---

Theses and Dissertations

Student Graduate Works

---

1-1997

## Manual Tracking Flight Control with Amplitude and Rate Constrained Dynamic Actuators

Russel B. Miller

Follow this and additional works at: <https://scholar.afit.edu/etd>



Part of the [Controls and Control Theory Commons](#)

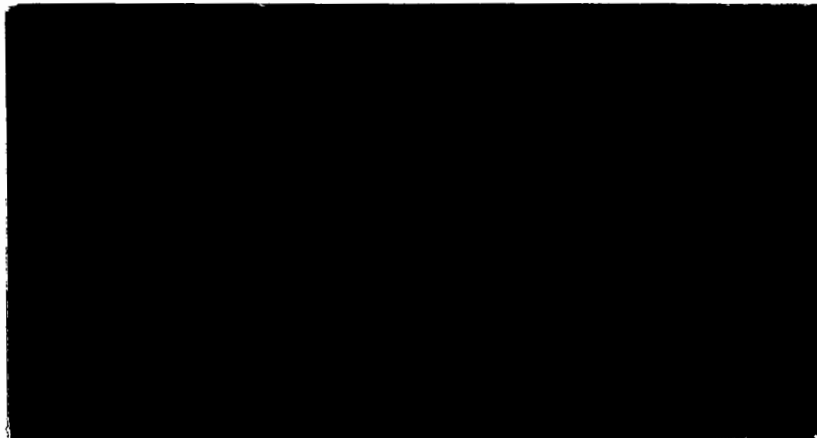
---

### Recommended Citation

Miller, Russel B., "Manual Tracking Flight Control with Amplitude and Rate Constrained Dynamic Actuators" (1997). *Theses and Dissertations*. 5814.

<https://scholar.afit.edu/etd/5814>

This Dissertation is brought to you for free and open access by the Student Graduate Works at AFIT Scholar. It has been accepted for inclusion in Theses and Dissertations by an authorized administrator of AFIT Scholar. For more information, please contact [AFIT.ENWL.Repository@us.af.mil](mailto:AFIT.ENWL.Repository@us.af.mil).



**DISTRIBUTION STATEMENT A**

Approved for public release,  
Distribution Unlimited

DEPARTMENT OF THE AIR FORCE  
AIR UNIVERSITY  
**AIR FORCE INSTITUTE OF TECHNOLOGY**

---

---

Wright-Patterson Air Force Base, Ohio

DTIC QUALITY INSPECTED 3



MANUAL TRACKING FLIGHT CONTROL  
WITH AMPLITUDE AND RATE  
CONSTRAINED DYNAMIC ACTUATORS

DISSERTATION

Russel B. Miller, Captain, USAF

AFIT/DS/ENG/96-15

**DISTRIBUTION STATEMENT A**

Approved for public release,  
Distribution Unlimited

DEPARTMENT OF THE AIR FORCE  
AIR UNIVERSITY

**AIR FORCE INSTITUTE OF TECHNOLOGY**

Wright-Patterson Air Force Base, Ohio

DTIC QUALITY IMPROVEMENT &

AFIT/DS/ENG/96-15

MANUAL TRACKING FLIGHT CONTROL  
WITH AMPLITUDE AND RATE  
CONSTRAINED DYNAMIC ACTUATORS

DISSERTATION

Russel B. Miller, Captain, USAF

AFIT/DS/ENG/96-15

Approved for public release; distribution unlimited

19970402 077

The views expressed in this dissertation are those of the author and do not reflect the official policy or position of the Department of Defense or the U.S. Government.

AFIT/DS/ENG/96-15

MANUAL TRACKING FLIGHT CONTROL WITH AMPLITUDE  
AND RATE CONSTRAINED DYNAMIC ACTUATORS

DISSERTATION

Presented to the Faculty of the Graduate School of Engineering  
of the Air Force Institute of Technology

Air University

In Partial Fulfillment of the  
Requirements for the Degree of  
Doctor of Philosophy

Russel B. Miller, B.S.E.E., M.S.E.E.

Captain, USAF

January, 1997

Approved for public release; distribution unlimited

MANUAL TRACKING FLIGHT CONTROL WITH AMPLITUDE  
AND RATE CONSTRAINED DYNAMIC ACTUATORS

Russel B. Miller, B.S.E.E., M.S.E.E.

Captain, USAF

Approved:

<u>M. Pachter</u>	<u>Jan 28, 97</u>
Dr. Meir Pachter, Committee Chairman	
<u>C.H. Houps</u>	<u>1/28/97</u>
Dr. C.H. Houps, Committee Member	
<u>Mark Oxley</u>	<u>28 Jan 97</u>
Dr. Mark Oxley, Committee Member	
<u>Dennis W Quinn</u>	<u>JAN 28, 97</u>
Dr. Dennis W. Quinn, Dean's Representative	

Robert A. Calico, Jr.

Robert A. Calico, Jr.  
Institute Senior Dean and  
Scientific Advisor

## *Preface*

During my course of studies at the Air Force Institute of Technology, I have had the pleasure of interacting with numerous highly professional and competent individuals, faculty and students alike. I am highly indebted to my research committee, Drs. Pachter, Houpis and Oxley, and greatly appreciate their immense levels of patience, understanding and guidance. I would like to give special thanks to my research advisor, Dr. Pachter, for giving me a new perspective on life in general. Also, a special thanks to Dr. Houpis, without whom I would have never had this opportunity at all.

I also wish to express my gratitude to Capt Odell Reynolds, colleague and friend, for the stimulating discussions, for keeping my computer resources intact, and for an occasional *search* for the big walleye. I am eternally indebted to him and his wife 1Lt Stacey Reynolds, for their tremendous hospitality and support. Also, I would like to thank Capt Bob Lewis for his assistance with the final draft, and Maj Pat Gardner for his friendship and inspiration.

Finally, and most importantly, I could never possibly express enough appreciation in words for the sacrifices, patience and support given to me by my loving wife Linda. Thank you, and I will spend the rest of my life trying to make up for lost time. I also need to apologize to my children Amy, Pam, Russel and Raleigh for their neglect and thank them for their support. Also, thanks to my parents, for making all the good things that have come to my life possible.

In closing, I have learned a valuable lesson which is not reported elsewhere in this dissertation: One can go 24 hrs without sleep, and one can go 24 hrs without food. One cannot, however, go 24 hrs without sleep nor food, as while quite different, one is often used as a substitute for the other.

Russel B. Miller



## *Table of Contents*

Preface .....	iii
List of Figures .....	vii
List of Tables .....	x
List of Abbreviations .....	xi
Abstract .....	xii
I. Introduction .....	1-1
1.1 Actuator Saturation .....	1-1
1.2 Overview of the Current Literature .....	1-5
1.2.1 General .....	1-5
1.2.2 Anti-Windup and Performance Enhancement Approaches .....	1-9
1.2.3 Miscellaneous Approaches .....	1-13
1.2.4 Saturation Avoidance .....	1-15
1.2.5 Summary .....	1-16
1.3 Problem Statement .....	1-17
1.4 Approach .....	1-17
1.5 Scope and Assumptions .....	1-18
1.6 Documentation .....	1-19
1.7 Summary .....	1-20
II. Problem Formulation and Modeling Issues .....	2-1
2.1 Overview .....	2-1
2.2 Manual Flight Control .....	2-1
2.3 Mathematical Formulation .....	2-2
2.3.1 The Unconstrained Open-Loop System .....	2-4
2.3.2 The Unconstrained Closed-Loop System .....	2-6
2.3.3 The Actuator Constraints .....	2-6

2.4	Model Windup .....	2-8
2.5	Discretization Issues .....	2-10
2.6	Summary .....	2-14
III.	Linear Quadratic Tracking .....	3-1
3.1	Overview .....	3-1
3.2	Improving Tracking Performance via Reference Signal Prediction ..	3-1
3.3	Optimization Methods in Tracking Control .....	3-4
3.4	LQT Control .....	3-6
3.5	The Unconstrained Optimal Control Solution Within Each Window	3-10
3.6	Transformation of Actuator Constraints .....	3-15
3.7	The Explicit LQT Control Law .....	3-17
3.8	Summary .....	3-18
IV.	The Feasible Reference Vector .....	4-1
4.1	Overview .....	4-1
4.2	Stage 1: Extrapolation of the Pilot Demanded Reference .....	4-2
4.3	Stage 2: Determining a Feasible Reference Vector .....	4-8
4.3.1	Strategy: Poly- $p$ + Poly- $p'$ .....	4-8
4.3.2	Strategy: Poly- $p$ + Asymptotic Convergence .....	4-13
4.3.3	Strategy: Poly- $p$ + Parallel .....	4-16
4.4	Reference Signals with Corners and Jumps .....	4-18
4.5	Summary .....	4-20
V.	Mitigation of the Hard Constraints Effects .....	5-1
5.1	Overview .....	5-1
5.2	A "Simple" Example .....	5-1
5.3	LQT with Saturation Effects Mitigation .....	5-10
5.4	Simulation Examples and Discussion .....	5-14

5.5	A Globally Bounded Output LQT Controller .....	5-20
5.6	Summary .....	5-30
VI.	Conclusion .....	6-1
6.1	Overview .....	6-1
6.2	Contributions and Accomplishments .....	6-1
6.3	Research Conclusions .....	6-6
6.4	Recommendations .....	6-7
	Appendix: Additional Simulation Results .....	A-1
	Bibliography .....	BIB-1
	Vita .....	VITA-1

## *List of Figures*

Figure	Page
2.1 Tracking Problem Block Diagram .....	2-3
2.2 Commonly Used Model for Constrained Actuators .....	2-8
2.3 Avoiding Model Windup .....	2-9
2.4 Actuator/Plant System .....	2-11
2.5 Linear Comparison of Discretization Methods .....	2-12
2.6 Nonlinear Comparison of Discretization Methods .....	2-13
2.7 DT/AUG Discretization Method Error .....	2-14
3.1 Benefits of Predictive Control .....	3-3
3.2 Overall Closed-Loop Configuration .....	3-9
4.1 Poly- $p$ Extrapolation of the Pilot's Reference .....	4-4
4.2 Poly-2 Test Reference Signals .....	4-7
4.3 Poly-2 Extrapolation Test Results .....	4-7
4.4 Poly- $p$ + Poly- $p'$ Prediction of the Reference .....	4-9
4.5 Poly- $p$ + Asymptotic Convergence Prediction .....	4-13
4.6 Modified Poly- $p$ + Asymptotic Convergence .....	4-15
4.7 Poly- $p$ + Parallel Prediction of the Reference .....	4-16
4.8 Parabolic Extrapolation of a Reference with Corners .....	4-19
4.9 Linear Extrapolation of a Reference with Corners .....	4-20
5.1 Closed Loop Control System .....	5-2
5.2 Sets of Interest .....	5-3
5.3 Stable and Unstable Equilibria .....	5-5
5.4 Transformed Closed-Loop System .....	5-7
5.5 Unmitigated System Responses .....	5-9

5.6	Scalar Example Results with Saturation Mitigation .....	5-10
5.7	LQT/LQR Comparison .....	5-15
5.8	LQT/LQR Actuator Responses .....	5-16
5.9	LQT vs LQT/DTRG with First Order Prediction .....	5-18
5.10	LQT and LQT/DTRG Actuator Response Comparisons .....	5-18
5.11	1-Step LQT vs LQT/DTRG with Second-Order Prediction .....	5-19
5.12	LQT 1-Step, 10-Step and LQR/DTRG Comparison .....	5-20
5.13	Unconstrained Actuator Step Responses .....	5-27
5.14	High Amplitude Step with $tol = 0.5$ .....	5-28
5.15	The Sticking Phenomenon .....	5-29
5.16	High Amplitude Step with Artificial State Bounds .....	5-30
A.1	Unconstrained Poly-0 + Poly-0 vs. $N$ .....	A-3
A.2	Unconstrained Poly-0 + Poly-1 vs. $N$ .....	A-3
A.3	Unconstrained Poly-0 + Poly-2 vs. $N$ .....	A-4
A.4	Unconstrained Poly-1 + Poly-1 vs. $N$ .....	A-4
A.5	Unconstrained Poly-1 + Poly-2 vs. $N$ .....	A-5
A.6	Unconstrained Poly-2 + Poly-2 vs. $N$ .....	A-5
A.7	Unconstrained Poly-0 + AC vs. $N, k_a = 0.4$ .....	A-6
A.8	Unconstrained Poly-0 + AC vs. $k_a, N = 10$ .....	A-6
A.9	Unconstrained Poly-1 + AC vs. $k_a, N = 10$ .....	A-7
A.10	Unconstrained Poly-2 + AC vs. $k_a, N = 10$ .....	A-7
A.11	Constrained Poly-2 + Poly-2, $N = 15$ .....	A-8
A.12	Constrained Poly-2 + Poly-2 Actuator Activity .....	A-8
A.13	Constrained Poly-2 + AC .....	A-9
A.14	Constrained Poly-2 + AC Actuator Activity .....	A-9

A.15 Constrained Poly-2 + Parallel Response .....	A-10
A.16 Constrained Poly-2 + Parallel Actuator Activity .....	A-10

*List of Tables*

Table	Page
4.1 Poly- $p$ Extrapolation Coefficients .....	4-5
4.2 Explicit Poly- $p$ + Poly- $p'$ Coefficients, $p'=1$ .....	4-11
4.3 Explicit Poly- $p$ + Poly- $p'$ Coefficients, $p'=2$ .....	4-12
4.4 Explicit Poly- $p$ + Asymptotic Convergence Coefficients .....	4-14
4.5 Explicit Poly- $p$ + Parallel Coefficients .....	4-17
A.1 Constrained Simulation Parameters .....	A-2

## *List of Abbreviations*

- BIBO - Bounded Input Bounded Output
- CAD - Computer Aided Design
- CAW - Conventional Anti-Windup
- CG - Center of Gravity
- CT - Continuous Time
- DT - Discrete-Time
- DTRG - Discrete-Time Reference Governor
- EDT - Equivalent Discrete-Time
- FCS - Flight Control System
- IMC - Internal Model Control
- LP - Linear Programming
- LQR - Linear Quadratic Regulator
- LQT - Linear Quadratic Tracking
- LTI - Linear Time-Invariant
- MAW - Modified Anti-Windup
- MIMO - Multiple Input Multiple Output
- MPC - Model Predictive Control
- PIO - Pilot Induced Oscillation
- RH - Receding Horizon
- RHC - Receding Horizon Control
- RHP - Right-Half-Plane
- RHPC - Receding Horizon Predictive Control
- RHW - Receding Horizon Window
- SISO - Single Input Single Output
- ZOH - Zero-Order Hold



## *Abstract*

A new control methodology for manual flight control, viz., real-time tracking control, is developed. Amplitude and rate constrained dynamic actuators are considered. Optimal *tracking* control is made possible by the use of unique reference signal prediction strategies which extrapolate the reference signal over the optimization horizon. Since it would be ill-advised to rely on long term predictions, a receding horizon formulation is employed. A linear-quadratic inner-loop controller which yields good small signal performance is used in conjunction with an outer-loop nonlinear element which modifies the exogenous reference signal so that downstream actuator constraints are not violated. The novel 2-stage prediction strategies result in reference signals over the optimization horizon that are parameterized in the current reference value. The constraint effects mitigation strategy is to optimally track a modified reference signal which yields feasible actuator commands over the optimization horizon when the pilot demanded reference is too aggressive to be tracked by the inner-loop optimal control law. Thus, the current reference value is modified by the outer-loop nonlinear element. A discrete-time implementation yields computationally inexpensive, closed-form solutions which are implementable in real-time and which afford the optimal tracking of an exogenous, unknown ahead of time, reference signal. A stability analysis of the ensuing nonlinear tracking control system is also performed. The developed control algorithm is applied to an open-loop unstable aircraft model, with attention being given to the trade-offs associated with the conflicting objectives of aggressive tracking and saturation avoidance. One-step ahead constraint mitigation is shown to provide substantial improvement in the constrained system response, while slightly more complicated constraint mitigation strategies yield stronger stability properties.

# *MANUAL TRACKING FLIGHT CONTROL WITH AMPLITUDE AND RATE CONSTRAINED DYNAMIC ACTUATORS*

## *I. Introduction*

### *1.1 Actuator Saturation*

Dynamic systems are commonly modeled as linear systems, whereas in practice, all physical control systems are subject to hard (nonlinear) actuator displacement and rate saturation constraints. Moreover, in control systems the actuating element is critically located between the controller and the linear plant. Unfortunately, it is not uncommon for academic controller designs to fail to acknowledge the presence of "downstream" actuator constraints. Now, it is desired not only to confine one's attention to small perturbations situations, viz., regulation, but high amplitude maneuvering control is also of interest. Then the presence of actuator constraints cannot and should not be overlooked. In addition, the absence of the ubiquitous sensor noise in deterministic control paradigms also "shoves under the rug" the unavoidable and detrimental actuator rate saturation caused effects.

Moreover, with the current emphasis on robustness, the attendant high gain control laws will bring into the foreground the actuator saturation problem. A large number of robust linear control design methodologies, as well as model following control design paradigms, have been proposed. Unfortunately, these high gain approaches will only exacerbate the actuator saturation problem. Although many of the above mentioned design paradigms have merit with regard to their intended objectives, the preordained existence of hard actuator constraints in physical systems precludes their practical application without significant ad hoc post-design modifications. This is one manifestation of the often lamented about disparity between control theory and practice. Thus, the impact of actuator displacement and rate constraints upon the performance of closed-loop feedback control systems needs to be addressed.

In conventional well designed plants the operational requirements have been taken into consideration, and, in addition, the performance specifications which the plant will be expected to meet, are in line with the applicable physical constraints. For instance, in flight control the sizing and placement of control surfaces on an aircraft are determined by the performance requirements. Also, realistic performance specifications must be stipulated. Moreover, the available control authority must be properly allocated among the tasks at hand. For example, the 23 degrees of available deflection of an elevator of a modern fighter aircraft might be allocated as follows: 4° for stabilization (or stability augmentation), 2° for differential roll control, 7° for trim, and 10° for maneuvering. Thus, 10° of effector deflection should suffice for the maneuvers that the vehicle is expected to perform. Furthermore, an extreme maneuver requiring, say 12° of effector deflection, will not necessarily result in saturation, as one would have to be unfortunate enough to be simultaneously using all of the remaining control authority for the other tasks. In well designed plants then, and where the control design goals are not too ambitious, the aforementioned saturation constraints are generally of minimal impact, and industry has

fared well in plant design and closed-loop feedback control. Evidently, in this context, the "actuator saturation problem" while real, is, in truth, somewhat contrived.

Hence, one should guard against overzealous performance objectives in feedback control, e.g., excessively tight tracking or excessive robustness specifications which invariably require high gain controllers upstream of the actuators. In addition, in nonconventional air vehicle concepts one moves the center of gravity (CG) back and reduces the size of the control surfaces to reduce drag and improve performance. As a result, one abandons the static stability requirement thus forcing the use of feedback control for stabilization. This is conducive to making actuator saturations a problem. Actuator saturation then becomes a major obstacle to exploiting the benefits of feedback. Also, misguided dynamic control power apportionment among the various control effectors can contribute to and/or exacerbate actuator saturation phenomena.

Typical flight control systems in operational practice generally consist of relatively simple, low gain, but gain-scheduled compensators which, for the most part have been highly successful. There are, however, situations where actuator saturation can become a problem in operational flight control systems. For example, dogfights and aerial demonstrations at the boundary of the aircraft's operational envelope may require high amplitude slewing maneuvers at the extreme edge of an aircraft's capabilities. In the quest for high performance, and when these systems are "pushed to their limits," it is reasonable to expect that actuator saturations may, in fact, occur and the consideration of these nonlinear effects in the design phase might indeed reduce the degree of conservativeness of a flight control system (FCS) and thus enhance the FCS performance. Additionally, there is currently a quest for reconfigurable flight control which is driven by the need to accommodate failed or battle damaged control surfaces. Saturation of the actuators may realistically become a problem in the event of a control surface failure or when battle damage is sustained, and performance is to be recovered.

Deflection (or displacement) limits are probably the most commonly studied type of actuator saturation, but rate limitations are equally significant, and in practical applications more important than the former. In flight control, actuator rate saturations have most recently been implicated in the departure and subsequent crash of a new fighter at an air show [1],[2], and the YF-22 crash landing [14].

Both amplitude and rate actuator saturations change, to some extent the otherwise linear and familiar response of a linearly designed FCS and one then refers to "windup." In particular, in FCS's which employ controllers with integral action, this is colloquially referred to as "integrator windup." In general, actuator saturation invariably causes *windup* whenever linear dynamic compensation is used. Indeed, it is important to note that actuators are necessarily located in the inner-most control loop and at the plant's input. When the actuator is saturated the plant's output no longer instantaneously affects its input, in particular with respect to pulling out of saturation, and the system is, roughly speaking, in open-loop operation. Hence, during periods of saturation, the effects of (dynamic) feedback compensation are reduced or even eliminated. It is obvious then, from this observation, that actuator displacement and/or rate saturation is especially dangerous when feedback control is used for stabilization of an open-loop unstable plant, e.g., the F-16, the Swedish JAS 39, and the X-29 aircraft, with doubling times in the pitch channel of 0.5, 0.3, and 0.2 seconds, respectively. Thus, windup translates into degraded performance, limit cycling, and/or closed-loop instability/departure - a litany of adverse effects listed in increasing order of severity.

Concerning the issue of windup in manual flight control: During periods of actuator saturation and windup, aircraft exhibit nonlinear, abnormal, responses which may momentarily bewilder the human operator, or pilot, who creates an outer-feedback loop. This will prompt the pilot to raise his "gain" and further push the FCS into saturation. Thus, in manual flight control systems in which there exist both an inner feedback loop with a physical actuator which is subject to saturation, and an outer feedback loop which is

closed by a human operator, pilot induced oscillations (PIO) can occur [1],[2],[14],[49]. PIO's caused by actuator saturation are therefore referred to as *nonlinear PIO's*.

Robustness optimized *small signal* designs perform well only when subjected to small signal stimuli, so that the control constraints are not activated and system linearity is preserved. A control design methodology which yields high performance, viz., robustness and tight (dynamic) tracking characteristics, while at the same time *mitigates* the actuator saturation problem during high amplitude maneuvers, is desired. The simultaneous satisfaction of these conflicting objectives is indeed a rich research area. Thus, actuator saturation must be considered during the control design process, and hence, one must call upon nonlinear control design.

## 1.2 Overview of the Current Literature

*1.2.1 General.* Actuator saturation is a topic of active research in control theory [1]-[63]. Numerous compensation approaches related to actuator saturation have been proposed in the literature. Different approaches have different objectives: The predominant focus is on minimizing or eliminating windup, while the preferable, but less common, approach entails avoiding saturation altogether. Computational complexity and practical (real-time) implementability, as well as stability, must be considered in the design process, and weighed against improvements in tracking performance. Nonlinear methods (see, e.g., [28], [29], [19], [50]) may be used to prevent saturations from occurring in the first place but are, in general, computationally intense and thus not very practical for real-time implementation, whereas simpler linear approaches (see, e.g., [3], [11], [23], [25], [30]), by reducing the effects and duration of saturations when they occur, may provide limited benefits in some applications.

The likelihood of actuator saturation can be greatly reduced by the acceptance of sluggish "small signal" performance, however, this is, in general, an undesirable approach.

Even with reasonable gain, linear controllers do not operate at maximum efficiency when the error signals are small [16], rather maximum control effort (as dictated by the saturation nonlinearities) must be reserved for the largest allowable reference signals. Consistent with the solution of the time-optimal control problem for constrained linear systems (see e.g., [39]), it may be preferential to go "full-bore" (e.g., bang-bang, maximum rate) until the desired objective is achieved - provided that stability can be guaranteed "in the large." Thus, when designing controllers for constrained linear systems, the designer must take into consideration the capabilities of the plant, the performance requirements, and the impact of the constraints on achieving these requirements.

Based on the calculus of variations and Pontryagin's Minimum Principle, the linear control constrained optimal control problem has been posed, and, at least, in theory, "solved" for a variety of low-order plants with simple constraints and performance functionals (see, e.g., [5], [13], [32], [39]). The controllability problem is mainly considered, where the emphasis is on steering the system's state to a known target state. The optimal control framework yields necessary conditions which generally lead to nonlinear two-point boundary value problems. The solutions may be of an open-loop and nonlinear nature (e.g., bang-bang in the case of minimum time or minimum fuel problems) which are difficult to implement and are very sensitive to model uncertainty, disturbances, and sensor noise [11], [28], [29]. Additionally, analytical solutions for higher order systems are generally impossible to obtain [32]. For these reasons, these solutions are seldom used in practice [11], [28], [29]. Rather, sub-optimal, but more practical solutions are used, and the motivation is thus provided for the large number of ad hoc design approaches for treating constrained actuators which abound in the current literature. The optimal control solution does, however, when it can be constructed, provide a quantitative measure for assessing the performance of other sub-optimal (but practical) control systems [32].

In applied control work, saturation nonlinearities are seldom considered during the control design process. Traditionally, the most common approach is to first design a controller without consideration to the saturation elements (often referred to as the "linear controller"), and then to subsequently design additional compensation to mitigate the effects of actuator saturation. This is referred to as a *2-step design process*. With a 2-step process, there are two basic philosophies: The first being that the modified compensator perform identical to the original linear controller in the absence of saturation, and provide a "graceful degradation of system performance in the face of saturation," see e.g., [3], [15], [20], [23]. The alternative design philosophy is to obtain linear performance as long as possible, but without allowing the actuators to saturate at all (see, e.g., [19], [24], [28], [29], [50]). One disadvantage of a 2-step design approach is that it is not always clear how the initial controller design may affect the performance properties of the completed design. Alternatively, a *1-step design process* acknowledges the existence of the saturation nonlinearities at the outset so that windup cannot occur, e.g., as in constrained optimal control theory.

Research papers in which state and/or control constraints are considered in the tracking control problem are few, but notable exceptions exist [12], [46]. The majority of the literature on constrained control addresses the constrained regulation problem, as opposed to the *(dynamic) tracking* problem which is concerned with following an exogenous reference input  $r(t)$ , such that the output  $y(t) \approx r(t)$ . When the reference signal  $r$  is not of an exogenous nature and one employs the "internal model" approach, one merely considers an augmented regulation problem. The problem with this approach is that the behavioral assumptions on the reference signal's dynamics feature in the ensuing control law, thus rendering the controller noncausal. In particular, when the reference signal  $r$  is restricted to constant values (i.e. steps), or varies slowly as compared to the system dynamics, this may be referred to as a *setpoint* control problem: These however are not tracking control



problems. In fact, problems of this type are often rewritten in terms of *error coordinates* and treated as regulator problems, see e.g., [34], [42]. In *manual flight control*, the emphasis is on dynamic reference signals which are not known ahead in time. Additionally, in most of the current literature, only stable open-loop plants are considered. This is true particularly for the two-step anti-windup approaches, as they are not generally applicable to unstable open-loop plants.

In tracking control systems, there are basically two saturation mechanisms: 1) "Temporary" saturation occurs because of a large initial error (e.g., at the onset of a step command), or saturation is caused by the system's transient dynamics (e.g., an underdamped response in which the overshoot violates the constraints), or saturation is induced by the dynamic nature of the reference signal, and is henceforth referred to as *transient saturation*. 2) State and/or control constraints may impose bounds on the achievable steady-state output of a given system. Thus, a reference signal  $r(t)$ , which converges to some steady-state value  $r_{ss}$ , is said to be *statically admissible* with respect to a tracking system with output  $y(t)$ , if the equilibrium condition  $y(t) = y_{ss} = r_{ss}$  can be statically maintained without violating the constraints. Static admissibility does not imply that transient saturations will not be encountered en route to the steady-state equilibrium, only that the constraints are not violated in the steady-state.

Stability/performance analysis of the complete nonlinear control system is also an important issue. In the case of 2-step designs, saturation effect compensation strategies consist of modifications to the "linear controller" for which certain stability and performance guarantees can be made. The question is, what can be said about the nonlinearly modified system? While the stability analysis of linear systems is generally straightforward, analyzing nonlinear systems and guaranteeing their stability is not in general an easy task. A number of methods have been used to assess the stability characteristics of constrained and "saturation compensated" systems. Some of these are based on traditional methods used for the analysis of linear systems, while others employ a

nonlinear framework. Stability analysis of regulators is generally based on Lyapunov stability theory, see e.g., [7], [8], [9], [21], [22], [56]. Other methods include the use of Nyquist and describing function methods [59], direct nonlinear analysis techniques [10], [11], [20], [38], or the treatment of nonlinear effects as (additive [24], multiplicative [40], or other nonlinear [10]) perturbations to the linear signals. In [5], [11], nonlinear system components are replaced with linear approximations and the approximation errors are characterized by norm bounds. The multi-loop circle criterion [52] provides MIMO versions of gain and phase margins, and has been used in several works [28], [29], [30], [50]. A similar theorem which provides sufficient conditions for a saturating linear control system with bounded states is presented in [33]. Bounds of convergence for regulators which maximizes the set of initial conditions for which stability can be guaranteed, have been given in [7], [9], [21], [56]. The limitations imposed by right-half-plane (RHP) compensator poles and RHP plant zeros on the frequency domain properties of constrained systems are examined in [41]. The existence of smooth, nonlinear feedback stabilizers for a class of constrained LTI systems has been demonstrated in [53].

*1.2.2. Anti-Windup and Performance Enhancement Approaches.* The concept of "windup", "integrator windup", or "reset windup" is an important issue in the analysis of the effects of saturation in control systems. Most commonly, these terms are used to refer to the windup or continual growth of the output of integrators, especially in the context of PI controllers, during periods of actuator saturation. However, any, and particularly, slow, dynamic compensation can "windup" in the face of downstream actuator saturation nonlinearities. Strictly speaking, the input to the plant ceases to change in response to changes in the error signal, and, moreover, for the command signal to move away from the actuator saturation level a period of time needs to elapse in order for the states of the dynamical elements in the compensator to return to "normal" values. The result of windup is degraded performance (including the possibility of instability), generally in the form of large overshoots and increased settling times. A characterization of windup has been given

in [11] as "windup occurs when the states of the controller are driven by the error while the actuator is in saturation."

One of the most basic anti-windup methods is the concept of "intelligent" or "conditional" integration, which has often been used in the literature (see, e.g., [3], [6], [11], [30], [34], [35], [58], [59]). The basic idea is to turn off or modify the integration of error signals during actuator saturation. In this case, a nonlinear feedback loop is placed around an integrator such that under "small signal" operation, the feedback loop is open and the system is simply an integrator. When the integrator output exceeds some preset threshold (presumably the saturation value), the feedback kicks in, modifying the input-output relationship depending on the dynamics of the linear feedback compensation  $H$ .  $H$  can be a dynamic compensator, or a simple gain. In the latter case, the system becomes a first-order lag, with its bandwidth determined by the magnitude of the gain. Of course, this requires physical accessibility of the integrator. The idea of using a deadband in the feedback loop to obtain "intelligent" integration was proposed by Krikelis [35], but this particular implementation may be subject to "chatter" [3]. An alternative approach is to feed back the difference between the limiter's input and output, which does not explicitly introduce any additional nonlinearity into the system. Conditional integration, when applicable, can be effective in reducing the degradation in system performance associated with the windup phenomenon. It should be noted, however, that when an integrator is modified to another type of dynamical compensation, the stored energy of the modified compensation can still result in windup problems, i.e., degraded performance, albeit generally less severe.

The concept of *conventional* or *classical* anti-windup (CAW) is based on the idea of feeding back the difference between the constrained and unconstrained control signals (see, e.g., [11], [15]). The block diagram of a CAW system can appear in many different forms which seem unrelated at first glance, but block diagram manipulation can be used to show that a number of existing anti-windup compensation schemes are equivalent to the basic

CAW structure. A particularly convenient form for analysis and comparison purposes is given in [11], where by a simple parameter modification the CAW structure is readily shown to decompose or generalize into other techniques [11], e.g., conditional integration or *Internal Model Control* (IMC) [11], [15], [17].

Hanus, et al. [23], Campo and Morari [11], and Åström and Rundquist [3] have each independently developed basically the same anti-windup controller for control constrained systems, but by using completely different approaches. In each case, the compensation technique is developed using a 2-step design process, in that a linear controller which provides satisfactory performance with the unconstrained system is specified up front. The resulting controllers in [23] and [11] are actually special cases of the controller developed by Åström and Rundquist, but the minor differences in their resulting algorithms are primarily due to the form in which the original linear controller is specified. The most general development of this method, is the "conditioning technique" presented by Hanus, et al., where the approach is based on "realizable references," i.e., a reference signal which results in a linear controller output that matches the constrained plant input corresponding to the actual desired reference. Åström and Rundquist develop the controller using an observer approach. Using this formulation, it is readily apparent that the windup problem is caused by feeding back the controller output to the observer as opposed to the actual plant input. Campo and Morari attack the problem from a state space perspective, with the goal of not allowing the error  $e$  to drive the controller states during saturation. Hence, their approach is to drive the controller states by the actual plant input, as opposed to the error signal. A large number of existing anti-windup schemes can be related to this basic structure [58], which has been used in an anti-windup context as early as 1984 [4]. In the absence of saturation, the modified controller is equivalent to the prespecified linear controller. During saturation, windup is avoided. By using the "velocity form" (see [4]) implementation of a PI controller, an example is presented in [23] which demonstrates that

the algorithm can effectively avoid windup when a rate saturation of the controller output occurs.

In multiple-input (MI) systems, actuator or input saturations generally are in the form of single channel operations on the individual elements of the control vector. In MI systems the *alignment* or *directionality* of the control signal is of interest. If only some elements of the control vector become saturated, or different elements exceed the saturation limit(s) by different amounts, the control vector becomes directionally distorted in the control space, which results in additional degradation of performance [6], [11], [22], [49]. Hence, successful SISO compensation schemes are not always applicable to MIMO systems. The application of CAW has primarily been restricted to SISO systems, but Doyle, et al., [15] has presented a modified anti-windup (MAW) scheme which does ensure preservation of the control vector "direction," which is basically a MIMO implementation of conditional integration around a pre-specified, linear controller.

Anti-windup compensation techniques attempt to eliminate or reduce windup effects, but do not necessarily have any direct bearing on the onset of actuator saturations. If windup is eliminated/reduced, it would generally be expected that the duration of any saturations may be shortened, and subsequent saturation avoided, since the "unwinding" period is shortened or eliminated. That is, anti-windup compensators may result in fewer/shorter saturations, but this can to some extent be regarded as a byproduct of the compensation as opposed to a primary objective. For stable plants, these techniques generally reduce the large overshoots and degraded performance associated with the windup problem. Simply avoiding windup when the open-loop plant is unstable and feedback control is used for stabilization, is not a viable control solution: A departure may occur even when windup is avoided. Hence, it is apparent that anti-windup compensators are generally not applicable (or, at least, are not sufficient) for stable closed-loop operation in the presence of actuator saturation when the open-loop plant is unstable. Windup is not an issue when saturation is avoided altogether.

Similar to the anti-windup approaches are performance enhancement techniques. For example, Horowitz [25] has devised a frequency domain approach to "drive the system out of saturation quickly". This ad hoc approach proposed for SISO systems entails introducing an additional degree of freedom by placing a linear feedback loop around the saturation element. The loop transmission  $L_n$  around the saturation element can be shaped independently of the other important loop transmissions of the system. Hence, by appropriate selection of  $L_n$ , the system can be made to drive itself out of saturation "quickly," thus reducing the impact of saturation. An extension to the case of stable plants with rate saturations is provided in [26]. In [27] and [36] additional nonlinear compensation is introduced to provide an extension to the case of unstable plants. The goal is to improve performance under saturations caused by large reference signals. Hess and Snell [24] have presented an alternative approach to extend the method of [25] to include the case of unstable plants. The original technique was not appropriate for application to unstable plants, because the resultant compensator  $G$  includes zeros intended to cancel plant poles. Hess has shown that by allowing  $L_n$  to include the unstable poles of the plant, along with mirroring zeros in the left-half-plane, the stable plant restriction can be removed.

*1.2.3. Miscellaneous Approaches.* There are a number of other unique and/or ad hoc approaches to the saturation problem in the literature. Some brief comments regarding some of these methods are provided here.

A number of research efforts have established stability and convergence properties for adaptive control methods with input constraints [31], [37], [43], [44], [48], [57], [60], [61], [62], [63]. Most of these have focused on stable plants, and many are limited to stable, type 1, and minimum-phase plants. Nonminimum-phase plants have specifically been addressed in [44], [60], [63]. The usual approach has been to consider d-step ahead or adaptive pole placement methods followed by a saturation element, with special care taken in the design of the estimation algorithm to ensure stability of the constrained closed loop system [44]. Rate saturations are explicitly considered only in [44]. Except for [57],

which has specifically addressed the issue of windup, these efforts consider only stability and convergence properties. In [57], a generalization of Hanus' conditioning technique is applied to a setpoint control problem.

Using modified versions of the quadratic performance functional which result in a one point boundary value problem, Frankena and Sivan [16] and Ryan [51] developed bang-bang control laws for the (elliptically and rectangularly, respectively) control constrained linear quadratic regulator (LQR) problem for stable plants. By considering a similar performance functional but with a discontinuous integrand, Bernstein [9] developed an optimal continuous (saturated linear) control law for stable plants with both types of constraints, which avoids the problem of singular extremals. A *near time optimal control* law which consists of a combination of bang-bang and linear control action is presented in [45]. The control level saturation in this case is restricted below full deflection to reserve some control authority for disturbance rejection and plant uncertainty.

An interesting concept referred to as *time regulation* is presented in [54]. The basic idea, presented in a fault tolerant robot control context, proposes an on-line time scaling procedure for partially failed robot arms. The idea is to have the robot arm follow the same (unfailed) geometric trajectory, but over a longer time period because of the reduced control authority imposed by actuator failure.

Model predictive control (MPC) schemes are those which explicitly include a model of the plant, and are of an open-loop, moving horizon, optimal control nature [17], [47], [55]. MPC is attractive for constrained systems because of its ability to explicitly handle constraints, and feedback can be incorporated via an estimator to eliminate some of the disadvantages associated with open-loop control solutions, hence enhancing robustness with respect to the modeling inadequacies. The basic internal model control (IMC) structure is inherent in all MPC methods [17]. In the absence of model uncertainty, the IMC system effectively operates open-loop, and the preservation of stability under

saturation is not an issue only when the open-loop plant is stable. Unfortunately, the performance of IMC with constrained systems is generally overly sluggish [15].

*1.2.4. Saturation Avoidance.* Saturation avoidance schemes are necessarily anti-windup schemes as well, since by definition, actuator saturation must exist for windup to occur. Kpasouris [29] has addressed the MIMO problem with amplitude control (i.e., controller output) constraints using a set theoretic/functional analysis approach. His 2-step design process, results in an "inner-loop" gain reduction scheme, referred to as an *error governor*. The error governor is essentially a nonlinear, time-varying gain  $\lambda(t)$ , which operates on the error signal using integral action, i.e., the error governor modifies the linear controller's input signal. The variable gain  $0 \leq \lambda(t) \leq 1$  is selected in a manner which prevents the linear controller from achieving states from which the unforced controller output will saturate. Since the gain  $\lambda$  can be made arbitrarily small, saturation of the controller output can always be avoided. An extension to account for controller output rate saturations is made in [28] by applying the technique to the controller state equation as opposed to the controller output equation.

Rodriguez and Wang [50] have applied a modified version of the error governor to an unstable bank-to-turn missile problem. Consideration of this unstable plant requires two basic modifications to the procedures described above. First of all, selection of  $\lambda = 0$  is not acceptable since this represents open-loop operation. Hence, design of the error governor requires the determination of the value  $\lambda_{\min}$ , which is the smallest gain which maintains closed-loop stability. Instead of  $0 \leq \lambda \leq 1$ , the error governor design in this case must only consider  $\lambda_{\min} \leq \lambda \leq 1$ . The obvious disadvantage is that sufficiently large reference signals and/or disturbances can now cause saturations to occur. Measures are taken to account for possible saturations due to large reference signals by means of a *reference governor*. The



reference governor is an "outer-loop" gain reduction strategy (which operates on the reference signal), and its design is similar to that of the error governor.

The error and reference governor strategies discussed above are quite intense from a computational perspective. Gilbert and Tan [18] have applied the concept of maximal output admissible sets to streamline the mathematical analysis and reduce the computational burden of the error governor implementation. Further, Gilbert, et al., [19] have established the existence of finitely determined approximations to output admissible sets for discrete-time systems and developed a discrete-time reference governor (DTRG) with global convergence properties. Indeed, the work of Gilbert is quite impressive, and is the most pertinent to the actuator saturation problem as addressed in this dissertation. Hence, further development of the DTRG concept, and implementations theory are pursued in subsequent chapters of this dissertation.

Finally, Pachter, et al., [12], [46] have recognized that a receding horizon predictive control (RHPC) approach is well suited to the tracking control problem and thus applicable to manual flight control, and have combined the LQ and linear programming (LP) optimization paradigms into a hybrid approach to the control-constrained tracking problem within the RHPC framework. This work establishes the basic premises on which this dissertation is based.

*1.2.5 Summary.* For the most part, the literature consists of a number of ad hoc approaches, each applicable to a limited class of plants, each with a limited set of objectives, and each with limited claims of stability and/or performance. It is clear, that there does not exist a universal solution to the problems caused by actuator saturation. Many of the techniques from the literature (particularly the anti-windup approaches) are, however, closely related and oftentimes functionally identical. Most of the work is geared toward the regulation and set-point control problems as opposed to tracking control, and thus does not directly apply to maneuvering and manual flight control. Additionally, by neglecting actuator dynamics altogether, actuator constraints are often treated as control

constraints, whereas, particularly in "high gain" flight control, actuator dynamics should be included, in which case actuator displacement and rate constraints introduce state constraints into the control problem. Thus, the preponderance of the literature is not directly applicable to the constrained, real-time, manual tracking control problem. Most of the literature can be classified as anti-windup, with only a few research efforts that strive for saturation avoidance.

### *1.3 Problem Statement*

Investigate the actuator saturation problem, and develop a control design methodology which places a high degree of emphasis on both the dynamic tracking and actuator saturation mitigation aspect, for manual tracking flight control.

### *1.4 Approach*

The stated objectives necessitate the consideration of actuator saturation during the control design process, and hence, nonlinear control design must be employed. An optimization-based, linear (small signal) control signal synthesis algorithm, with emphasis on the tracking aspect, is developed. The control signal is explicitly expressed in terms of the dynamic reference signal, so that, when required, a nonlinear modification of the reference signal which minimizes the impact of the downstream actuator constraints on overall system performance is readily employed. An optimal control approach to the tracking problem invariably requires advance knowledge of the desired reference trajectory. Since this information is unavailable in the manual tracking context, means for predicting the desired (pilot commanded) reference is developed. The undesirable effects associated with a predictive control strategy are tempered through the use of a receding horizon control implementation. The latter also yields feedback action.

Since the optimal control signal is explicitly expressed in terms of the incoming reference, an additional nonlinear control loop can be placed around the existing system to address the actuator saturation aspect of the problem, when necessary. The appeal of this second stage "outer-loop" approach to saturation mitigation, i.e., the placement of an additional nonlinear feedback loop around an inner-loop closed-loop linear system, in order to modify the incoming reference signal as a means of averting saturation, lies in the following fact. If the boundedness of this modified reference signal can be ascertained, and if saturation is successfully averted, then linear analysis methods remain valid with respect to the inner, small signal, linearly compensated and stable system, and the overall control system's stability is guaranteed. Thus, BIBO stability of the overall nonlinear feedback control system is achieved. If, in addition, this outer, nonlinear control loop is activated only when saturation is imminent, then the desirable small signal tracking characteristics of the pre-modified system are also preserved. Thus, the strategy is to optimally track, when necessary, a less aggressive reference, as a means of avoiding saturation.

Finally, the use of equivalent discrete-time models for the aircraft (plant) and actuator dynamics makes it possible to obtain straightforward, explicit control solutions which are readily implementable in real-time.

### *1.5 Scope and Assumptions*

The development is specifically directed toward the manual tracking flight control problem with dynamic actuators subjected to hard constraints in both rate and amplitude. Attention is confined to the single-input single-output (SISO) case, although full state feedback is employed. Open-loop unstable plants are considered. The constraints' effect mitigation aspect of the development is directly applicable to a multiple actuator situation, while the tracking control aspect is extendible to multiple-input situations. Tracking

control, as opposed to regulation or set-point control is addressed, and the trade-offs between achievable tracking performance and stability guarantees are investigated. In manual flight control, a human operator - the pilot - generates the reference signal and closes the outermost loop around the flight control system. Since evidence exists which links actuator rate saturation to PIO situations, the saturation mitigation strategies developed in this dissertation contribute to the alleviation of PIO problems.

The primary assumption on which this research is based, is that adequate control authority has been allocated to the non-tracking tasks, e.g., maintaining trim and the rejection of unmodeled disturbances. Finally, it is assumed that the pilot will not intentionally and deliberately stress the flight control system, which could bring about a situation where the pilot supplied reference yields an output signal which, although as close as possible to the reference, is nevertheless very far from the reference; and notwithstanding BIBO stability of the FCS and thus the boundedness of the output, the pilot flies the aircraft into the ground.

## *1.6 Documentation*

The dissertation is organized as follows. Chapter 2 provides background information, an explicit formulation of the problem, and discusses some important observations regarding the modeling of hard constrained nonlinear flight control systems. A novel control approach for the actuator constrained manual tracking control problem, *Linear Quadratic Tracking* (LQT), which simultaneously addresses the conflicting objectives of aggressive tracking and actuator saturation effects mitigation, is introduced in Chapter 3. Chapter 4 is devoted to the development of new methods for predicting the pilot demanded reference into the future, in a manner which facilitates the subsequent mitigation of the actuator constraints, and also includes the derivation of the explicit closed-form LQT control solutions for each prediction strategy. Several simulation examples using the LQT

control method with unconstrained actuators are provided. In Chapter 5, the impact of hard actuator constraints on tracking and control system stability, particularly for an open-loop unstable plant, is first illustrated via a simple example. This is followed by a detailed examination of the constraint mitigation implementation and tracking and stability performance within the LQT framework. Next, a special case of the LQT control method which sacrifices a certain degree of tracking performance in favor of stronger stability characteristics is discussed. Concluding remarks, and recommendations for future work are given in Chapter 6. Finally, additional simulation results are provided in the Appendix.

### *1.7 Summary*

The primary emphasis of this research is on the effects of actuator saturations (both displacement and rate) on control systems and the mitigation of those effects. Secondly, but equally important, is that the research is done in the context of (manual) tracking control, and NOT regulation. Specifically, the goal here is to examine and compensate for the effects of actuator saturations from a manual tracking perspective. Although "tracking" is a common term among controls engineers, manual tracking control design and analysis is relatively rare. Perhaps this lack of attention is vested in the fact that the manual tracking problem cannot be directly posed in an optimization framework because of the need to "see into the future." Thus, one approach is to heuristically devise "practical" tracking control methods, and then mathematically assess the resultant system to determine any BIBO stability guarantees that may be made.

Generally, "tracking" systems found in the literature are based on the concepts of regulation and are deeply rooted in steady state analysis. These trackers, for the most part, are made possible only because of the extensive understanding of the time domain/frequency domain connection in simple second-order systems and the design for second-order dominant dynamics; frequency domain arguments are (often) used. The

manual tracking problem, however, is a multivariable control problem of a continually transient nature - there is, in general, no steady-state. It does not, therefore, make sense to design controllers for this class of problems based on steady-state analyses. Hence, the problem is a time domain problem - certainly, in the case of hard actuator constraints, and should be attacked in the time domain.

In this dissertation, a number of established time domain control system design and optimization methods are combined in a novel manner to properly attack the manual tracking problem with actuator constraints. Among these, are the concepts of receding horizon control (also referred to as model predictive control), full state feedback and LQ optimal control, constrained optimization and reference signal polynomial extrapolation and interpolation. It is shown that these tools are instrumental to developing a sound control strategy for the constrained dynamic tracking problem at hand.

## *II. Problem Formulation and Modeling Issues*

### *2.1 Overview*

In this chapter, a mathematical formulation of the manual tracking control problem as addressed in this dissertation is provided. First, an elaboration on the concept of "manual tracking" is presented, followed by the mathematical representations of the aircraft and actuator models under investigation. Additionally, there are many subtleties associated with the modeling of nonlinear physical (continuous-time) systems on a digital computer which are easily, and consequently, often overlooked. Procedures which are commonplace for the modeling of linear systems may be inherently flawed when applied in nonlinear modeling. For example, artificial model windup may occur in discrete-time models of nonlinear dynamical systems, or, the nonlinear effects of a system may be unfairly mitigated by improper nonlinear modeling. Thus, the chapter is concluded with a discussion of these issues.

### *2.2 Manual Flight Control*

Manual flight control entails a pilot flying an aircraft "by the seat of his pants" in order to satisfy a mission objective. In military aviation this objective could be to engage enemy aircraft, or to attack ground targets. Thus, manual flight control calls for tracking control. The tracking problem begins at some point subsequent to take-off and cruise (where the aircraft could be flown by the autopilot), and ends when the mission is completed. Thus, the manual tracking task is an "open-ended" problem which evolves in time; its duration is indefinite.

Manual tracking control problems are strictly of a dynamic and transient nature. Hence, "steady state" is meaningless in maneuvering and manual flight control, which stands in stark contrast to the classical regulation paradigm. For these reasons, and bearing in mind the very point-wise in time nature of hard actuator constraints, the manual flight control problem should be addressed in the time domain. However, the tracking situation arises where the reference signal is not known in advance, and thus the optimal tracking control paradigm cannot be directly applied to manual, real-time tracking control. Receding horizon control (RHC) formulations have traditionally been used in process control, in the absence of viable feedback measurements. In this dissertation, however, and as suggested by Pachter, et. al., [12], [46], RHC is combined with reference signal prediction strategies to overcome the shortcoming in the required knowledge regarding the reference signal over the planning horizon.

### *2.3 Mathematical Formulation*

The constrained actuator control problem is often treated in the literature as a control constrained problem. When actuator dynamics are included, however, the problem should be addressed as a state constrained problem. Consider the single-input single-output (SISO) feedback control system depicted in the block diagram of Figure 2.1, which represents the tracking feedback control problem at hand. The physical aircraft includes control surfaces which are positioned by dynamic actuators. The controller output is  $u \equiv \delta_c$ , which, when linear controllers are employed, is in general, unconstrained. The control surface deflection  $\delta$  which is the plant's input, is however, constrained due to physical limitations of the dynamic actuators. Thus an appropriate aircraft model requires an augmentation of the airframe dynamics with the actuator dynamics.



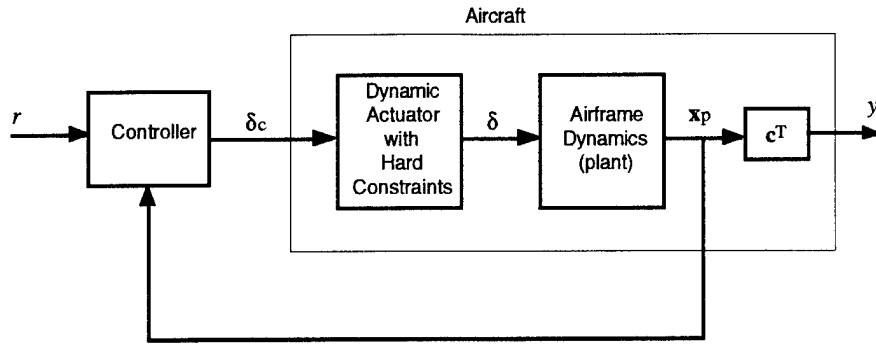


**Figure 2.1.** Tracking Problem Block Diagram

The equivalent discrete-time model representation of the resultant single-input *closed-loop* linear control system is thus described by

$$\begin{aligned}\mathbf{x}_{k+1} &= \mathbf{A}_{cl}\mathbf{x}_k + \mathbf{b}_{cl}r_{k+1} \\ y_{k+1} &= \mathbf{c}^T\mathbf{x}_{k+1}\end{aligned}$$

where  $\mathbf{x}_k \in \mathbf{R}^n$  is the closed-loop state vector and includes both the actuator dynamics and aircraft dynamics.  $\mathbf{A}_{cl} \in \mathbf{R}^{n \times n}$  and  $\mathbf{b}_{cl} \in \mathbf{R}^n$  are the closed-loop dynamics matrix and input vector respectively, and  $k = 0, 1, 2, \dots$  is the time step index. The required tracking task entails the output following an exogenous, unknown a priori reference sequence  $(r_1, r_2, \dots)$ . Because the actuator dynamics are imbedded in the closed-loop system's augmented state vector, the actuator displacements and rates can be expressed in the general form  $\mathbf{C}\mathbf{x} + \mathbf{d}r$ , and defined as follows:

$$\begin{bmatrix} \delta_{k+1} \\ \frac{1}{T}(\delta_{k+1} - \delta_k) \end{bmatrix} = \mathbf{C}\mathbf{x}_k + \mathbf{d}r_{k+1}$$

Thus, the displacement and rate constrained manual tracking problem is treated as a state and "control" constrained problem. Finally,  $r_{k+1}$  is the exogenous reference signal which becomes available at time  $k$ . Note that the convention is employed such that the pilot

supplies the desired reference value  $r_{k+1}$  at time  $k$  and thus, in the discrete-time formulation, the control signal at time  $k$ ,  $u_k$ , is computed such that the resultant output at the subsequent time step,  $y_{k+1}$ , is driven toward the desired reference  $r_{k+1}$ . Thus, the difference between the current desired reference value and the actual system response  $y_{k+1}$  is the tracking error at time  $k+1$ .

*2.3.1 The Unconstrained Open-Loop System.* Linear aircraft dynamics (plant) models are considered, with discrete-time representations of the form

$$\mathbf{x}_{p_{k+1}} = \mathbf{A}_p \mathbf{x}_{p_k} + \mathbf{b}_p \delta_k + \zeta d, \quad k = 0, 1, \dots \quad (2.1)$$

where  $\mathbf{x}_{p_k}$  is the plant (aircraft dynamics) state vector at time  $k$ ,  $\mathbf{A}_p \in \mathbf{R}^{n_p \times n_p}$  and  $\mathbf{b}_p \in \mathbf{R}^{n_p}$  are the dynamics matrix and input vector respectively,  $\delta_k$  is the control surface deflection at time  $k$ ,  $\zeta$  is a disturbance vector,  $d$  is a known and constant disturbance input, and the output of interest is

$$y_{k+1} = \mathbf{c}_p^T \mathbf{x}_{p_{k+1}} + d_p \delta_k$$

where the output matrix  $\mathbf{c}_p^T \in \mathbf{R}^{1 \times n_p}$  and the feedforward coefficient  $d_p \in \mathbf{R}$ . The inclusion of the known constant disturbance  $d$  is motivated by the need to linearize the aircraft equations of motion about a non-trim point. The dynamics matrix  $\mathbf{A}_p$  is not necessarily stable, i.e., it may have eigenvalues outside the unit circle.

The control system supplies actuator commands (the control signal  $u_k \equiv \delta_{c_k}$ ), resulting in control surface deflections according to the actuator dynamics. Proper, linear dynamic actuator models of the form

$$\mathbf{x}_{\delta_{k+1}} = \mathbf{A}_\delta \mathbf{x}_{\delta_k} + \mathbf{b}_\delta \delta_{c_k}$$

are considered, where  $\mathbf{x}_{\delta_k} \in \mathbf{R}^{n_\delta}$  is the internal state of the actuator at time  $k$ ,  $\mathbf{A}_\delta \in \mathbf{R}^{n_\delta \times n_\delta}$  and  $\mathbf{b}_\delta \in \mathbf{R}^{n_\delta}$  are the actuator dynamics matrix and input vector respectively. The resultant (unconstrained) actuator displacement is given by

$$\delta_{k+1} = \mathbf{c}_\delta^T \mathbf{x}_{\delta_{k+1}}$$

An integrator state  $z$  such that

$$\dot{z} = r - y$$

for the purpose of implementing integral action in the time domain is also included, which adds a pole at the ( $s$ -plane) origin. When full state feedback control is implemented, integral control is not necessary to meet steady state performance criteria, however in practical applications the utility of integral control is with respect to model uncertainty and disturbance rejection. The discrete-time representation of this integral state is given by

$$z_{k+1} = z_k + T(r_{k+1} - y_{k+1})$$

where  $T$  is the sample interval.

Hence (in the absence of actuator constraints), the (linear) augmented open-loop system ensues

$$\begin{aligned} \mathbf{x}_{k+1} &\equiv \begin{bmatrix} \mathbf{x}_{p_{k+1}} \\ \mathbf{x}_{\delta_{k+1}} \\ z_{k+1} \end{bmatrix} = \begin{bmatrix} \mathbf{A}_p & \mathbf{b}_p \mathbf{c}_\delta^T & \mathbf{0} \\ \mathbf{0} & \mathbf{A}_\delta & \mathbf{0} \\ -T\mathbf{c}_p^T \mathbf{A}_p & -Td_p \mathbf{c}_\delta^T & 1 \end{bmatrix} \begin{bmatrix} \mathbf{x}_{p_k} \\ \mathbf{x}_{\delta_k} \\ z_k \end{bmatrix} + \begin{bmatrix} \mathbf{0} \\ \mathbf{b}_\delta \\ 0 \end{bmatrix} \delta_{c_k} + \begin{bmatrix} \mathbf{0} \\ \mathbf{0} \\ T \end{bmatrix} r_{k+1} + \begin{bmatrix} \zeta \\ \mathbf{0} \\ 0 \end{bmatrix} d \\ &\equiv \mathbf{A}\mathbf{x}_k + \mathbf{b}u_k + \boldsymbol{\gamma}_1 r_{k+1} + \boldsymbol{\gamma}_2 d \\ y_{k+1} &= \begin{bmatrix} \mathbf{c}_p^T & d_p \mathbf{c}_\delta^T & 0 \end{bmatrix} \mathbf{x}_{k+1} \equiv \mathbf{c}^T \mathbf{x}_{k+1} \end{aligned} \quad (2.2)$$

where the respective augmented state, input, output and disturbance input vectors are  $\mathbf{x}_k$ ,  $\mathbf{b}$ ,  $\mathbf{c}^T$ ,  $\boldsymbol{\gamma}_2 \in \mathbf{R}^n$ , the augmented dynamics matrix  $\mathbf{A} \in \mathbf{R}^{n \times n}$ , the control signal, the output and the (constant and known) disturbance are  $u_k$ ,  $y_{k+1}$ ,  $d \in \mathbf{R}$ , respectively, the "time" variable is  $k = 0, 1, 2, \dots$ , and the initial state  $\mathbf{x}_0 \in \mathbf{R}^n$  is known. Note that the additional input

vector  $\gamma_1 \in \mathbf{R}^n$  is needed to accommodate the inclusion of integral control, and  $T$  is the sampling interval.

2.3.2 *The Unconstrained Closed-loop System.* Consider, e.g., the simplest stabilizing state feedback tracking control law given by

$$u_k = \delta_{c_k} = \mathbf{k}_x^T \mathbf{x}_k + k_r r_{k+1}$$

where  $\mathbf{k}_x^T = [\mathbf{k}_p^T \ \vdots \ \mathbf{k}_\delta^T \ \vdots \ k_z] \in \mathbf{R}^{1 \times n}$ , with  $n = n_p + n_\delta + 1$ . Inserting this control law into Eq. (2.2) yields the closed-loop state equation

$$\mathbf{x}_{k+1} = \mathbf{A}_{cl} \mathbf{x}_k + \mathbf{b}_{cl} r_{k+1} + \boldsymbol{\gamma}_2 d \quad (2.3)$$

where  $\mathbf{A}_{cl} = \mathbf{A} + \mathbf{b} \mathbf{k}_x^T$ , and  $\mathbf{b}_{cl} = \gamma_1 + \mathbf{b} k_r$ . Clearly, the state feedback gain  $\mathbf{k}_x^T$  must be selected such that all the eigenvalues of  $\mathbf{A}_{cl}$  are inside the unit circle. Thus, the closed-loop system of Eq. (2.3) is said to be *stable by design*.

2.3.3 *The Actuator Constraints.* The control surface displacement is constrained in both amplitude and rate, viz.,

$$\delta_{\min} \leq \delta(t) \leq \delta_{\max}$$

$$\dot{\delta}_{\min} \leq \dot{\delta}(t) \leq \dot{\delta}_{\max}$$

In the discrete-time case, these constraints are accounted for by enforcing

$$\delta_{\min} \leq \delta_{k+1} \leq \delta_{\max}$$

$$\Delta_{\min} \leq (\delta_{k+1} - \delta_k) \leq \Delta_{\max}, \quad k = 0, 1, \dots$$

where  $\Delta_{\min}$  and  $\Delta_{\max}$  are given by  $T\dot{\delta}_{\min}$  and  $T\dot{\delta}_{\max}$ , respectively. In practical applications, it is not unrealistic to assume that  $\delta_{\min} = -\delta_{\max}$ ,  $\Delta_{\min} = -\Delta_{\max}$ , and that  $\delta_{\max}, \Delta_{\max} > 0$ . These constraints are imposed by the physical limitations of the dynamic actuator. A mathematical representation of these constraints is as follows. First, define the saturation function

$$sat(x) = \begin{cases} 1, & x > 1 \\ x, & -1 \leq x \leq 1 \\ -1, & x < -1 \end{cases}$$

where  $x$  is a scalar. Similarly,  $sat(\mathbf{x})$  where  $\mathbf{x}$  is a vector with components  $x_i$ , is the vector with elements  $sat(x_i)$ . In terms of this function, then, the symmetric hard *amplitude* constraints (with bounds  $\pm\delta_{\max}$ ) can be characterized by

$$sat_a(\delta_{k+1}) = \delta_{\max} sat\left(\frac{\delta_{k+1}}{\delta_{\max}}\right)$$

This  $sat$  function can also be used to characterize the *rate* constraints alone, viz.,

$$sat_r(\delta_{k+1}, \delta_k) = \Delta_{\max} sat\left(\frac{\delta_{k+1} - \delta_k}{\Delta_{\max}}\right) + \delta_k$$

or to simultaneously characterize *both* the amplitude and rate constraints, viz.,

$$sat_2(\delta_{k+1}, \delta_k) = \Delta_{\max} \cdot sat\left(\frac{1}{\Delta_{\max}} \left( \delta_{\max} \left[ sat\left(\frac{\delta_{k+1}}{\delta_{\max}}\right) - sat\left(\frac{\delta_k}{\delta_{\max}}\right) \right] \right)\right) + \delta_{\max} sat\left(\frac{\delta_k}{\delta_{\max}}\right)$$

The term *small signal operation* can now be defined. In the most general case where there are both displacement and rate actuator constraints, *small signal operation* implies that for all  $\delta_k$ ,  $k = 0, 1, \dots$ , resulting from the linear system of Eq. (2.3),  $sat_2(\delta_{k+1}, \delta_k) = \delta_{k+1}$ .

During small signal operation, the dynamic behavior of the closed loop system is governed by the linear system Eq. (2.3). However, when the hard saturation constraints are encountered, the system behavior is nonlinear and much more complicated. The unstable plant dynamics of Eq. (2.1) are no longer driven by  $\delta_k$ , but by  $sat_2(\delta_k, \delta_{k-1})$ .

Consider, e.g., the case of a persistent amplitude saturation where  $\delta_k = \delta_{k+1} = \dots = \delta_{\max}$ . If the tracking control law does not alleviate this situation, the result is a constant input to an unstable system which will ultimately result in a departure. When the saturation is of the

transient type, recovery may be possible, but if the saturation is the result of a reference signal which is not statically admissible, departure is inevitable.

## 2.4 Model Windup

When modeling nonlinear systems, one must take special care to avoid *model windup*. That is, windup which is unrelated to the system's physics, and rather is an artifact of poor modeling which, at least to some extent, invalidates the model. For example, consider the simple first-order actuator model whose dynamics are described by

$$\dot{\delta} = a\delta + b\delta_c$$

When such an actuator is subject to amplitude and rate constraints, a commonly used (see, e.g., [12]) block diagram level model is as shown in Figure 2.2.

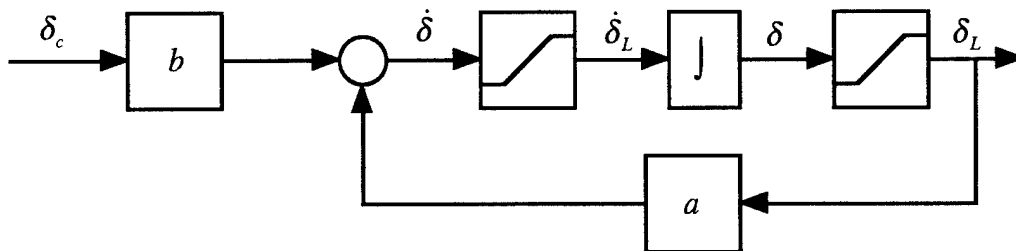


**Figure 2.2.** Commonly Used Model for Constrained Actuators

This actuator model, however, is subject to "model windup" and physical inconsistencies. Actuators are translational devices, and thus, zero rates should dictate constant displacements and vice versa. In addition to this model being subject to model windup, regardless of which of the variables depicted in Figure 2.2 are used to represent the physical quantities of actuator displacement and rate, inconsistencies can arise. Consider the case where the actuator has encountered a hard displacement constraint. Clearly, in order to obtain the desired displacement limiting, the variable  $\delta_L$  must be used to represent

the physical actuator displacement. According to the model depicted in Figure 2.2, a hard saturation in displacement in no way implies that either of the quantities  $\dot{\delta}$  or  $\dot{\delta}_L$  is zero. Specifically,  $\dot{\delta} = b\dot{\delta}_c + a\dot{\delta}_L$  which is zero only if

$$\dot{\delta}_c = -\frac{a}{b}\dot{\delta}_L$$

Moreover, when  $\dot{\delta}_L \neq 0$  the variable  $\delta$  will windup. Thus, even after  $\dot{\delta}_L$  reverses direction, a period of time will have to elapse before  $\delta = \delta_L$ , and only then will the displacement begin to move away from the saturation value. Unfortunately, one is pushed into this type of block diagram modeling by the modern or "graphical" CAD paradigms, e.g., MATRIXx System Build or MATLAB Simulink; whereas proper nonlinear modeling mandates a reversion to the physical state space.

A more realistic model which maintains the translational characteristics of the actuator could be obtained by ceasing to drive the integrator when a displacement saturation occurs, as illustrated in Figure 2.3. The switch would remain in the position shown any time that

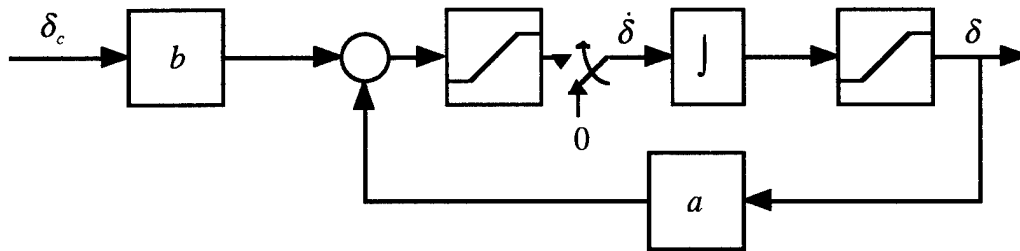


**Figure 2.3.** Avoiding Model Windup

the displacement is at the limit, thus preventing both physical inconsistencies and model windup. The concept of conditional integration, used in the literature to prevent integrator windup in controllers, could thus be used in the modeling process to avoid model windup.

Perhaps the best approach, and the method incorporated into this dissertation, is to use a physical variable state space representation for the actuator state vector so that the

actuator displacement appears as an explicit state. In a discrete-time formulation, rate saturations can be readily accommodated via appropriate hard limiting of the displacement state.

## 2.5 Discretization Issues

Discrete-time models basically play two distinct roles in the control design process. First of all, digital controllers are often used because of powerful digital computers which can be used to implement these controllers. Secondly, simulations of physical systems is essential in the controls design process. Since most of these simulations are performed on digital computers, equivalent discrete-time (EDT) models are often used to represent continuous-time systems.

Given a linear, continuous-time model of a physical system that consists of a linear plant and actuator (as illustrated in Fig 2.1), the model should be discretized as a single unit. That is, if the plant is of order  $n_p$  and the actuator is of order  $n_a$  then the entire system can be represented with a  $n = n_p + n_a$  order state space model determined by augmenting the plant and actuator continuous time models as described in Section 2.3.

For a linear plant/actuator system, one could then use canned controls tools, e.g., the *c2d* command in MATLAB, to obtain an EDT model. However, when the actuator is subject to hard constraints a canned discretization routine, e.g., *c2d* mentioned above, may yield invalid results when applied to the augmented system and one attempts to enforce the constraints in the EDT system. In fact, when simulating complicated systems, these invalid models have been observed to actually mitigate the actuator saturation effects. It has been observed, that more realistic results can be obtained by discretizing the actuator and plant models separately, and then augmenting the EDT models of each subsystem. While this approach implies the use of a sampling device between the plant and actuator, which by no



means exists in the physical reality, the selection of a sufficiently small sampling interval allows one to *hide behind the sample rate*.

The phenomenon described here is best described by way of example. Thus, consider the actuator/plant continuous-time (CT) system of Figure 2.4:

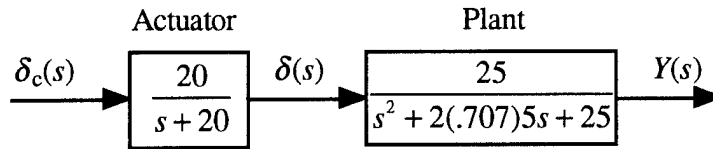


**Figure 2.4.** Actuator/Plant System

Further, let the actuator displacement  $\delta$  be constrained in displacement to 1.0 units. A state-space formulation of the augmented CT system is given by

$$\begin{bmatrix} \dot{x}_1 \\ \dot{x}_2 \\ \dot{x}_\delta \end{bmatrix} = \begin{bmatrix} -7.07 & -25 & 20 \\ 1 & 0 & 0 \\ 0 & 0 & -20 \end{bmatrix} \begin{bmatrix} x_1 \\ x_2 \\ x_\delta \end{bmatrix} + \begin{bmatrix} 0 \\ 0 \\ 1 \end{bmatrix} \delta_c$$

where the system output is  $y = \mathbf{c}^T \mathbf{x} = [0 \ 25 \ 0] \mathbf{x}$ , and the actuator displacement is  $\delta = \mathbf{c}_\delta^T \mathbf{x} = [0 \ 0 \ 20] \mathbf{x}$ . The MATLAB *c2d* command yields the "equivalent" discrete-time model

$$\begin{bmatrix} x_1[k+1] \\ x_2[k+1] \\ x_\delta[k+1] \end{bmatrix} = \begin{bmatrix} 0.9305 & -0.2413 & 0.1747 \\ 0.0097 & 0.9988 & 0.0009 \\ 0 & 0 & 0.8187 \end{bmatrix} \begin{bmatrix} x_1[k] \\ x_2[k] \\ x_\delta[k] \end{bmatrix} + \begin{bmatrix} 0.0009 \\ 0 \\ 0.0091 \end{bmatrix} \delta_c[k] \quad (2.4)$$

An obvious problem lies in the fact that in the discrete-time (DT) model of Eq. (2.4), the plant can be directly affected by the actuator command  $\delta_c$  whereas in reality and as clearly illustrated in Figure 2.4, this should not be the case. The preferred method entails discretization of the plant and actuator models individually, then augmenting the resultant DT models, which yields

$$\begin{bmatrix} x_1[k+1] \\ x_2[k+1] \\ x_\delta[k+1] \end{bmatrix} = \begin{bmatrix} 0.9305 & -0.2413 & 0.1930 \\ 0.0097 & 0.9988 & 0.0010 \\ 0 & 0 & 0.8187 \end{bmatrix} \begin{bmatrix} x_1[k] \\ x_2[k] \\ x_\delta[k] \end{bmatrix} + \begin{bmatrix} 0 \\ 0 \\ 0.0091 \end{bmatrix} \delta_c[k]$$

which is more in line with the physical system. In all three cases, the CT augmented model, the discretization of the augmented CT model (denoted AUG/DT), and the augmentation of the individually discretized plant and actuator (denoted DT/AUG) yield nearly identical linear (i.e., without constraints) performance, as illustrated in Figure 2.5.

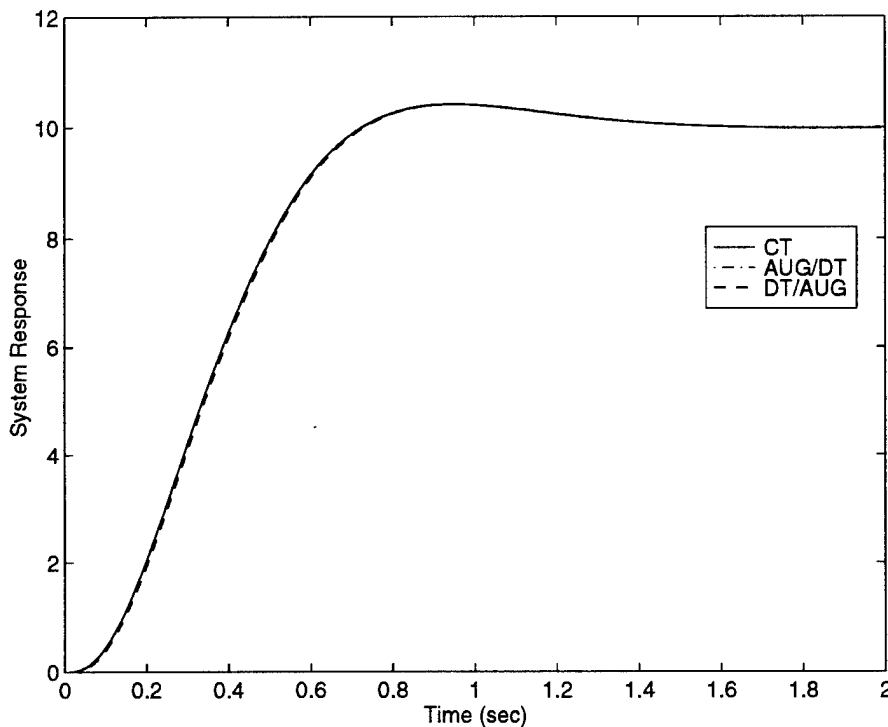


**Figure 2.5.** Linear Comparison of Discretization Methods

The input command is a 10 unit step command, and all discretizations use a sample interval of 0.01 seconds, and assume a zero order hold.

However, when the actuator displacement constraint is enforced, performance of the AUG/DT model is quite poor as compared to the CT system, as shown in Figure 2.6. The

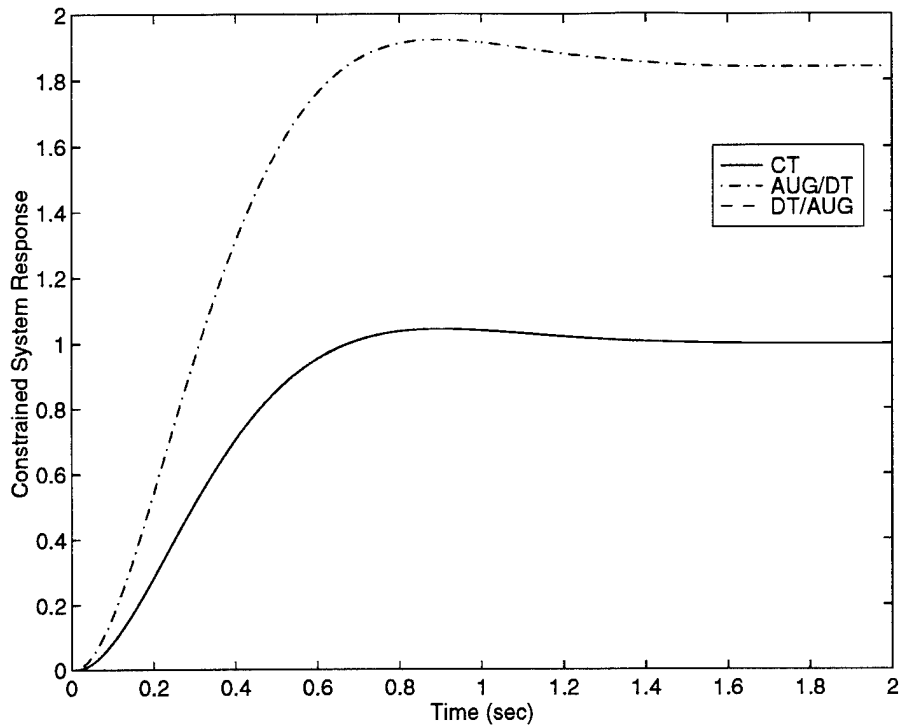


**Figure 2.6.** Nonlinear Comparison of Discretization Methods

DT/AUG method on the other hand, is essentially an exact overlay, and the difference in the two responses are shown in Figure 2.7. Aside from the obvious problems illustrated in the preceding example, significant discrepancies in the CT and AUG/DT model responses may occur even with minimal periods of saturation. However, in realistic situations, viz., where the actuator dynamics are relatively fast as compared to the plant, these additional effects are minimal and very difficult to discern. In order to amplify those effects, however, one can examine the same situation but with a much slower actuator, or choose a much longer sampling interval, and see that discretization of the nonlinear, augmented CT model performs even worse than demonstrated in the above example.

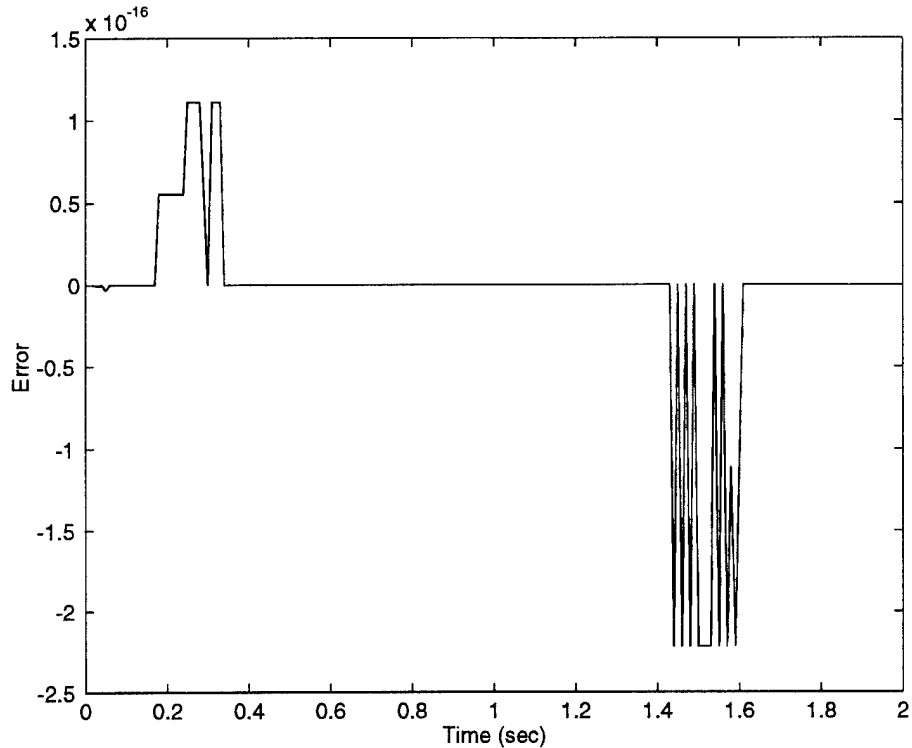


**Figure 2.7.** DT/AUG Discretization Method Error

## 2.6 Summary

The emphasis of this chapter has been to clearly define the aircraft actuator and plant models used throughout the remainder of the dissertation. In the context of the augmented system models, it is clear that actuator constraints impose state constraints on the problem, and thus control constraint mitigation strategies are not directly applicable. Explicit mathematical representations of the actuator displacement and rate constraints was provided, as well as a discussion of two important modeling issues, viz., model windup, and the appropriate approach for the discretization of the aforementioned augmented system models. Straightforward, canned discretization tools are not necessarily directly applicable to the problem at hand. Indeed, one must model nonlinear systems carefully by reverting to their state-space representation.

### *III. Linear Quadratic Tracking*

#### *3.1 Overview*

In this chapter, a new control strategy for addressing the manual flight control problem with constrained actuators, *Linear Quadratic Tracking (LQT)*, is devised. A receding horizon (RH) implementation of Linear Quadratic (LQ) optimal control, is combined in a novel manner with a unique two-stage reference signal prediction strategy. By parameterizing this predicted reference over the planning horizon in terms of its value at "time now"  $r_1'$  the mitigation of hard actuator constraints effects is made possible in an effective and efficient manner without sacrificing the aggressive tracking characteristics of the otherwise linear system. First, an example which demonstrates potential tracking performance enhancement through the use of a predictive tracking control strategy over that of a regulator-based approach is presented, followed by an overview of the LQT methodology. Next, the finite horizon optimal control problem which presents itself within each RH window is solved in terms of the parameterized predicted reference vector. A straightforward reflection of the actuator constraints into constraints on  $r_1'$  is then made to afford an effective, yet computationally inexpensive, constraint mitigation strategy. This entails the relaxation of the reference signal (pilot commanded) at "time now." Specific reference prediction strategies are developed in Chapter 4, and considerable attention is given to the constraint mitigation aspect in Chapter 5.

#### *3.2 Improving Tracking Performance via Reference Signal Prediction*

Optimal control methods cannot be directly applied to the manual tracking control problem, because the desired reference trajectory is not known in advance. Thus, optimal

control tracking systems are traditionally based on a somewhat adaptation of the regulation paradigm. This research is, in part, motivated by the following insight.

In a manual tracking situation, tracking performance can be improved over the performance achieved by using regulator based approaches, by employing accurate, short-term predictions of the reference signal.

This is supported by the following example.

*Example 3.1.*

Consider the two state (short period dynamics) longitudinal aircraft model of an F-16 derivative, for a flight condition of 10000 ft, Mach 0.7. The bare plant's state space model is given by

$$\begin{bmatrix} \dot{\alpha} \\ \dot{q} \end{bmatrix} = \begin{bmatrix} Z_\alpha & Z_q \\ M_\alpha & M_q \end{bmatrix} \begin{bmatrix} \alpha \\ q \end{bmatrix} + \begin{bmatrix} Z_\delta \\ M_\delta \end{bmatrix} \delta_e \quad (3.1)$$

where the units of angle of attack  $\alpha$  and pitch rate  $q$  are rad and rad/sec respectively, with  $Z_\alpha = -1.15$ ,  $Z_q = 0.9937$ ,  $Z_\delta = -0.177$ ,  $M_\alpha = 3.724$ ,  $M_q = -1.26$ , and  $M_\delta = -19.5$ . Also,  $\delta_e$  represents the elevator deflection in rad. A first-order actuator model with bandwidth of 20 rad/sec is considered. The tracking task requires pitch rate  $q$  to follow an exogenous reference signal  $r$ . Furthermore, an integral control state  $\dot{z} = r - y$  is augmented into the system. Using a sample interval of  $T = 0.01$  sec and assuming a zero-order hold on the input yields an equivalent discrete-time system given by  $\mathbf{x}_{k+1} = \mathbf{A}\mathbf{x}_k + \mathbf{b}\delta_{ek} + \gamma r_{k+1}$ , viz.,

$$\begin{bmatrix} \alpha_{k+1} \\ q_{k+1} \\ \delta_{k+1} \\ z_{k+1} \end{bmatrix} = \begin{bmatrix} 0.9887 & 0.0098 & -0.0025 & 0 \\ 0.0368 & 0.9877 & -0.1756 & 0 \\ 0 & 0 & 0.8187 & 0 \\ -0.000368 & -0.009877 & .001938 & 1 \end{bmatrix} \begin{bmatrix} \alpha_k \\ q_k \\ \delta_k \\ z_k \end{bmatrix} + \begin{bmatrix} 0 \\ 0 \\ 0.1813 \\ 0 \end{bmatrix} \delta_{ek} + \begin{bmatrix} 0 \\ 0 \\ 0 \\ 0.01 \end{bmatrix} r_{k+1} \quad (3.2)$$

and  $y_{k+1} = q_{k+1} = \mathbf{c}^T \mathbf{x}_{k+1}$ , where  $\mathbf{c}^T = [0 \ 1 \ 0 \ 0]$ , and  $\mathbf{x}_0 = \mathbf{0}$ .

Two control strategies are considered. First, a finite receding horizon optimal control approach is employed, using  $N$ -point second-order polynomial (parabolic) extrapolations of the reference signal. Thus, at each time step  $k$  the cost functional

$$J = \sum_{m=k}^{k+N-1} [Q_p (y_{m+1} - \hat{r}_{m+1})^2 + Q_r z_{m+1}^2 + R u_m^2] \quad (3.3)$$

is minimized, where the weights  $Q_p = 0.29$ ,  $Q_r = 47$ ,  $R = 0.91$ ,  $\hat{r}_{k+1} = r_{k+1}$ , and the  $\hat{r}_{k+2}, \dots, \hat{r}_{k+N}$  are the results of the extrapolation. These are determined by  $r_{k+1}$ ,  $r_k$  and  $r_{k-1}$ . The (relatively long) planning horizon  $N = 60$  is used in this example, and thus the reference is predicted 0.6 sec into the future. The second control strategy consists of a regulator-based tracking system. Here the LQR performance functional

$$J = \sum_{m=0}^{\infty} [Q_P (y_{m+1})^2 + Q_I z_{m+1}^2 + R u_m^2] \quad (3.4)$$

is minimized, where the LQ weights are the same as in the previous case. No emphasis is put on tracking the reference signal. This yields the optimal regulator solution  $u_k^* = -\mathbf{k}_{LQR}^T \mathbf{x}_k$ , but in order to meet the tracking objective, the modified input given by  $u_k = -(r_{k+1} + -\mathbf{k}_{LQR}^T \mathbf{x}_k)$  is used. (Note  $-r_{k+1}$  is used because  $M_\delta < 0$ .)

Now, in the first case, the control law is given by

$$\delta_{c_k} = \mathbf{k}_x^T \mathbf{x}_k + [k_{r1} \quad k_{r2} \quad k_{r3}] \begin{bmatrix} r_{k-1} \\ r_k \\ r_{k+1} \end{bmatrix} = \mathbf{k}_x^T \mathbf{x}_k + \mathbf{k}_r^T \mathbf{r}_k \quad (3.5)$$

with  $\mathbf{k}_x^T = [0.3522 \quad 1.1372 \quad -0.9183 \quad -6.6087]$ , and  $\mathbf{k}_r^T = [-33.1533 \quad 75.5399 \quad -43.6337]$ . The regulator based control law is given by

$$\delta_{c_k} = -r_{k+1} - \mathbf{k}_{LQR}^T \mathbf{x}_k \quad (3.6)$$

where  $-\mathbf{k}_{LQR}^T = [0.3509 \quad 1.1373 \quad -0.9184 \quad -6.6107]$ . It should be noted that the long planning horizon ( $N = 60$ ) yields the state feedback gains  $\mathbf{k}_x \approx -\mathbf{k}_{LQR}$ , thus the only real difference between the two strategies is the predictive information made available by the reference signal extrapolation (which makes it possible to include the  $r_k$ 's in the optimization and thus enforce tracking). The system response to a filtered pitch doublet using each control strategy is shown in Figure 3.1.

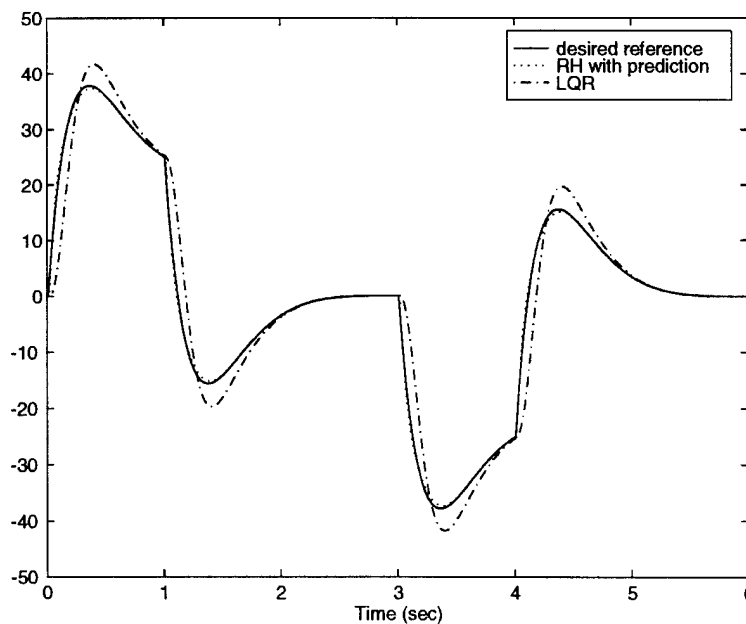


**Figure 3.1** Benefits of Predictive Control

Clearly, as seen in this figure, the RH predictive response essentially lies on top of the desired reference, and the predictive information has improved the tracking performance. Thus, receding horizon control is well suited to the manual flight control problem, where it is required to track the pilot's commands over a finite time interval.

Remark: It should be noted that the two control strategies differ even in the case where the simplest (ZOH) extrapolation rule

$$r_m = r_{k+1}, m = k+1, k+2, \dots, k+N \quad (3.7)$$

is used; in which case both control strategies operate on the same information. In this case,

$$\delta_{c_x} = \mathbf{k}_x^T \mathbf{x}_k + k_r r_{k+1} \quad (3.8)$$

where  $k_r = -1.2471$  and  $\mathbf{k}_x \approx \mathbf{k}_{LQR}$  is the same as before. ■

### 3.3 Optimization Methods in Tracking Control

The time domain Linear Quadratic (LQ) optimal control theory addresses the regulation and/or set-point control problem, particularly in the control unconstrained case, where the linear control system  $\dot{\mathbf{x}} = \mathbf{A}\mathbf{x} + \mathbf{b}u$ ,  $\mathbf{x}(0) = \mathbf{x}_0$ ,  $t \geq 0$  is considered. In tracking control, it is required that the system output of the general form  $y(t) = \mathbf{c}^T \mathbf{x}(t) + du(t)$  follow a reference signal  $r(t)$ . Regulation and set-point control consider reference signals that are known in advance, viz.,  $r(t)$  is zero or a constant for all time. Having upfront knowledge of the desired system trajectory for all time of interest, optimization methods can be employed to determine the optimal control  $u^*(t) = \mathbf{k}_x^T \mathbf{x}(t)$ ,  $0 \leq t < \infty$ , which minimizes a given quadratic performance functional, typically of the form

$$J = \int_0^{\infty} \left\{ (y(t) - r(t))^2 Q + u^2(t) R \right\} dt$$

Thus, the entire control signal time history (as a function of the state) is determined prior to the execution of the control task, based on prior knowledge of the entire reference signal  $r(t)$ ,  $0 \leq t < \infty$ . That is, optimization requires advance knowledge of the reference signal  $r(t)$  over the entire *planning horizon* on which the performance functional is based. This obviously is indeed the case in regulation and set-point control, whereas, the goal in



manual tracking control is to follow an unknown a priori, exogenous, reference signal  $r(t)$  as it becomes available in real-time. A causal control strategy is needed; indeed, only in batch simulations does one have the luxury of knowing the entire simulation time history upfront. Consequently, classical LQ optimal control can not be directly applied to manual flight control. On the other hand, automatic control of an aircraft, e.g., as is the case in autopilot design, where, during cruise, it is required to regulate the aircraft at a prespecified and fixed altitude or maintain the airspeed, is a regulation/set-point control problem. Thus, regulation and set-point control play an important role in autopilot design, but these are merely *special cases* of the *tracking* control problem and therefore are not adequate for the full gamut of manual flight control system design, where the tracking control paradigm applies.

In a discrete-time formulation, the optimal control tracking task requires the system output to follow an exogenous reference, i.e., it is required that  $y_{k+1} \approx r_{k+1}$ ,  $k = 0, 1, \dots$ . An LQ optimal control approach would thus entail the minimization of a performance functional of the general form

$$J = \sum_{k=0}^{\infty} \left[ Q(y_{k+1} - r_{k+1})^2 + Ru_k^2 \right] \quad (3.9)$$

where the scalar weights  $Q$  and  $R \geq 0$ . An optimal control tracking solution thus requires that the reference signal  $r_{k+1}$ , be known for all  $k$  in advance.

The manual tracking problem, however, is an "open-ended" task, that is, tracking is not about moving from point A to a prespecified and known point B, but rather to continually follow an unknown, exogenous reference as it becomes available in time. Thus,  $r_{k+1}$  is not known until time  $k$  (recall that the convention is used such that the pilot provides  $r_{k+1}$  at time  $k$ ), at which time  $r_{k+2}, \dots, r_{k+N}, \dots$  are not known. Hence, at time  $k$  it is impossible to explicitly evaluate (or much less minimize) a performance functional  $J$  of the form in Eq. (3.9) for a given tracking task until it is over; clearly, at this point it is too late to utilize this information in the control of the vehicle during the tracking task.

### 3.4 LQT Control

In order to employ the optimal control method, the reference signal time history, viz., each  $r_k$ , must be prespecified over the *planning horizon* ( $N$ ). This is not feasible in the case of manual, viz., real-time tracking control at time  $k$ , however the reference can be predicted into the future based on the currently available reference signal  $r_{k+1}$  and the recent past history of the reference signal. It would be ill-advised to rely on long term predictions, thus a receding horizon approach is logical and is used to break up the indefinite horizon tracking problem into an open-ended sequence of finite horizon optimization problems based on short-term only predictions of the pilot demanded reference signal. Thus, at each time step  $k$ , i.e., within each receding horizon window (RHW), the reference signal is extrapolated (details of the reference prediction are provided in Chapter 4) over the planning horizon  $N$ , denoted by  $\hat{r}_{k+n}$ ,  $n = 2, \dots, N$ , and the finite horizon performance functional

$$J = \sum_{m=k}^{k+N-1} \left[ Q_P (y_{m+1} - \hat{r}_{m+1})^2 + Q_I z_{m+1}^2 + R u_m^2 \right] \quad (3.10)$$

is minimized, in accordance with the prescribed system dynamics, and where  $z$  represents the integral state described in Chapter 2. The result is an  $N$ -dimensional optimal control vector  $\mathbf{u}^*$ , where the optimality is with respect to tracking the extrapolated reference vector from the current system state forward to the end of the current window. In the unconstrained case, the first element of this control vector is used to physically drive the system (the remaining elements are discarded) and the procedure is repeated at each subsequent time step. In the presence of downstream actuator constraints, however, within any given window the resultant control vector may not be *feasible*, i.e., it may induce actuator saturations which invalidate the linear system representation, nullify the optimality of the control vector, and adversely impact the stability of the closed-loop system. Hence, special measures must be taken to prevent this state of affairs from occurring.

Within the window initiated at time  $k$ , an optimization problem over  $\mathbf{R}^N$  is posed by considering the vectors

$$\mathbf{u} = [u_n] = [u_0, u_1, \dots, u_{N-1}]^T \in \mathbf{R}^N \quad (3.11)$$

$$\hat{\mathbf{r}} = [\hat{r}_n] = [\hat{r}_1, \hat{r}_2, \dots, \hat{r}_N]^T \in \mathbf{R}^N \quad (3.12)$$

$$\mathbf{y} = [y_n] = [y_1, y_2, \dots, y_N]^T \in \mathbf{R}^N \quad (3.13)$$

$$\mathbf{z} = [z_n] = [z_1, z_2, \dots, z_N]^T \in \mathbf{R}^N \quad (3.14)$$

where  $\mathbf{u}$  represents an  $N$ -point input vector,  $\hat{\mathbf{r}}$  is the extrapolated reference vector,  $\mathbf{y}$  is the corresponding  $N$ -point output vector, and  $\mathbf{z}$  is the  $N$ -point integrator "charge."

The performance functional Eq. (3.10) can now be written in the form

$$J = \sum_{n=0}^{N-1} \left[ Q_P (y_{n+1} - \hat{r}_{n+1})^2 + Q_I z_{n+1}^2 + R u_n^2 \right] \quad (3.15)$$

where the *initial* (i.e., with respect to the current window) state  $\mathbf{x}_0$  is  $\mathbf{x}_k$  and thus state feedback action is achieved via the receding horizon formulation. The *optimal control vector*  $\mathbf{u}^* = [u_0^*, u_1^*, \dots, u_{N-1}^*]^T \in \mathbf{R}^N$  is obtained at each real time step  $k$ , corresponding to optimal tracking of the extrapolated reference vector  $\hat{\mathbf{r}} = [\hat{r}_1, \hat{r}_2, \dots, \hat{r}_N]^T$ . Note that the first element of  $\hat{\mathbf{r}}$  is the currently demanded pilot reference signal, and thus does not have to be predicted. Moreover, it transpires,  $\mathbf{u}^* = \mathbf{u}^*(\hat{\mathbf{r}}; \mathbf{x}_0)$  is linear in both  $\mathbf{x}_0$  and  $\hat{\mathbf{r}}$ . If the vector  $\hat{\mathbf{r}}$  is too aggressive in the sense that it can not be optimally tracked with respect to the designated performance criteria and within the bounds of the actuator constraints, the strategy is to *optimally* track the closest *feasible* reference,  $\mathbf{r}'$ . In light of the preceding observations, the corresponding *feasible control vector* is readily determined, viz.,

$$\mathbf{u}' = \mathbf{u}^*(\mathbf{r}'; \mathbf{x}_0)$$

which is the optimal control vector corresponding to the feasible reference  $\mathbf{r}'$ . Moreover,  $\mathbf{r}'$  is the *best* reference vector that can be tracked with the given optimal control law without violating the actuator constraints. In other words, the relaxed reference vector  $\mathbf{r}'$  is as "close" as possible to the pilot demanded  $\hat{\mathbf{r}}$ .

There are many important questions which need to be addressed when assessing the feasibility of the reference vector. For example, since only the first element of the vector  $\mathbf{u}'$  will actually drive the system, is it really necessary to be so conservative as to ensure that each and every element of  $\mathbf{u}'$  does not induce saturation? Thus, specific *feasibility criteria* must be stipulated, which best serve the specific problem at hand. Furthermore, one must assess the long term stability implications of the criteria, as well as whether or not guarantees can be made regarding the existence of a feasible reference at subsequent time steps. The investigation of these issues is pursued in Chapter 5.

Further elaboration is also required regarding the use of the terms *best* and *closest* in the preceding. In the following chapter, innovative methods of predicting the pilot demanded reference are devised in which the feasible reference vector is expressed in the linear relationship

$$\mathbf{r}' = \mathbf{k}r_1' + \mathbf{h} \quad (3.16)$$

The term *best* (or *closest*) *reference vector* is used to imply the minimization of  $|r_1 - r_1'|$  subject to the specified feasibility criteria. It is important to note that  $r_1$  is the only reference value which is ever explicitly tracked, and thus this implication is stronger than it may appear at first glance. Under certain conditions the resultant  $\mathbf{r}'$  sequence is the solution to  $\min_{\mathbf{r}'} \|\hat{\mathbf{r}} - \mathbf{r}'\|$ , subject to the specified feasibility criteria, for any norm. Furthermore, during small signal operation  $\mathbf{r}' = \hat{\mathbf{r}}$ , and optimal (with respect to the extrapolated pilot reference and within the given window) tracking ensues. In any event, this novel formulation yields

a computationally efficient solution which is highly amenable to real-time tracking control applications.

The closed-loop system configuration is illustrated in Figure 3.2. When the exogenous reference signal is such that it attempts to drive the system out of its small signal

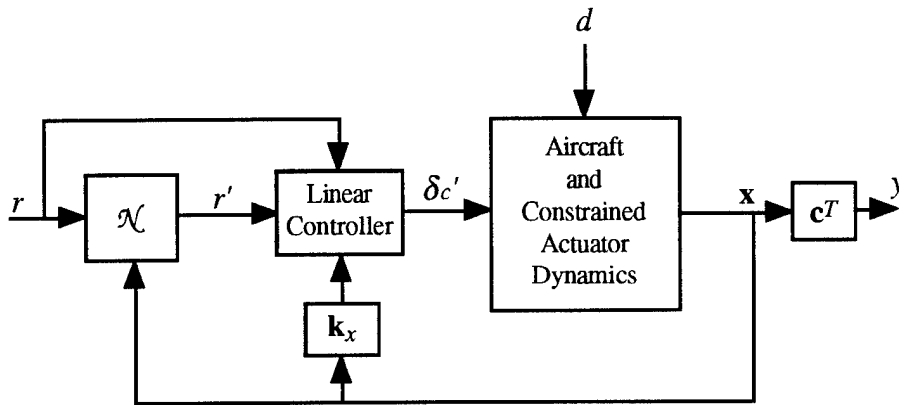


**Figure 3.2.** Overall Closed-Loop Configuration

operating range, the result is tantamount to a nonlinear scaling (represented by the nonlinear operator  $\mathcal{N}$  in Figure 3.2) of  $r_1 = r_{k+1}$ , yielding a feasible reference  $r'_1 = r'_{k+1}$ . Hence, using this control architecture the state feedback structure is unaffected and BIBO stability of the inner-loop feedback system (from  $r'$  to  $y$ ) is maintained. Although BIBO stability from  $r'$  to  $y$  is guaranteed provided that the LQT solution exists, BIBO stability from  $r$  to  $y$  requires an assurance that  $r'$  remains bounded. The mere preclusion of downstream actuator saturation does not provide this assurance when the open-loop plant is unstable. Stronger feasibility criteria must be enforced to prevent the feasible reference  $r'$  from simply "following" the unstable output of an open-loop unstable plant. This issue is discussed further in Chapter 5. Furthermore, in this control scheme, during small signal operation,  $r'_{k+1} = r_{k+1}$ , and the linear performance characteristics are preserved: Small signal performance is not sacrificed to accommodate the actuator constraints. Finally, it should be noted that  $|r'_{k+1}| \leq |r_{k+1}|$  does not necessarily hold. The case  $|r'_{k+1}| > |r_{k+1}|$  is indeed possible,

and, e.g., it is also possible that  $r_{k+1} = 0$  whereas  $r'_{k+1} \neq 0$ . Hence, a rather general adjustment of the reference signal is employed in order to address the manual tracking problem with both amplitude and rate constrained actuators.

### 3.5 The Unconstrained Optimal Control Solution Within Each Window

In this section, the finite horizon optimization problem is solved from within each window. At this point in time, the actuator constraints are not explicitly addressed. The only concern here is the determination of the optimal control vector  $\mathbf{u}^* = [u_0^* \ \cdots \ u_{N-1}^*]^T$  which minimizes the finite horizon performance functional Eq. (3.15). The development is based on the discrete-time control system given by

$$\mathbf{x}_{k+1} = \mathbf{A}\mathbf{x}_k + \mathbf{b}u_k + \boldsymbol{\gamma}_1 r_{k+1} + \boldsymbol{\gamma}_2 d \quad (3.17)$$

$$y_{k+1} = \mathbf{c}^T \mathbf{x}_{k+1} \quad (3.18)$$

where it is assumed that  $\mathbf{x}_k = \mathbf{x}[k] = [x_1[k] \ \cdots \ x_{n-1}[k] \ z_k]^T \in \mathbf{R}^n$  where  $z_k$  is the integrator state described in Chapter 2. The following development remains valid without the integrator state by letting  $Q_1$  (and possibly  $\gamma_1$ ) = 0. Within the window initiated at time  $k$ , the initial state is  $\mathbf{x}_k$ , and thus the notation  $\mathbf{x}_0 = \mathbf{x}_k$  is employed. During the ensuing development, it is evident that the reference signal has been predicted into the future, and thus, the "hat" notation is temporarily suppressed.

Given the discrete-time system described by Eqs. (3.17) and (3.18), and with the reference signal  $r_k$  stipulated for all  $1 \leq k \leq N$ , the unconstrained tracking problem with *finite* planning horizon  $N$  can be posed as a linear quadratic optimization problem in the control sequence  $[u_0, u_1, \dots, u_{N-1}]^T \in \mathbf{R}^N$  by considering the vectors of Eqs. (3.11)-(3.14). Throughout the remainder of this document, the subscript  $k$  ( $0 \leq k < \infty$ ) is used to represent real-time instants, while, within a given receding horizon window, the subscript

$n$  ( $0 \leq n \leq N$ ) is used. Thus, each  $u_k$  and  $r_{k+1}$  over the tracking task will be represented by a  $u_0$  and  $r_1$  respectively in one of the receding horizon windows.

According to the receding horizon modulus operandi,  $u_0$  represents an actual system input. The remaining control signals  $u_1, \dots, u_{N-1}$  do not represent physically realized inputs to the system. Furthermore, at any given time instant  $k$  in the *system time reference*  $\mathbf{x}_0$  from the *window time reference* represents  $\mathbf{x}_k$ , thus state feedback action is achieved via the receding horizon formulation. Thus, the second through  $N$ -th components of  $\mathbf{u}$  are never actually used to drive the system, nor are the second through  $N$ -th elements of  $\mathbf{y}$  actually realized.

Using the notation of Eqs. (3.11)-(3.14), the convex cost functional Eq. (3.15) can be written

$$J = Q_p[\mathbf{y} - \mathbf{r}]^T[\mathbf{y} - \mathbf{r}] + Q_l \mathbf{z}^T \mathbf{z} + \mathbf{R} \mathbf{u}^T \mathbf{u}, \quad (3.19)$$

and the optimal control sequence  $\mathbf{u}^* = \mathbf{u}^*(\mathbf{r}; \mathbf{x}_0)$  for the unconstrained problem over the planning horizon  $N$  is given by  $\mathbf{u} = \mathbf{u}^*$  such that  $\partial J / \partial \mathbf{u}^* = \mathbf{0}$ . Thus, it is required to express  $J$  as a function of  $\mathbf{u}$  only.

The explicit solution of the difference Eq. (3.17) is

$$\mathbf{x}_n = \mathbf{A}^n \mathbf{x}_0 + \sum_{k=0}^{n-1} \mathbf{A}^k (\mathbf{b} u_{n-1-k} + \boldsymbol{\gamma}_1 r_{n-k} + \boldsymbol{\gamma}_2 d), \quad n = 1, 2, \dots, N \quad (3.20)$$

Direct substitution of Eq. (3.20) into the quadratic functional Eq. (3.15) yields

$$J = \sum_{m=0}^{N-1} \left[ Q_p \left( \mathbf{c}^T \mathbf{A}^{m+1} \mathbf{x}_0 + \sum_{k=0}^m \mathbf{c}^T \mathbf{A}^k (\mathbf{b} u_{m-k} + \boldsymbol{\gamma}_1 r_{m-k+1} + \boldsymbol{\gamma}_2 d) - r_{m+1} \right)^2 \right] \\ + \sum_{m=0}^{N-1} \left[ Q_l \left( \mathbf{c}_z^T \mathbf{A}^{m+1} \mathbf{x}_0 + \sum_{k=0}^m \mathbf{c}_z^T \mathbf{A}^k (\mathbf{b} u_{m-k} + \boldsymbol{\gamma}_1 r_{m-k+1} + \boldsymbol{\gamma}_2 d) \right)^2 + \mathbf{R} u_m^2 \right]$$

where the row vector  $\mathbf{c}_z^T = [\mathbf{0}_{n-1} \mid 1]$ , i.e.,  $\mathbf{c}_z^T \mathbf{x} = z$ .

Now,

$$\frac{\partial J}{\partial \mathbf{u}} = \left[ \frac{\partial J}{\partial u_0} \quad \frac{\partial J}{\partial u_1} \quad \cdots \quad \frac{\partial J}{\partial u_{N-1}} \right]^T$$

Setting  $\partial J / \partial u_n = 0$  for each  $n = 0, 1, \dots, N-1$ , and after some algebraic manipulation, the optimal control vector  $\mathbf{u}^*$  is expressed in vector notation as

$$\mathbf{u}^* = \begin{bmatrix} u_0^* \\ \vdots \\ u_{N-1}^* \end{bmatrix} = \mathbf{X}^{-1}(\mathbf{Y}\mathbf{r} + \mathbf{Z}\mathbf{x}_0 + \mathbf{V}\mathbf{d})$$

where the vector  $\mathbf{d} = \mathbf{1}_{N \times 1} d$ , and  $\mathbf{V}$ ,  $\mathbf{X}$ ,  $\mathbf{Y}$  and  $\mathbf{Z}$  are matrices depending only on the known system parameters. Specifically,  $\mathbf{V}$ ,  $\mathbf{X}$ ,  $\mathbf{Y} \in \mathbf{R}^{N \times N}$  and  $\mathbf{Z} \in \mathbf{R}^{N \times n}$  are explicitly given by

$$\mathbf{V} = \begin{bmatrix} v_{0,0} & \cdots & v_{0,N-1} \\ \vdots & \ddots & \vdots \\ v_{N-1,0} & \cdots & v_{N-1,N-1} \end{bmatrix}_{N \times N} \quad \mathbf{X} = \begin{bmatrix} x_{0,0} & \cdots & x_{0,N-1} \\ \vdots & \ddots & \vdots \\ x_{N-1,0} & \cdots & x_{N-1,N-1} \end{bmatrix}_{N \times N} \quad \mathbf{Y} = \begin{bmatrix} y_{0,0} & \cdots & y_{0,N-1} \\ \vdots & \ddots & \vdots \\ y_{N-1,0} & \cdots & y_{N-1,N-1} \end{bmatrix}_{N \times N}$$

and

$$\mathbf{Z} = \begin{bmatrix} \mathbf{z}_0^T \\ \vdots \\ \mathbf{z}_{N-1}^T \end{bmatrix}_{N \times n}$$

where the entries

$$v_{i,j} = \begin{cases} -\sum_{m=i}^{N-1} \sigma_m(\gamma_2), & i \geq j \\ -\sum_{m=j}^{N-1} \sigma_m(\gamma_2), & j > i \end{cases}$$

$$x_{i,j} = \begin{cases} \sum_{m=i}^{N-1} \sigma_m(\mathbf{b}), & j < i \\ \sum_{m=i}^{N-1} \sigma_m(\mathbf{b}) + \frac{R}{Q_P}, & j = i \\ \sum_{m=j}^{N-1} \sigma_m(\mathbf{b}), & j > i \end{cases}$$



$$y_{i,j} = \begin{cases} -\sum_{m=i}^{N-1} \sigma_m(\gamma_1), & i > j \\ -\sum_{m=i}^{N-1} \sigma_m(\gamma_1) + \mathbf{c}^T \mathbf{b}, & i = j \\ -\sum_{m=j}^{N-1} \sigma_m(\gamma_1) + \mathbf{c}^T \mathbf{A}^{j-i} \mathbf{b}, & i < j \end{cases}$$

and where

$$\sigma_m(\mathbf{v}) = \mathbf{c}^T \mathbf{A}^{m-i} \mathbf{b} \mathbf{c}^T \mathbf{A}^{m-j} \mathbf{v} + \frac{Q_l}{Q_p} \mathbf{c}_z^T \mathbf{A}^{m-i} \mathbf{b} \mathbf{c}_z^T \mathbf{A}^{m-j} \mathbf{v}, \quad \mathbf{v} \in \mathbf{R}^n$$

and

$$\mathbf{z}_i^T = -\sum_{m=i}^{N-1} (\mathbf{c}^T \mathbf{A}^{m-i} \mathbf{b}) (\mathbf{c}^T \mathbf{A}^{m+1}) + \frac{Q_l}{Q_p} (\mathbf{c}_z^T \mathbf{A}^{m-i} \mathbf{b}) (\mathbf{c}_z^T \mathbf{A}^{m+1})$$

The indices  $i, j = 0, 1, \dots, N-1$ . Now, define the matrices  $\mathbf{K}_r = \mathbf{X}^{-1} \mathbf{Y}$ ,  $\mathbf{K}_x = \mathbf{X}^{-1} \mathbf{Z}$ ,  $\mathbf{k}_d = \mathbf{X}^{-1} \mathbf{V} \mathbf{1}_{N \times 1}$ . Then the unconstrained optimal control vector can be expressed in closed form, viz.,

$$\mathbf{u}^*(\mathbf{r}; \mathbf{x}_0) = \mathbf{K}_x \mathbf{x}_0 + \mathbf{K}_r \mathbf{r} + \mathbf{k}_d d$$

where the matrices  $\mathbf{K}_x \in \mathbf{R}^{N \times n}$ ,  $\mathbf{K}_r \in \mathbf{R}^{N \times N}$  and  $\mathbf{k}_d \in \mathbf{R}^N$  depend only on the system parameters  $(\mathbf{A}, \mathbf{b}, \mathbf{c}, \gamma_1, \gamma_2)$  and the LQ weights  $Q_p, Q_l$  and  $R$ . An important observation is that  $\mathbf{u}^*$  is linear in both  $\mathbf{r}$  and the initial state  $\mathbf{x}_0 \equiv \mathbf{x}_k$ .

The corresponding *optimal state vector* time history over the planning horizon can thus be obtained

$$\mathbf{x}^* = \begin{bmatrix} \mathbf{x}_1^{*T} & \cdots & \mathbf{x}_N^{*T} \end{bmatrix}^T = \mathbf{M}_x \mathbf{x}_0 + \mathbf{M}_r \mathbf{r} + \mathbf{m}_d d$$

where  $\mathbf{M}_x \in \mathbf{R}^{Nn \times n}$ ,  $\mathbf{M}_r \in \mathbf{R}^{Nn \times N}$ , and  $\mathbf{m}_d \in \mathbf{R}^{Nn}$ . Let  $\mathbf{M}_A(\mathbf{v}) \in \mathbf{R}^{Nn \times Nn}$  be the lower block triangular matrix with dummy variable  $\mathbf{v} \in \mathbf{R}^n$ , and with block elements  $[\mathbf{M}_A(\mathbf{v})]_{ij} \in \mathbf{R}^n$  given by

$$[\mathbf{M}_A(\mathbf{v})]_{i,j} = \begin{cases} \mathbf{A}^{i-j}\mathbf{v}, & i \geq j \\ \mathbf{0}_{n \times 1}, & i < j \end{cases}$$

Then,

$$\mathbf{M}_x = \begin{bmatrix} \mathbf{A} \\ \dots \\ \mathbf{A}^2 \\ \dots \\ \vdots \\ \dots \\ \mathbf{A}^N \end{bmatrix} + \mathbf{M}_A(\mathbf{b})\mathbf{K}_x, \quad (3.21)$$

$$\mathbf{M}_r = \mathbf{M}_A(\mathbf{b})\mathbf{K}_r + \mathbf{M}_A(\boldsymbol{\gamma}_1) \quad (3.22)$$

and

$$\mathbf{m}_d = \begin{bmatrix} \mathbf{I} \\ \dots \\ (\mathbf{I} + \mathbf{A}) \\ \dots \\ \vdots \\ \dots \\ \sum_{m=0}^{N-1} \mathbf{A}^m \end{bmatrix} \boldsymbol{\gamma}_2 + \mathbf{M}_A(\mathbf{b})\mathbf{K}_d \quad (3.23)$$

Additionally, the control surface deflection  $\delta$  is contained in  $\mathbf{x}$ , viz.,  $\delta = \mathbf{c}_\delta^T \mathbf{x}$ . Thus, over the planning horizon the *optimal control surface deflection vector* is given by

$$\boldsymbol{\delta}^* = [\delta_1^* \quad \dots \quad \delta_N^*]^T = (\mathbf{I}_N \otimes \mathbf{c}_\delta^T) \mathbf{x}^*$$

where  $\otimes$  is the Kronecker product. Hence,

$$\boldsymbol{\delta}^* = (\mathbf{I}_N \otimes \mathbf{c}_\delta^T) \mathbf{M}_x \mathbf{x}_0 + (\mathbf{I}_N \otimes \mathbf{c}_\delta^T) \mathbf{M}_r \mathbf{r} + (\mathbf{I}_N \otimes \mathbf{c}_\delta^T) \mathbf{m}_d d$$

Thus, define

$$\mathbf{N}_x \triangleq (\mathbf{I}_N \otimes \mathbf{c}_\delta^T) \mathbf{M}_x, \quad \mathbf{N}_r \triangleq (\mathbf{I}_N \otimes \mathbf{c}_\delta^T) \mathbf{M}_r, \quad \mathbf{n}_d \triangleq (\mathbf{I}_N \otimes \mathbf{c}_\delta^T) \mathbf{m}_d \quad (3.24)$$

and  $\boldsymbol{\delta}^*$  can be written

$$\boldsymbol{\delta}^* = [\delta_1^* \quad \dots \quad \delta_N^*]^T = \mathbf{N}_x \mathbf{x}_0 + \mathbf{N}_r \mathbf{r} + \mathbf{n}_d d \quad (3.25)$$

where  $\mathbf{N}_x \in \mathbf{R}^{N \times n}$ ,  $\mathbf{N}_r \in \mathbf{R}^{N \times N}$ , and  $\mathbf{n}_d \in \mathbf{R}^N$ .

Since the actuator rates are also of concern, the calculated *optimal actuator displacement difference vector* is given by

$$\Delta_{\delta^*} = \begin{bmatrix} \delta_1^* - \delta_0 \\ \delta_2^* - \delta_1^* \\ \vdots \\ \delta_N^* - \delta_{N-1}^* \end{bmatrix} = \mathbf{E} \begin{bmatrix} \delta_1^* \\ \delta_2^* \\ \vdots \\ \delta_N^* \end{bmatrix} - \mathbf{e}_{1_N} \delta_0$$

where  $\mathbf{E} = \mathbf{I}_N - \mathbf{D}_{U_N}^T$ ,  $\mathbf{D}_{U_N}$  is the upper triangular matrix given by

$$\mathbf{D}_{U_N} = \begin{bmatrix} 0 & 1 & & & \\ & 0 & 1 & \mathbf{0} & \\ & & 0 & \ddots & \\ & \mathbf{0} & & \ddots & 1 \\ & & & & 0 \end{bmatrix}_{N \times N}$$

$\mathbf{e}_{1_N} = [1 \ 0 \ \dots \ 0]_{N \times 1}^T$ , and  $\delta_0 = \mathbf{c}_\delta^T \mathbf{x}_0$ . Now, let

$$\mathbf{P}_x = (\mathbf{I}_N - \mathbf{D}_{U_N}^T) \mathbf{N}_x - \mathbf{e}_{1_N} \mathbf{c}_\delta^T \quad (3.26)$$

$$\mathbf{P}_r = (\mathbf{I}_N - \mathbf{D}_{U_N}^T) \mathbf{N}_r \quad (3.27)$$

$$\mathbf{p}_d = (\mathbf{I}_N - \mathbf{D}_{U_N}^T) \mathbf{n}_d \quad (3.28)$$

Finally,  $\Delta_{\delta^*}$  can be written

$$\Delta_{\delta^*} = \mathbf{P}_x \mathbf{x}_0 + \mathbf{P}_r \mathbf{r} + \mathbf{p}_d d \quad (3.29)$$

where  $\mathbf{P}_x \in \mathbf{R}^{N \times n}$ ,  $\mathbf{P}_r \in \mathbf{R}^{N \times N}$ , and  $\mathbf{p}_d \in \mathbf{R}^N$ .

### 3.6 Transformation of Actuator Constraints

In Chapter 4 several reference prediction schemes are devised in which the feasible reference vector  $\mathbf{r}'$  is parameterized by  $r'_1$ , and written in the form

$$\mathbf{r}' = \mathbf{k} r'_1 + \mathbf{h} \quad (3.30)$$

Assume for the moment that the reference is feasible and thus  $\mathbf{r}' = \mathbf{r}$ . Then, the optimal control vector can be written

$$\mathbf{u}^* = \mathbf{K}_x \mathbf{x}_0 + \mathbf{K}_r \mathbf{k} r'_1 + \mathbf{K}_r \mathbf{h} + \mathbf{k}_d d \quad (3.31)$$

Hence, the unconstrained LQT optimal control vector is specified linearly in terms of the current plant state  $\mathbf{x}_0$ , the known and constant disturbance  $d$ , the present reference signal value  $r_1$  and possibly known past values of the reference signal in  $\mathbf{h}$ . The known plant parameters and the LQ weights feature in the coefficient matrices  $\mathbf{K}_x$ ,  $\mathbf{K}_r$  and  $\mathbf{k}_d$ .

The control vector  $\mathbf{u}^*(\mathbf{r}; \mathbf{x}_0)$  produced by the inner-loop control law Eq. (3.31) indeed induces optimal tracking of the stipulated reference over the given planning horizon, but does not necessarily satisfy the actuator constraints. Thus, a modified control signal  $\mathbf{u}'$  is sought which does not infringe upon the actuator constraints. This modified control vector is based on the determination of the feasible reference vector  $\mathbf{r}'$ . Specifically, this *feasible control vector* is given by

$$\mathbf{u}' = \mathbf{K}_x \mathbf{x}_0 + \mathbf{K}_r \mathbf{k}_r r_1' + \mathbf{K}_r \mathbf{h} + \mathbf{k}_d d \quad (3.32)$$

Taking into consideration Eqs. (3.25), (3.29) and (3.30), it is readily apparent that the actuator constraints (both amplitude and rate) can be transformed into linear constraints on the current reference value  $r_1$ . Thus, a nonlinear "scaling" is performed on  $r_1$  to yield  $r_1'$  which in turn defines the feasible reference vector  $\mathbf{r}'$ . Furthermore,  $\mathbf{u}'$  is the optimal control for tracking the relaxed reference  $\mathbf{r}'$ . However, it is not necessarily true that  $\mathbf{u}'$  is the optimal control solution to the original constrained problem.

The amplitude constraints yield

$$\delta_{\min} \leq \mathbf{N}_x \mathbf{x}_0 + \mathbf{N}_r \mathbf{k}_r r_1' + \mathbf{N}_r \mathbf{h} + \mathbf{n}_d d \leq \delta_{\max} \quad (3.33)$$

and thus

$$\delta_{\min} - \mathbf{N}_x \mathbf{x}_0 - \mathbf{N}_r \mathbf{h} - \mathbf{n}_d d \leq \mathbf{N}_r \mathbf{k}_r r_1' \leq \delta_{\max} - \mathbf{N}_x \mathbf{x}_0 - \mathbf{N}_r \mathbf{h} - \mathbf{n}_d d \quad (3.34)$$

Similarly, the rate constraints yield

$$T \dot{\delta}_{\min} \leq \mathbf{P}_x \mathbf{x}_0 + \mathbf{P}_r \mathbf{k}_r r_1' + \mathbf{P}_r \mathbf{h} + \mathbf{p}_d d \leq T \dot{\delta}_{\max} \quad (3.35)$$

and thus

$$T \dot{\delta}_{\min} - \mathbf{P}_x \mathbf{x}_0 - \mathbf{P}_r \mathbf{h} - \mathbf{p}_d d \leq \mathbf{P}_r \mathbf{k}_r r_1' \leq T \dot{\delta}_{\max} - \mathbf{P}_x \mathbf{x}_0 - \mathbf{P}_r \mathbf{h} - \mathbf{p}_d d \quad (3.36)$$

Each of the Eqs. (3.34) and (3.36) yield up to  $2N$  constraints which  $r_1'$  must satisfy, for a total of  $4N$  constraints. Moreover, the saturation avoidance/mitigation strategies discussed in Chapter 5 are readily employed. Regardless of the particular mitigation scheme selected, the end result is a single inequality of the form

$$r_{\min} \leq r_1' \leq r_{\max} \quad (3.37)$$

which satisfies some or all of the constraints dictated in Eqs. (3.34) and (3.36). Thus, the scalar  $r_1'$  is chosen accordingly, viz.,

$$r_1' = \begin{cases} r_{\min}, & r_1 < r_{\min} \\ r_1, & r_{\min} \leq r_1 \leq r_{\max} \\ r_{\max}, & r_1 > r_{\max} \end{cases} \quad (3.38)$$

The details regarding the selection of  $r_1'$  are provided in Chapter 5.

### 3.7 The Explicit LQT Control Law

It is reiterated that regardless of the prediction method or constraint enforcement strategy selected, the only element of  $\mathbf{u}'$  which is actually used to drive the system is  $u_0' \equiv u_k$ , which can be written

$$u_k \equiv u_0' = \mathbf{e}_{1_N}^T \mathbf{u}' = \mathbf{e}_{1_N}^T (\mathbf{K}_x \mathbf{x}_0 + \mathbf{K}_r \mathbf{k} r_1' + \mathbf{K}_r \mathbf{h} + \mathbf{k}_d d) \quad (3.39)$$

Thus, in the spirit of Eq. (3.17) the actual control signal  $u_k$  applied at each time step is explicitly given by

$$u_k = \mathbf{k}_x^T \mathbf{x}_k + k_r r_{k+1}' + k_d d + \phi_k \quad (3.40)$$

where the *state feedback gain*

$$\mathbf{k}_x^T = \mathbf{e}_{1_N}^T \mathbf{K}_x \quad (3.41)$$

is constant, as is the *current reference signal gain*

$$k_r = \mathbf{e}_{1_N}^T \mathbf{K}_r \mathbf{k} \quad (3.42)$$

and the *disturbance signal gain*

$$k_d = \mathbf{e}_{1_N}^T \mathbf{k}_d \quad (3.43)$$

The control signal  $u_k$  thus consists of four components, viz., the state feedback component  $\mathbf{k}_x^T \mathbf{x}_k$ , the *reference signal component*  $k_r r'_{k+1}$  which is used not only for tracking, but also to ensure feasibility of the control signal, the *disturbance component*  $k_d d$ , and the *prediction-induced memory component*  $\phi_k = \mathbf{e}_{1_N}^T \mathbf{K}_r \mathbf{h}$ , where information from previous reference signal values is contained. Except during small signal operation, the feasible reference value  $r'_{k+1}$  is nonlinearly determined and depends on the particular saturation mitigation strategy employed, while the gain  $k_r$  is constant but depends on the prediction method employed, i.e., the vector  $\mathbf{k}$  as described in Chapter 4. The explicit formula for  $\phi_k$ , which may include previously demanded and/or previously applied reference values, also depends on the specific reference prediction method used, and is explicitly computed for each method devised in the following chapter.

### 3.8 Summary

A new approach to manual tracking control with amplitude and rate constrained actuators, referred to as LQT, has been presented. A motivational example, demonstrating potential benefits of a reference predictive control strategy was followed by a discussion of the problems which preclude the direct application of optimization methods in a real-time tracking control situation. Subsequently, the LQT methodology, which combines the established tools of LQ optimal control and receding horizon control was outlined. Next the finite horizon unconstrained optimization problem which arises in each receding horizon window was posed and solved yielding an optimal control vector  $\mathbf{u}^*$ , which is expressed linearly in terms of a predicted reference vector  $\mathbf{r}$ . Taking advantage of this linear relationship, the hard actuator constraints are transformed into constraints on the predicted

reference vector. A nonlinear scaling of the predicted reference vector can then be performed which precludes saturation of the downstream actuators, thus preserving linearity of the closed-loop system. The resultant computationally inexpensive control law is of the form

$$u_k = \mathbf{k}_x^T \mathbf{x}_k + k_r r'_{k+1} + k_d d + \phi_k$$

where each of the gains  $\mathbf{k}_x$ ,  $k_r$ , and  $k_d$  is constant. Specific reference prediction strategies are devised in Chapter 4, and the issue of constraint effects mitigation and the achievement of BIBO stability is addressed in Chapter 5.

## IV. The Feasible Reference Vector

### 4.1 Overview

In the previous chapter, the LQT control laws were developed, and the optimal control solution within each receding horizon window (RHW) was expressed linearly in terms of an  $N$ -dimensional reference vector,  $\hat{\mathbf{r}}$ . Subsequently, it was noted that optimal tracking of  $\hat{\mathbf{r}}$  may not be feasible due to the existence of the hard displacement and rate actuator constraints, and a feasible reference vector,  $\mathbf{r}'$  was alluded to. This Chapter is concerned with the generation of this feasible reference vector, viz.,

$$\mathbf{r}' = [r'_1 \ \cdots \ r'_N]^T \quad (4.1)$$

The crux of an optimal tracking control approach to manual control lies in the suitable and accurate prediction of the reference signal over the planning horizon. One of the goals of this research is to explore prediction methods which meet these criteria and readily extend themselves to an efficient handling of the downstream actuator constraints. At the same time, it is desired to keep computational requirements to a minimum.

Several two-stage prediction schemes are examined which yield a *feasible reference vector* of the form

$$\mathbf{r}' = [r'_n] = \begin{bmatrix} r'_1 \\ r'_2 \\ r'_3 \\ \vdots \\ r'_N \end{bmatrix} = \begin{bmatrix} k_1 \\ k_2 \\ k_3 \\ \vdots \\ k_N \end{bmatrix} r'_1 + \begin{bmatrix} h_1 \\ h_2 \\ h_3 \\ \vdots \\ h_N \end{bmatrix} = \mathbf{k}r'_1 + \mathbf{h} \quad (4.2)$$

Thus, the reference vector is parameterized in the reference signal at "time now,"  $r'_1$ . Within each RHW the  $\mathbf{k}$  and  $\mathbf{h}$  column vectors are constant, and  $\mathbf{r}'$  is (in some sense)



*feasible*. The latter comment is further explained in Chapter 5. Since the entire reference vector is parameterized by the scalar  $r_1$ , the door is opened to employ a variety of relatively simple saturation avoidance strategies.

A two-stage reference signal extrapolation scheme is developed. First, an extrapolation of past reference values is performed to predict the desired reference signal from the pilot into the future, yielding the *extrapolated reference vector*

$$\hat{\mathbf{r}} = [\hat{r}_1 \quad \cdots \quad \hat{r}_N]^T \quad (4.3)$$

Due to the actuator constraints it may not be possible for the linear controller to track this reference. Thus,  $\hat{\mathbf{r}}$  is subsequently modified to obtain the closest feasible reference vector  $\mathbf{r}'$ .

For each strategy presented, a heuristic description is provided, followed by the derivation of the explicit formulae in terms of past and present pilot demanded reference signal values. Finally, the explicit LQT control law is derived. While each of the two-stage prediction strategies are devised with constraint mitigation in mind, the unconstrained performance needs to be assessed as well, since this is the small-signal performance which will be obtained when these prediction strategies are employed. Simulation examples are deferred to Chapter 5 and the Appendix.

## 4.2 Stage 1: Extrapolation of the Pilot Demanded Reference

In the first stage of the prediction process, the pilot's reference is predicted into the future using a  $p$ -th order polynomial (*poly- $p$* ) extrapolation. Thus, over the planning horizon, each  $\hat{r}_n$  satisfies an equation of the form

$$\hat{r}_n = a_0 + a_1 n + a_2 n^2 + \cdots + a_p n^p, \quad n = 1, 2, \dots, N \quad (4.4)$$

Determination of the polynomial coefficients requires  $p + 1$  known solutions, viz., the present and  $p$  past values of the pilot demanded reference.

The polynomial coefficients in Eq. (4.4) are determined by solving the linear system of equations

$$\begin{bmatrix} r_{1-p} \\ \vdots \\ r_{-1} \\ r_0 \\ r_1 \end{bmatrix} = \begin{bmatrix} 1 & 1-p & (1-p)^2 & \cdots & (1-p)^p \\ \vdots & \vdots & \vdots & \ddots & \vdots \\ 1 & -1 & 1 & \cdots & (-1)^p \\ 1 & 0 & 0 & \cdots & 0 \\ 1 & 1 & 1 & \cdots & 1 \end{bmatrix} \begin{bmatrix} a_0 \\ a_1 \\ a_2 \\ \vdots \\ a_p \end{bmatrix} = \mathbf{E}\mathbf{a}$$

thus,  $\mathbf{E}_{ij} = (i-p)^{j-1}$ ,  $i, j = 1, \dots, p+1$ . Now,

$$\hat{r}_n = \sum_{m=0}^p a_m n^m$$

and the coefficients

$$\mathbf{a} = \mathbf{E}^{-1} [r_{1-p} \quad \cdots \quad r_{-1} \quad r_0 \quad r_1]^T$$

$\mathbf{E}$  is a Vandermonde matrix, and therefore invertible. Thus, let

$$\mathbf{E}^{-1} \triangleq \begin{bmatrix} \mathcal{E}_{1,1} & \mathcal{E}_{1,2} & \cdots & \mathcal{E}_{1,p+1} \\ \mathcal{E}_{2,1} & \mathcal{E}_{2,2} & \cdots & \mathcal{E}_{2,p+1} \\ \vdots & \vdots & \ddots & \vdots \\ \mathcal{E}_{p+1,1} & \mathcal{E}_{p+1,2} & \cdots & \mathcal{E}_{p+1,p+1} \end{bmatrix} \quad (4.5)$$

Then

$$a_m = \sum_{j=1}^{p+1} \mathcal{E}_{m+1,j} r_{j-p}, \quad m = 0, \dots, p, \text{ and}$$

$$\begin{aligned} \hat{r}_n &= \sum_{m=0}^p \left( \sum_{j=1}^{p+1} [\mathcal{E}_{m+1,j} r_{j-p}] \right) n^m \\ &= \sum_{j=1}^{p+1} \left[ \left( \sum_{m=0}^p n^m \mathcal{E}_{m+1,j} \right) r_{j-p} \right] \\ &= \sum_{j=1}^{p+1} c_{n,j} r_{j-p} \end{aligned} \quad (4.6)$$

where the  $c_{n,j}$  are constants given by

$$c_{n,j} = \sum_{m=0}^p n^m \varepsilon_{m+1,j} \quad (4.7)$$

and the  $\varepsilon_{i,j}$  are as defined in Eq. (4.5). Thus,  $\hat{\mathbf{r}}$  can be written in the general form

$\hat{\mathbf{r}} = \mathbf{k}r_1 + \mathbf{h}$ , where

$$\begin{aligned} \hat{r}_n &= c_{n,p+1}r_1 + \sum_{j=1}^p c_{n,j}r_{j-p} \\ &= k_n r_1 + h_n \end{aligned} \quad (4.8)$$

and thus

$$k_n = c_{n,p+1} \quad (4.9)$$

and

$$h_n = \sum_{j=1}^p c_{n,j}r_{j-p}$$

It should be noted that  $\hat{r}_1 \equiv r_1 \equiv r_{k+1}$ .

The general case poly- $p$  extrapolation is illustrated in Figure 4.1. Each of the  $r_{1-p}, \dots, r_1$  represent actual past pilot inputs and are explicitly known. Each of these, as well

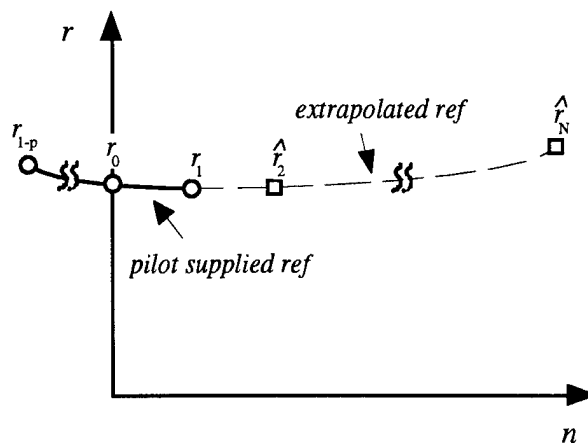


**Figure 4.1.** Poly- $p$  Extrapolation of the Pilot's Reference

as the  $\hat{r}_2, \dots, \hat{r}_N$  satisfy the polynomial Eq. (4.4). For the simplest case  $p = 0$ , each  $\hat{r}_n = \hat{r}_1 = r_1 = r_{k+1}$ ,  $n = 1, \dots, N$ , i.e., each  $r_{k+1}$  is assumed to be the beginning of a step input. The case  $p = 1$  provides for a linear extrapolation, and  $p = 2$  is a parabolic extrapolation. An explicit evaluation of the reference vector coefficients is provided in Table 4.1 for the values  $p = 0, 1$ , and  $2$ .

**Table 4.1.** Poly-p Extrapolation Coefficients

$p$	$k_n$	$h_n$
0	1	0
1	$n$	$(1-n)r_0$
2	$0.5(n^2+n)$	$0.5(n^2-n)r_{-1} + (1-n^2)r_0$

In the unconstrained case with poly- $p$  extrapolation, the extrapolated reference vector  $\hat{\mathbf{r}}$  can be written in the form  $\mathbf{K}r_1 + \mathbf{h}$ , where the elements of  $\mathbf{K}$  are defined in Eq. (4.9). The component  $\mathbf{h}$  can be written in the form

$$\mathbf{h} = \begin{cases} \mathbf{H} [r_{1-p} \ r_{2-p} \ \cdots \ r_0]^T, & p > 0 \\ \mathbf{0}_N, & p = 0 \end{cases} \quad (4.10)$$

where  $\mathbf{H} = [h(i,j)] \in \mathbf{R}^{N \times p}$ , whose elements are given by  $h(i,j) = c_{n=i,j}$  where the  $c_{n,j}$  are as defined in Eq. (4.7). Thus,

$$h(i,j) = \sum_{m=0}^p i^m \epsilon_{m+1,j}, \quad i = 1, \dots, N, \quad j = 1, \dots, p$$

where the  $\epsilon_{m+1,j}$  are as defined in Eq. (4.5). Hence, (for  $p > 0$ ),

$$\phi_k = \mathbf{e}_{1N}^T \mathbf{K}_r \mathbf{H} [r_{1-p} \ r_{2-p} \ \cdots \ r_0]^T$$

where  $\phi_k$  is the prediction-induced component mentioned in Chapter 3, and the optimal control vector is given by

$$\begin{aligned}\mathbf{u}^* &= \mathbf{K}_x \mathbf{x}_0 + \mathbf{K}_r \mathbf{k} r_1 + \mathbf{K}_r \mathbf{h} + \mathbf{k}_d d \\ &= \mathbf{K}_x \mathbf{x}_0 + \mathbf{K}_r \mathbf{k} r_1 + \mathbf{K}_r \mathbf{H} \begin{bmatrix} r_{1-p} & r_{2-p} & \cdots & r_0 \end{bmatrix}^T + \mathbf{k}_d d\end{aligned}$$

which yields the control signal

$$u_k = \mathbf{k}_x^T \mathbf{x}_k + k_r r_{k+1} + k_d d + \mathbf{k}_r^T \begin{bmatrix} r_{k+1-p} & r_{k+2-p} & \cdots & r_k \end{bmatrix}^T \quad (4.11)$$

where  $\mathbf{k}_r^T \in \mathbf{R}^{1 \times p}$  is given by  $\mathbf{k}_r^T = \mathbf{e}_{1_N}^T \mathbf{K}_r \mathbf{H}$  and the remaining components are as defined previously in Eqs. (3.41)-(3.43) with  $\mathbf{k}$  as defined in Eq. (4.9). For the case  $p = 0$ , the last term of Eq. (4.11) does not exist. Note that in the unconstrained case, the parameterization of  $\hat{\mathbf{r}}$  by  $r_1$  is of no particular use. The above is provided only for consistency. Alternatively, the optimal control vector could simply be written as

$$\mathbf{u}^* = \mathbf{K}_x \mathbf{x}_0 + \mathbf{K}_r \hat{\mathbf{r}} + \mathbf{k}_d d \quad (4.12)$$

where the elements of  $\hat{\mathbf{r}}$  are defined in Eq. (4.8). It follows then, that  $u_k = \mathbf{e}_{1_N}^T \mathbf{u}^*$ .

This poly- $p$  extrapolation scheme yields reasonable approximations, provided that the actual (pilot) reference is relatively smooth. This implies that it may be prudent to prefilter the pilot reference prior to the extrapolation. This issue is discussed further in Section 4.4. The performance of this poly- $p$  extrapolation scheme is demonstrated with some smooth reference signals in the following example.

*Example 4.1.*

Consider the reference signals of Figure 4.2. The base reference signal is a 6 second doublet. The two smooth references, filter 1 and filter 2, are obtained by filtering the base reference with

$$\frac{32}{s^2 + 8s + 32} \quad \text{and} \quad \frac{109}{s^2 + 6s + 109}$$

respectively. The two responses are quite different, but the poly- $p$  extrapolation scheme does a nice job of extrapolating each, as demonstrated in Figure 4.3 where a sampling interval of  $T = 0.01$  sec, a prediction horizon  $N = 10$ , and polynomial order  $p = 2$  are used. Each plot shows an overlay of the loci of  $\hat{r}_n$  from each window, shifted to the right by  $(n-1)T$  seconds. That is, the first trace is given by the locus of the  $\hat{r}_1$ 's from each window, and the next is the locus of  $\hat{r}_2$ 's from each window, but

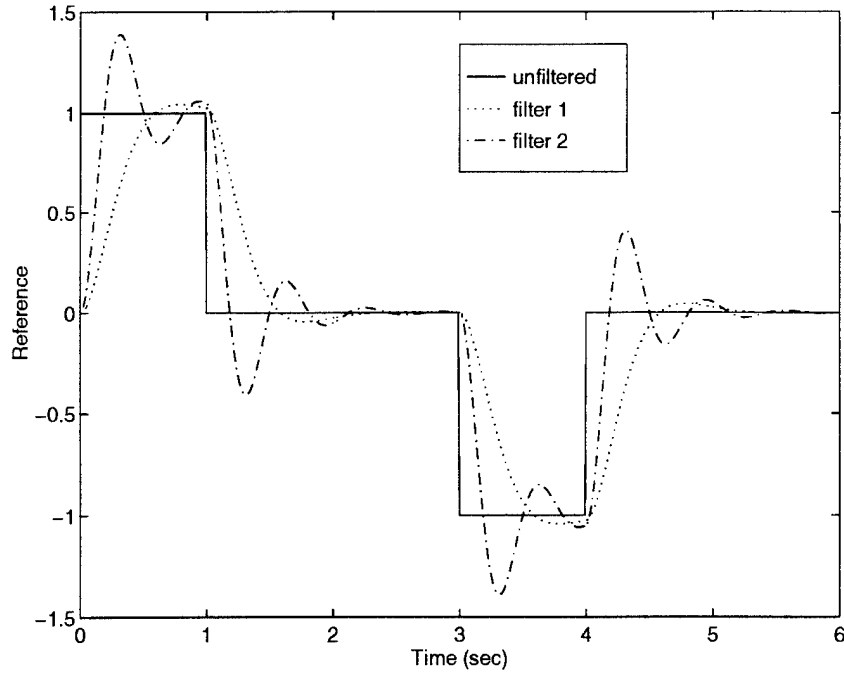


**Figure 4.2.** Poly-2 Test Reference Signals

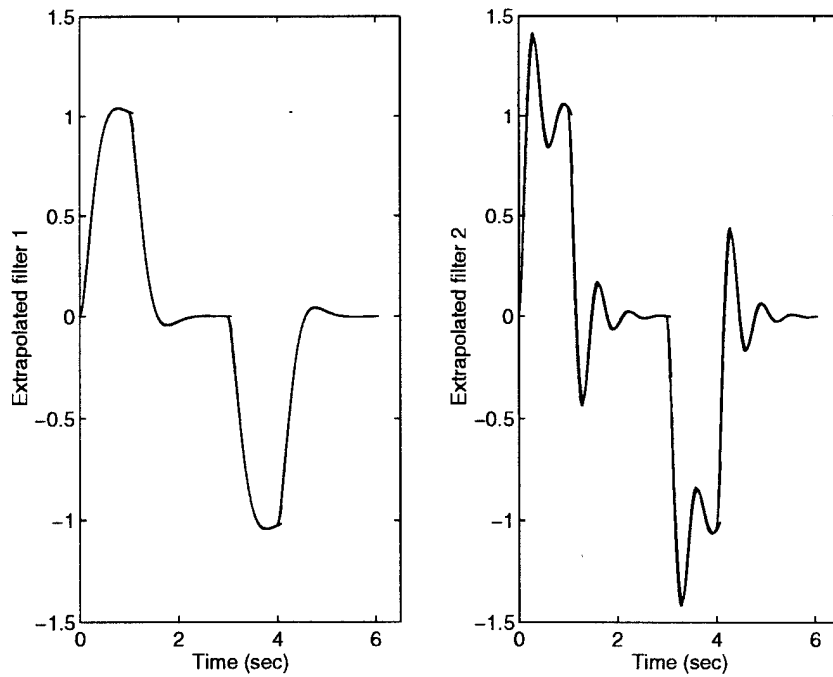


**Figure 4.3.** Poly-2 Extrapolation Test Results

shifted to the right by one time step. Every locus of  $\hat{r}_n$  points is shown for  $n = 1, \dots, N=10$ , with each locus shifted  $n-1$  time steps to the right. Recall that  $\hat{r}_1=r_1$ , thus the locus of  $\hat{r}_1$ 's is simply the

original reference signal shown in Figure 4.2. Hence, the accuracy of the predictions is apparent since the actual reference is included inside the tightly packed responses. Of course, the maximum width (error) of the locus of plots is  $NT$  seconds, viz., 0.1 s in this case. ■

### 4.3 Stage 2 - Determining a Feasible Reference Vector

In this section the extrapolated reference vector  $\hat{\mathbf{r}}$  is modified into a feasible reference vector  $\mathbf{r}'$  expressed linearly in  $r'_1$  which is as of yet unknown. During the constraint enforcement phase,  $r'_1$  is determined such that the resultant reference vector satisfies the prescribed feasibility criteria. The exact meaning of the term feasible depends on the particular saturation mitigation strategy, and is discussed in Chapter 5.

*4.3.1 Strategy: Poly- $p$  + Poly- $p'$ .* According to this strategy, a  $p'$ -th order polynomial fit is considered for the second stage. Since  $r'_1$  is assumed known, only  $p'$  points of the polynomial solution need to be explicitly stipulated. One of these points will be  $\hat{r}_N$ , viz., set  $r'_N = \hat{r}_N$ , so that the feasible vector  $\mathbf{r}'$  still ends up at the same place as the pilot demanded  $\hat{\mathbf{r}}$ . In extreme cases, it may be prudent to modify this endpoint. The remaining  $p' - 1$  polynomial values needed to determine the polynomial coefficients consist of previously applied reference commands, i.e., the corresponding  $r'_1$  from the previous  $p' - 1$  windows.

This method is similar to the extrapolation of stage 1, in the sense that each  $r'_n$  satisfies a polynomial equation of the form

$$r'_n = a'_0 + a'_1 n + a'_2 n^2 + \cdots + a'_p n^{p'}, \quad n = 1, 2, \dots, N$$

The poly- $p$  + poly- $p'$  prediction strategy is illustrated in Figure 4.4. The reference signals  $r_1$  and  $r_{1-p}, \dots, r_0$ , are known. They represent the current and  $p$  previous values of the pilot supplied (desired) reference, viz.,  $r_{k+1}$  and  $r_{k-p+1}, \dots, r_k$  respectively. That is, in the  $k$ -th window  $r_{k+1}$  is the specified reference value and is referred to as  $r_1$ ,  $r_{k+2}$  is referred to as  $r_2$ ,

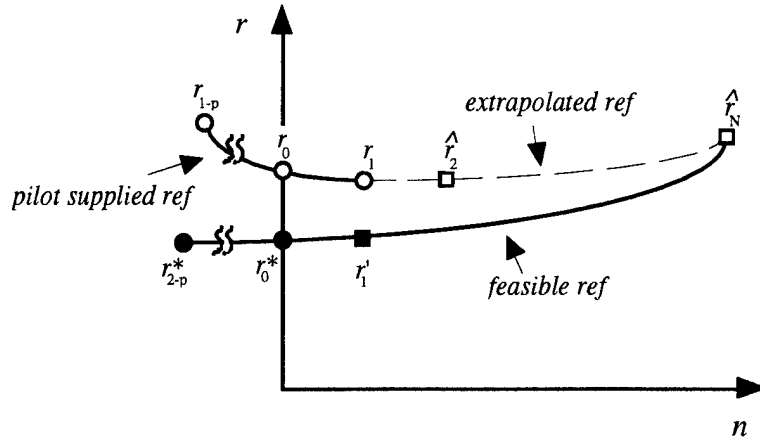


**Figure 4.4.** Poly- $p$  + Poly- $p'$  Prediction of the Reference

etc. Recall that  $r_{k+1}$  is known at time  $k$ , and  $u_k$  is used to drive the output  $y_{k+1}$  toward the desired value  $r_{k+1}$ . The  $r_{2-p}^*, \dots, r_0^*$  terms are also known. They represent the feasible reference values determined from previous windows, i.e.,  $r_{1-n}^* = r_1^*$  from the  $n$ -th previous window. Observe that if the constraints are never encountered, i.e.,  $r_1^* = r_1$  in every window, and if  $p = p'$ , then  $\mathbf{r}' = \hat{\mathbf{r}}$  holds.

The  $a_i'$  's are determined by solving the linear system

$$\begin{bmatrix} r_{2-p'}^* \\ \vdots \\ r_0^* \\ \hat{r}_N \\ r_1' \end{bmatrix} = \mathbf{T}\mathbf{a}' = \begin{bmatrix} 1 & 2-p' & (2-p')^2 & \cdots & (2-p')^{p'} \\ \vdots & \vdots & \vdots & \ddots & \vdots \\ 1 & 0 & 0 & \cdots & 0 \\ 1 & N & N^2 & \cdots & N^{p'} \\ 1 & 1 & 1 & \cdots & 1 \end{bmatrix} \begin{bmatrix} a_0' \\ a_1' \\ a_2' \\ \vdots \\ a_{p'}' \end{bmatrix} \quad (4.13)$$

The first  $p'-1$  terms on the left side of Eq. (4.13) are the previously applied feasible reference values, which appear only for  $p' > 1$ . The  $p'$ -th term corresponds to  $\hat{r}_N$  and is included only when  $p' \geq 1$ . The  $p'+1$ -th term appears for all  $p' \geq 0$ . That is, for  $p' = 1$ , Eq. (4.13) reduces to



$$\begin{bmatrix} \hat{r}_N \\ r'_1 \end{bmatrix}^T = \begin{bmatrix} 1 & N \\ 1 & 1 \end{bmatrix} \begin{bmatrix} a'_0 \\ a'_1 \end{bmatrix}$$

and for  $p' = 0$ ,

$$r'_1 = a'_0$$

Let

$$\mathbf{T}^{-1} = \begin{bmatrix} 1 & 2-p' & (2-p')^2 & \cdots & (2-p')^{p'} \\ \vdots & \vdots & \vdots & \ddots & \vdots \\ 1 & 0 & 0 & \cdots & 0 \\ 1 & N & N^2 & \cdots & N^{p'} \\ 1 & 1 & 1 & \cdots & 1 \end{bmatrix}^{-1} \triangleq \begin{bmatrix} \gamma_{1,1} & \gamma_{1,2} & \cdots & \gamma_{1,p'+1} \\ \gamma_{2,1} & \gamma_{2,2} & \cdots & \gamma_{2,p'+1} \\ \vdots & \vdots & \ddots & \vdots \\ \gamma_{p'+1,1} & \gamma_{p'+1,2} & \cdots & \gamma_{p'+1,p'+1} \end{bmatrix}$$

Then,

$$\mathbf{a}' = \mathbf{T}^{-1} \begin{bmatrix} r_{2-p'}^* & \cdots & r_0^* & \hat{r}_N & r'_1 \end{bmatrix}^T$$

Looking at the polynomial coefficients individually,

$$\begin{aligned} a'_{i-1} &= \sum_{j=1}^{p'-1} \gamma_{i,j} r_{j-p'+1}^* + \gamma_{i,p'} \hat{r}_N + \gamma_{i,p'+1} r'_1 \quad i = 1, 2, \dots, p+1 \\ &= \gamma_{i,p'+1} r'_1 + \sum_{j=1}^{p'-1} \gamma_{i,j} r_{j-p'+1}^* + \gamma_{i,p'} \sum_{j=1}^{p+1} \left[ \left( \sum_{m=0}^p N^m \varepsilon_{m+1,j} \right) r_{j-p} \right] \end{aligned}$$

Thus, the components of the feasible reference vector can be written in the form

$$\begin{aligned} r'_n &= \sum_{i=1}^{p'+1} a'_{i-1} n^{i-1} \\ &= \sum_{i=1}^{p'+1} \left\{ \left( \gamma_{i,p'+1} r'_1 + \sum_{j=1}^{p'-1} \gamma_{i,j} r_{j-p'+1}^* + \gamma_{i,p'} \sum_{j=1}^{p+1} \left[ \left( \sum_{m=0}^p N^m \varepsilon_{m+1,j} \right) r_{j-p} \right] \right) n^{i-1} \right\} \\ &= \left( \sum_{i=1}^{p'+1} \gamma_{i,p'+1} n^{i-1} \right) r'_1 + \sum_{j=1}^{p'-1} \left( \sum_{i=1}^{p'+1} \gamma_{i,j} n^{i-1} \right) r_{j-p'+1}^* + \sum_{j=1}^{p+1} \left[ \sum_{i=1}^{p'+1} \gamma_{i,p'} n^{i-1} \sum_{m=0}^p N^m \varepsilon_{m+1,j} \right] r_{j-p} \\ &= k_n r'_1 + \sum_{j=1}^{p'-1} c'_{n,j} r_{j-p'+1}^* + \sum_{j=1}^{p+1} d'_{n,j} r_{j-p} \\ &= k_n r'_1 + h_n \end{aligned}$$

where the  $k_n$ ,  $c'_{n,j}$  and  $d'_{n,j}$  are constants. Thus, the feasible reference sequence can be written in the desired form of Eq. (4.2), where the  $k_n$  are constants given by

$$k_n = \sum_{i=1}^{p'+1} \gamma_{i,p'+1} n^{i-1} \quad (4.14)$$

and the  $h_n = h_n(r_{2-p'}^*, \dots, r_0^*, r_{1-p}, \dots, r_1)$  are given by

$$h_n = \sum_{j=1}^{p'-1} c'_{n,j} r_{j-p'+1}^* + \sum_{j=1}^{p+1} d'_{n,j} r_{j-p}$$

where

$$c'_{n,j} = \sum_{i=1}^{p'+1} \gamma_{i,j} n^{i-1} \quad (4.15)$$

and

$$d'_{n,j} = \sum_{i=1}^{p'+1} \gamma_{i,p} n^{i-1} \sum_{m=0}^p N^m \epsilon_{m+1,j} \quad (4.16)$$

The  $h_n$ 's depend only on the past and present values of the desired and applied (feasible) references, thus, the coefficients vector  $\mathbf{h}$  is also constant within each window. Hence, as it relates to the required optimization,  $\mathbf{r}'$  is explicitly known as a linear function of  $r'_1$ . Note that  $k_1 = 1$  and  $h_1 = 0$ . Explicit off-line evaluations of the reference vector coefficients for the poly- $p$  + poly- $p'$  prediction strategy are provided in Tables 4.2 and 4.3. Note that for the case  $p' = 0$ ,  $r'_n = r'_1$  regardless of  $p$ , i.e.,  $k_n = 1$  and  $h_n = 0$ .

**Table 4.2.** Explicit Poly- $p$  + Poly- $p'$  Coefficients,  $p'=1$

$p$	$k_n$	$h_n$
0	$\frac{n-N}{1-N}$	$\frac{1-n}{1-N} r_1$
1	$\frac{n-N}{1-N}$	$(1-n)(1-N)r_0 + \frac{N(1-n)}{1-N} r_1$
2	$\frac{n-N}{1-N}$	$\frac{N}{2}(n-1)r_{-1} + (1-n)(1+N)r_0 + \frac{1}{2} \frac{N(1-n)(N+1)}{1-N} r_1$

**Table 4.3.** Explicit Poly- $p$  + Poly- $p'$  Coefficients,  $p'=2$

$p$	$k_n$	$h_n$
0	$\frac{n(n-N)}{1-N}$	$\left[ \frac{N(1-n)+n(n-1)}{N} \right] r_0^* + \frac{n(1-n)}{N(1-N)} r_1$
1	$\frac{n(n-N)}{1-N}$	$\left[ \frac{N(1-n)+n(n-1)}{N} \right] r_0^* + \frac{n(1-n)}{N} r_0 + \frac{n(1-n)}{(1-N)} r_1$
2	$\frac{n(n-N)}{1-N}$	$\left[ \frac{N(1-n)+n(n-1)}{N} \right] r_0^* + \frac{1}{2} n(n-1) r_{-1} + \frac{n(1-n)}{N(1+N)} r_0 + \frac{1}{2} \frac{n(1-n)(N+1)}{(1-N)} r_1$

Depending on the feasibility criteria, the end point  $\hat{r}_N$  may be deemed unacceptable. For example, it may be required that all  $r'_n$ ,  $n=1, \dots, N$  be statically admissible. In this case, a modified end point  $\tilde{r}_N$  which is acceptable may be selected. Thus, the elements of the feasible reference vector are given by

$$r'_n = k_n r'_1 + \sum_{j=1}^{p'-1} c'_{n,j} r_{j-p'+1}^* + d'_n \tilde{r}_N$$

where the  $k_n$  and  $c'_{j,n}$  are as in Eqs. (4.14) and (4.15), respectively, and the  $d'_n$  are given by

$$d'_n = \sum_{i=1}^{p'+1} \gamma_{i,p} n^{i-1} \quad (4.17)$$

For the case of poly- $p$  + poly- $p'$  reference prediction, the feasible reference vector  $\mathbf{r}'$  is written in the form  $\mathbf{k}r'_1 + \mathbf{h}$ , where  $\mathbf{k}$  is defined in Eq. (4.14). The component  $\mathbf{h}$  can be written in the form

$$\mathbf{h} = \begin{cases} \mathbf{H}_1 [r_{1-p} & r_{2-p} & \cdots & r_{p+1-p}]^T + \mathbf{H}_2 [r_{2-p'}^* & r_{3-p'}^* & \cdots & r_{p'-p'}^*]^T, & p' > 1 \\ \mathbf{H}_1 [r_{1-p} & r_{2-p} & \cdots & r_{p+1-p}]^T, & p' = 1 \\ \mathbf{0}_{N \times 1}, & p' = 0 \end{cases}$$

where  $\mathbf{H}_1 \in \mathbf{R}^{N \times p+1}$  and  $\mathbf{H}_2 \in \mathbf{R}^{N \times p'-1}$  and with elements

$$\mathbf{H}_1(i, j) = d'_{n=i, j}, \quad \mathbf{H}_2(i, j) = c'_{n=i, j}$$

where the  $d'_{n,j}$  and  $c'_{n,j}$  are defined in Eqs. (4.16) and (4.15) respectively. Clearly,  $\mathbf{H}_2$  exists only for  $p' > 1$ , and  $\mathbf{H}_1$  exists only for  $p' > 0$ , since for  $p' = 0$ ,  $\mathbf{r}'$  depends only on  $r'_1$  (and thus  $\mathbf{h} = 0$ ), and for  $p' = 1$ ,  $\mathbf{r}'$  depends only on  $r'_1$  and  $\hat{r}_N$ . The resultant control signal is thus

$$u_k = \begin{cases} \mathbf{k}_x^T \mathbf{x}_k + k_r r'_{k+1} + k_d d + \mathbf{k}_r^T [r_{k+1-p} \cdots r_{k+1}]^T + \mathbf{k}_{r^*}^T [r_{k+2-p'}^* \cdots r_k^*]^T, & p' > 1 \\ \mathbf{k}_x^T \mathbf{x}_k + k_r r'_{k+1} + k_d d + \mathbf{k}_r^T [r_{k+1-p} \cdots r_{k+1}]^T, & p' = 1 \\ \mathbf{k}_x^T \mathbf{x}_k + k_r r'_{k+1} + k_d d, & p' = 0 \end{cases}$$

where  $\mathbf{k}_r^T = \mathbf{e}_{1_N}^T \mathbf{K}_r \mathbf{H}_1$ ,  $\mathbf{k}_{r^*}^T = \mathbf{e}_{1_N}^T \mathbf{K}_r \mathbf{H}_2$  and the remaining components are as previously defined in Eqs. (3.41)-(3.43) with  $\mathbf{k}$  as defined in Eq. (4.14).

**4.3.2 Strategy: Poly- $p$  + Asymptotic Convergence.** This method consists of using a first-order filter to propagate the elements of  $\mathbf{r}'$  from  $r'_1$  to  $\hat{r}_N$ , as illustrated in Figure 4.5.

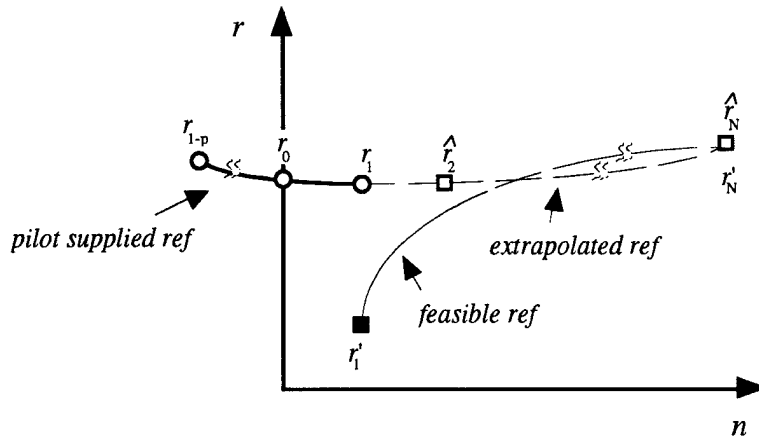


**Figure 4.5.** Poly- $p$  + Asymptotic Convergence

Specifically,  $\mathbf{r}'$  is generated from the equation

$$r'_{n+1} = k_a r'_n + (1 - k_a) \hat{r}_N, \quad n = 1, \dots, N-1, \quad 0 \leq k_a \leq 1$$

Thus, the  $r'_n$ 's asymptotically approach  $\hat{r}_N$ . The filter constant  $k_a$  is a tuning parameter and can be selected accordingly such that  $r'_N$  is arbitrarily close to  $\hat{r}_N$ . Furthermore, the resultant  $\mathbf{r}'$  can be represented in the desired form  $\mathbf{r}' = \mathbf{k}r'_1 + \mathbf{h}$ . Specifically, the elements of  $\mathbf{k}$  are given by

$$k_n = k_a^{n-1}, \quad n = 1, \dots, N \quad (4.18)$$

and the elements of  $\mathbf{h}$  are given by

$$\begin{aligned} h_n &= \hat{r}_N (1 - k_a) \sum_{j=0}^{n-2} k_a^j \\ &= \hat{r}_N (1 - k_a^{n-1}) \quad (0 \leq k_a \leq 1) \end{aligned} \quad (4.19)$$

Note that  $k_1 = 1$ , and  $h_1 = 0$ , and observe that  $\mathbf{h} = \hat{r}_N \mathbf{h}_0$ , where  $\mathbf{h}_0$  is a constant. Explicit reference vector coefficients for  $p = 0, 1, 2$  using the poly- $p$  + asymptotic convergence prediction strategy are provided in Table 4.4.

**Table 4.4.** Explicit Poly- $p$  + Asymptotic Convergence Coefficients

$p$	$k_n$	$h_n$
0	$k_a^{n-1}$	$(1 - k_a^{n-1})r_1$
1	$k_a^{n-1}$	$(1 - k_a^{n-1})[(1 - N)r_0 + Nr_1]$
2	$k_a^{n-1}$	$(1 - k_a^{n-1})\left[\frac{1}{2}(N^2 - N)r_{-1} + (1 - N^2)r_0 + \frac{1}{2}(N^2 + N)r_1\right]$

If the value  $\hat{r}_N$  is deemed not to be an acceptable endpoint, this scheme can also be modified such that the asymptotic convergence is not to  $\hat{r}_N$ , but rather the closest feasible value to  $\hat{r}_N$ ,  $\tilde{r}_N$ . For example, it could be required that this endpoint be statically admissible. This concept is illustrated in Figure 4.6. The equations corresponding to this approach are the same as before, except that  $\hat{r}_N$  is replaced with  $\tilde{r}_N$ .

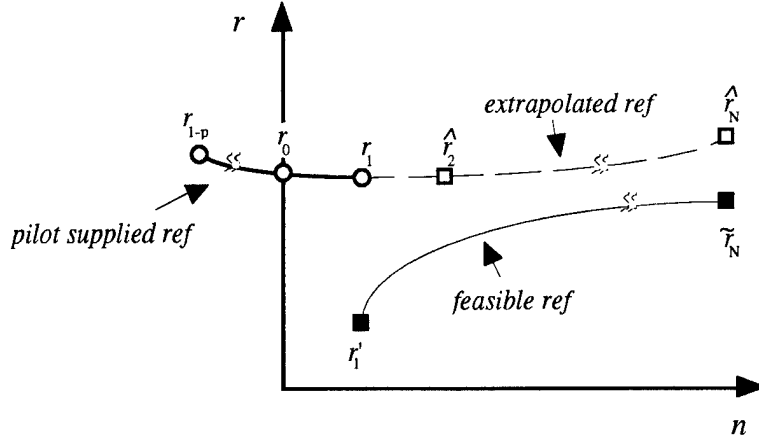


**Figure 4.6.** Modified Poly- $p$  + Asymptotic Convergence

In this case, the feasible reference vector is again written  $\mathbf{k}r'_1 + \mathbf{h}$ , but where the elements of  $\mathbf{k}$  are as defined in Eq. (4.18). For the unmodified strategy, the  $\mathbf{h}$  component can be written

$$\mathbf{h} = \mathbf{H} \begin{bmatrix} r_{1-p} & r_{2-p} & \cdots & r_{p+1-p} \end{bmatrix}^T$$

where  $\mathbf{H} \in \mathbf{R}^{N \times p+1}$  and has elements

$$\mathbf{H}(i, j) = (1 - k_a^{i-1}) c_{n=N, j}$$

where the  $c_{n, j}$  are as defined in Eq. (4.7). Hence, the prediction-induced component is

$$\phi_k = \mathbf{e}_{1N}^T \mathbf{K}_r \mathbf{H} \begin{bmatrix} r_{1-p} & r_{2-p} & \cdots & r_1 \end{bmatrix}^T$$

and the feasible control vector is given by

$$\mathbf{u}' = \mathbf{K}_x \mathbf{x}_0 + \mathbf{K}_r \mathbf{k} r'_1 + \mathbf{K}_r \mathbf{H} \begin{bmatrix} r_{1-p} & r_{2-p} & \cdots & r_1 \end{bmatrix}^T + \mathbf{k}_d d$$

which yields the feasible control signal

$$u_k = \mathbf{k}_x^T \mathbf{x}_k + k_r r'_{k+1} + \mathbf{k}_r^T \begin{bmatrix} r_{k+1-p} & r_{k+2-p} & \cdots & r_{k+1} \end{bmatrix}^T + k_d d$$

where  $\mathbf{k}_x^T$ ,  $k_r$ , and  $k_d$  are as in Eqs. (3.41)-(3.43) with  $\mathbf{k}$  determined by Eq. (4.18), and

$$\mathbf{k}_r^T = \mathbf{e}_{1N}^T \mathbf{K}_r \mathbf{H}$$

4.3.3 *Strategy: Poly- $p$  + parallel.* This strategy is the simplest of all proposed. Specifically,  $\mathbf{r}' = \hat{\mathbf{r}} - \mathbf{\Delta}$ , where  $\mathbf{\Delta}$  is a constant vector with elements  $\Delta_i = \Delta = \hat{r}_1 - r'_1$ . This parallel translation concept is illustrated in Figure 4.7.

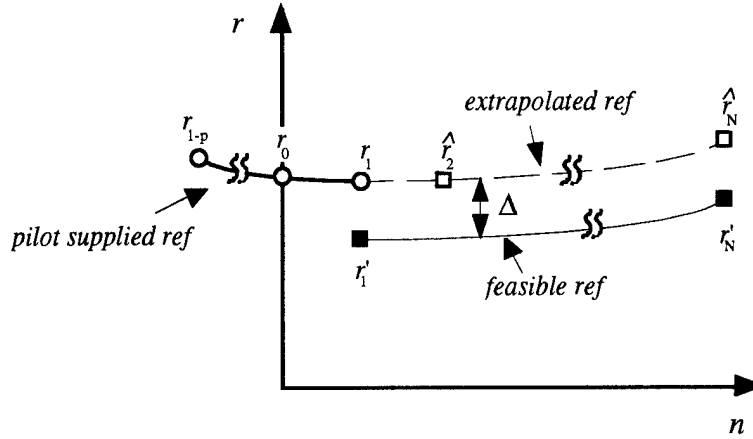


**Figure 4.7.** Poly- $p$  + Parallel Prediction of the Reference

In this case,  $r'_n = \hat{r}_n - \Delta$ ,  $n = 1, 2, \dots, N$ , and thus

$$\begin{aligned}
 r'_n &= \left( \sum_{j=1}^{p+1} c_{n,j} r_{j-p} \right) - \Delta \\
 &= \sum_{j=1}^{p+1} c_{n,j} r_{j-p} - r_1 + r'_1 \\
 &= r'_1 + \left( \sum_{j=1}^{p+1} c_{n,j} r_{j-p} - r_1 \right) \\
 &= k_n r'_1 + h_n
 \end{aligned}$$

Hence, as it relates to the required optimization,  $\mathbf{r}'$  is again explicitly known as a linear function of  $r'_1$ , where  $k_n = 1$ , and

$$h_n = h_n(r_{1-p}, \dots, r_1) = \sum_{j=1}^{p+1} c_{n,j} r_{j-p} - r_1 \quad (4.20)$$

where the  $c_{j,n}$  are defined as in Eq. (4.7). Explicit reference vector coefficients for  $p = 0, 1, 2$  using the poly- $p$  + parallel prediction method are given in Table 4.5.

**Table 4.5.** Explicit Poly- $p$  + Parallel Coefficients

$p$	$k_n$	$h_n$
0	1	0
1	1	$(n+1)r_0 + (n-1)r_1$
2	1	$0.5(n^2 - n)r_{-1} + (1 - n^2)r_0 + 0.5(n^2 + n - 2)r_1$

In this case, the feasible reference vector is given by  $\mathbf{r}' = \mathbf{k}r'_1 + \mathbf{h}$  where  $\mathbf{k} = \mathbf{1}_N$ , and  $\mathbf{h}$  can be written in the form

$$\mathbf{h} = \mathbf{H} \begin{bmatrix} r_{1-p} & \cdots & r_0 \end{bmatrix}^T$$

where  $\mathbf{H} \in \mathbf{R}^{N \times p+1}$  has elements  $\mathbf{H}(i,j)$  defined by

$$\mathbf{H}(i,j) = \begin{cases} c_{n,j}, & j \neq p+1 \\ c_{n,j} - 1, & j = p+1 \end{cases} \quad (4.21)$$

where the  $c_{n,j}$  are as defined in Eq. (4.7). Hence, the feasible control vector is given by

$$\mathbf{u}' = \mathbf{K}_x \mathbf{x}_0 + \mathbf{K}_r \mathbf{k} r'_1 + \mathbf{K}_r \mathbf{H}_{PL} \begin{bmatrix} r_{1-p} & r_{2-p} & \cdots & r_1 \end{bmatrix}^T$$

and

$$\phi_k = \mathbf{e}_{1_N}^T \mathbf{K}_r \mathbf{H}_{PL} \begin{bmatrix} r_{k+1-p} & r_{k+2-p} & \cdots & r_{k+1} \end{bmatrix}^T$$

It follows then, that the feasible control signal is given by

$$u_k = \mathbf{k}_x^T \mathbf{x}_k + k_r r'_{k+1} + \mathbf{k}_r^T \begin{bmatrix} r_{k+1-p} & \cdots & r_k \end{bmatrix}^T + k_d d$$

where  $\mathbf{k}_x^T$ ,  $k_r$ , and  $k_d$  are given by Eqs. (3.41)-(3.43) with  $\mathbf{k} = \mathbf{1}_N$ , and  $\mathbf{k}_r^T = \mathbf{e}_{1_N}^T \mathbf{K}_r \mathbf{H}$ ,

where  $\mathbf{H}$  is defined by Eq. (4.21).



#### 4.4 Reference Signals with Corners and Jumps

Polynomial extrapolation is not well suited to reference signals which contain corners and/or jumps, since it requires high order polynomials to come close to an accurate representation, and a perfect fit cannot in general be achieved. Linear extrapolation ( $p = 1$ ) is less sensitive to these problems, but is also generally less accurate than say parabolic extrapolation. Obviously, and as observed in simulations, the higher the order of the polynomial the greater the impact of the nonsmoothness of the pilot supplied reference signal. Thus, in a predictive control strategy it is wise to prefilter the pilot's reference signal prior to the extrapolation. First-order prefilters of the form

$$\frac{a}{s + a}$$

do a nice job of rounding out corners, e.g., as in a step or pulse type reference, but second-order prefilters of the form

$$\frac{\omega_n^2}{s^2 + 2\zeta\omega_n s + \omega_n^2}$$

may prove even more useful, since they additionally prevent instantaneous change in the first derivative of the reference, which is another source of corners. This, in turn, improves the performance of high-order reference extrapolation algorithms.

The performance of poly-2 extrapolation on smooth reference signals is considered in Example 4.1. Now, consider for example, the reference signal used in Example 3.1. This reference contains several corners. The trajectories for each  $\hat{r}_n$ ,  $n = 1, \dots, N$  are superimposed (and appropriately shifted) in Figure 4.8, using a poly-2 extrapolation with a sample interval  $T = 0.01$  sec and a planning horizon of  $N = 10$ . Note that at the corners, large spikes appear due to the inability of the second-order polynomial to fit these areas. It should be noted however, that these unidirectional spikes may not be as significant as they appear. Recall that this same method of extrapolation is used in Example 3.1, but with a

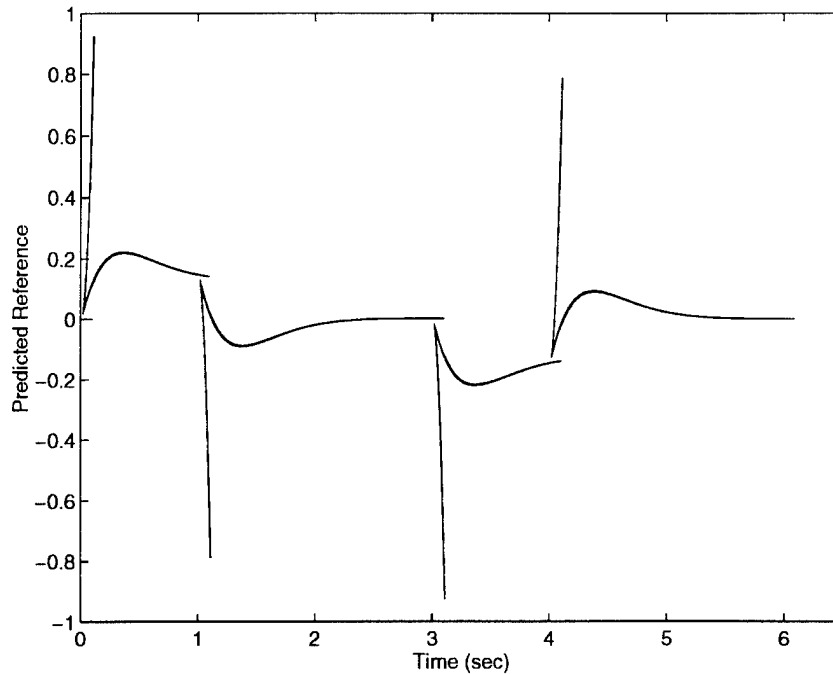


**Figure 4.8.** Parabolic Extrapolation of a Reference with Corners

longer prediction horizon (which exacerbates this phenomenon), yet the control system output is quite good. It is important to note that only  $\hat{r}_1 = r_1$  (which is always error free) is actually injected into the system. Thus, the system never tries to explicitly track these errors, but the optimization is based on the assumption that these errors are what is to come in the future. Since the spikes are always in the right direction, the result is perhaps a more aggressive approach toward  $r_1$  than actually necessary. When higher order polynomials are used in the extrapolation, spikes occur in both directions, and the peak magnitude grows with the polynomial order. Thus, it is believed that the maximum polynomial order used for extrapolation purposes should be 2, i.e., parabolic extrapolation. These spikes are eliminated when linear ( $p = 1$ ) extrapolation is used, as shown in Figure 4.9.

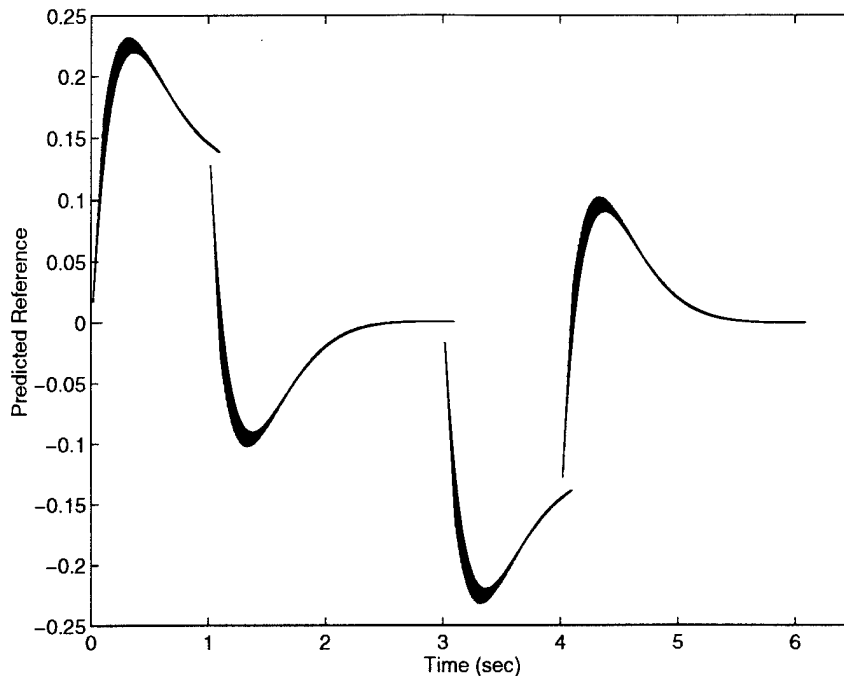


**Figure 4.9.** Linear Extrapolation of a Reference with Corners

#### 4.5 Summary

Several two-stage reference prediction strategies have been devised which can be used in support of the LQT methodology discussed in Chapter 3. The first stage entails a polynomial extrapolation of the pilot demanded reference signal, based on the currently available and previously demanded pilot input signals. A  $p$ -th order polynomial extrapolation has been shown to work well with smooth reference signals. This method is, however, less successful for predicting reference signals which contain corners or large jumps. Thus, prefiltering the reference signal (particularly with a second-order filter) greatly enhances the accuracy of the prediction.

Each of the second stage interpolation schemes, viz.,  $p'$ -th order polynomial interpolation, asymptotic convergence, and parallel, can be used with a receding horizon control strategy to express a feasible reference vector linearly in terms of the current feasible value  $r_1'$ . For each proposed strategy, the explicit LQT control algorithms are

derived. Unconstrained simulation examples (for selected parameter values) utilizing each of these strategies are provided in the appendix. These unconstrained simulation examples are important, because they represent the small-signal system performance when the given strategy is employed. However, final judgment on the performance of each technique should be reserved until after the constrained simulation results are examined as well.

Finally, the closed form and linear representation  $\mathbf{r}' = \mathbf{k}r_1' + \mathbf{h}$  attained by each of the investigated prediction strategies opens the door to a number of relatively simple constraint mitigation (saturation avoidance) strategies which are discussed in Chapter 5. Indeed, the concise representation and seamless integration into the LQT framework afforded by the polynomial extrapolation methods is the primary motivator for using polynomial prediction methods. An investigation into the application of more stable and accurate extrapolation methods to the LQT methodology would be a worthwhile endeavor.

## V. Mitigation of the Hard Constraints Effects

### 5.1 Overview

Chapters 3 and 4 have focused on the development of explicit control law formulations in terms of the "as of yet unknown" feasible reference value at time now  $r_1'$  which is then used to parameterize a *feasible* reference vector  $\mathbf{r}'$  for the duration  $N$  of the optimization horizon. This chapter is devoted to an investigation into the pertinent actuator saturation issues affecting the selection of  $r_1'$ , and the selection process itself, viz., explicitly obtaining the feasibility criteria alluded to in previous chapters. First, a simple, scalar control system example is investigated which clearly illustrates the critical tracking and stability aspects of the constrained actuator tracking control problem. Subsequently, a constraint mitigating control strategy is developed, and examined via extensive simulation. In each case, the feasibility criteria are specified and explicit closed form algorithms for the computation of  $r_1'$ , and thus, the derivation of the tracking control law, are developed. The two layers controller arrived at is nonlinear, where  $r_1'$  is determined such that the downstream actuator bounds are not violated and the control signal is then determined by  $r_1'$  such that a quadratic tracking performance functional is minimized. Finally, attention is given to ascertaining the BIBO stability of the ensuing nonlinear control system.

### 5.2 A "Simple" Example

A simple control constrained system is analyzed in order to demonstrate the critical tracking and stability aspects of the constrained tracking control problem. The continuous-time scalar plant with an amplitude constrained control is given by

$$\dot{x} = ax + b \cdot \text{sat}(u), \quad x(0) = x_0 \quad (5.1)$$

where the nonlinear  $\text{sat}(u)$  function is

$$\text{sat}(u) = \begin{cases} -1, & -1 < u \\ u, & -1 \leq u \leq 1 \\ 1, & u > 1 \end{cases}$$

Since the case of an open-loop unstable plant is of particular interest, assume  $a > 0$ . A state feedback control law is desired which yields tracking, i.e.  $x \approx r$ , for all  $t > 0$ , for the largest possible set of initial states  $x_0$ , and for "all" exogenous reference signals  $r(t)$ . The simplest continuous-time control law within this framework is of the form

$$u = k_x x + k_r r \quad (5.2)$$

Note that  $u$  is in the familiar form  $\mathbf{C}x + \mathbf{D}r$  (in which closed-loop actuator responses are often characterized), and thus actuator constrained problems relate to the example at hand. The linear control law of Eq. (5.2) combined with the open-loop plant of Eq. (5.1) yields the closed-loop control system whose block diagram is shown in Figure 5.1.

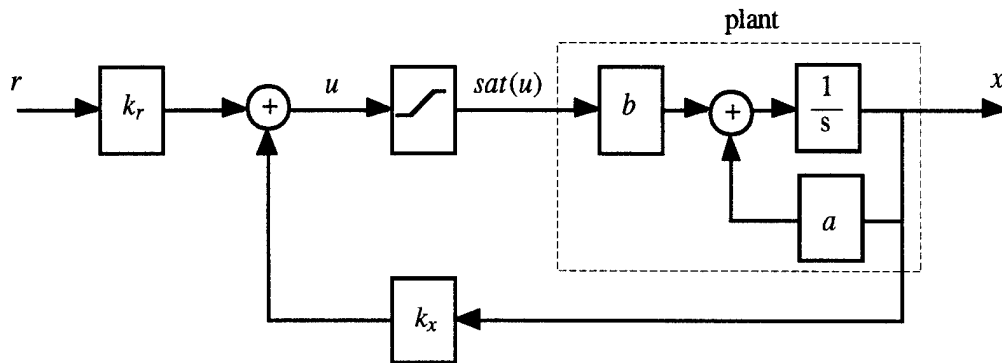


**Figure 5.1.** Closed-loop Control System

An examination of the relevant augmented (two-dimensional) space of  $r$  and  $x$ ,

$$V = R \times X = \left\{ \mathbf{v} \mid \mathbf{v} = \begin{bmatrix} r \\ x \end{bmatrix} \right\}$$

provides insight into the problem. There are several sets with respect to this space which are of importance - refer to Figure 5.2:

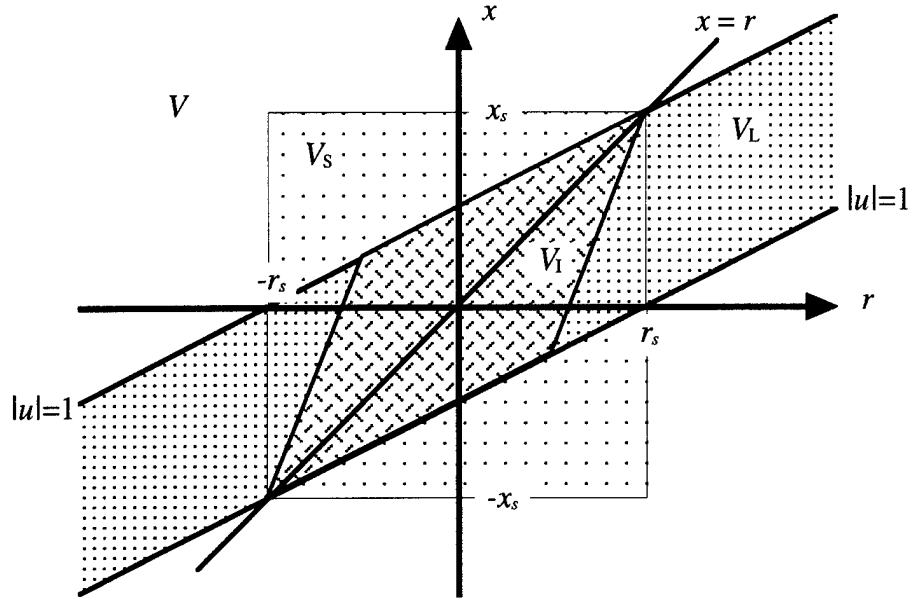


Figure 5.2. Sets of Interest

The set  $V_L$  is determined by the control constraint, and consists of the region of the space  $V$  in which the closed-loop system (Figure 5.1) operates linearly. The set of statically admissible references  $R_s = [-r_s, r_s]$  and the set of statically admissible states  $X_s = [-x_s, x_s]$  can thus be defined, where

$$r_s = \left| \frac{a + bk_x}{k_r a} \right|$$

and

$$x_s = \left| \frac{b}{a} \right|$$

The rectangular set  $V_S$  represents the portion of the space which contains statically admissible reference values and states, i.e.,  $V_S = R_s \times X_s$ , where each  $r \in R_s$  yields an equilibrium  $x_{ss} \in X_s$ , and such that the equilibrium control  $u_{ss} = k_x x_{ss} + k_r r$  does not violate

the control constraint - note however that this does NOT imply that every  $[r, x]^T \in V_S$  is an equilibrium point of the system. For example, for a tracking system which yields zero steady-state error, only the points which are contained in  $V_L$  and lie on the line  $x = r$  are equilibrium points. Finally, there exists an invariant set  $V_I \subset (V_L \cap V_S)$  such that for any constant  $r = r_\alpha$  and  $[r_\alpha, x_0]^T \in V_I$ , all subsequent  $[r_\alpha, x]^T$  resulting from the closed-loop dynamics is also inside  $V_I$ . Here,  $x$  is the response of the linear system of Eq. (5.1). In this simple (scalar) case,  $V_I = V_S \cap V_L$ , but this does not necessarily hold true for higher-order systems. For example, a second-order system whose constrained quantity of interest is underdamped would have a  $V_I$  of the general shape shown in Figure 5.2, since any fixed value of  $r$  yields a percentage overshoot in  $x$ .

The following interesting observations can be made. First of all, there exist trajectories  $\mathbf{v}(t) \in V_L$  which are unbounded; that is,  $r$  and  $x$  can both grow without bound, without violating the control constraints. Thus, although the closed-loop linear system is BIBO stable, saturation mitigation strategies which solely modify the incoming reference in order to avoid saturation do not necessarily yield a BIBO stable nonlinear control system. Another observation is that should the system ever achieve the valid, yet very special linear equilibrium point  $\mathbf{v}_s = [r_s, x_s]^T$ , the system becomes "stuck": The only two options after such an equilibrium state is reached is to stay there forever, or diverge. Additionally, for any  $x \in \text{int}(X_s)$ , i.e.,  $-x_s < x < x_s$ , there always exists an  $r$  which can bring the state toward the origin without violating the constraints. Conversely, for any  $|x| \geq x_s$ , the state can never be brought back to the origin. (If the open-loop plant were stable, recovery from this state of affairs would be possible, but would entail violations of the control constraints and periods of nonlinear operation.) This goes back to the previous observation regarding "open-loop" operation during periods of actuator saturation. This problem just described is illustrated in the state diagram shown in Figure 5.3. Note: In this particular figure it is



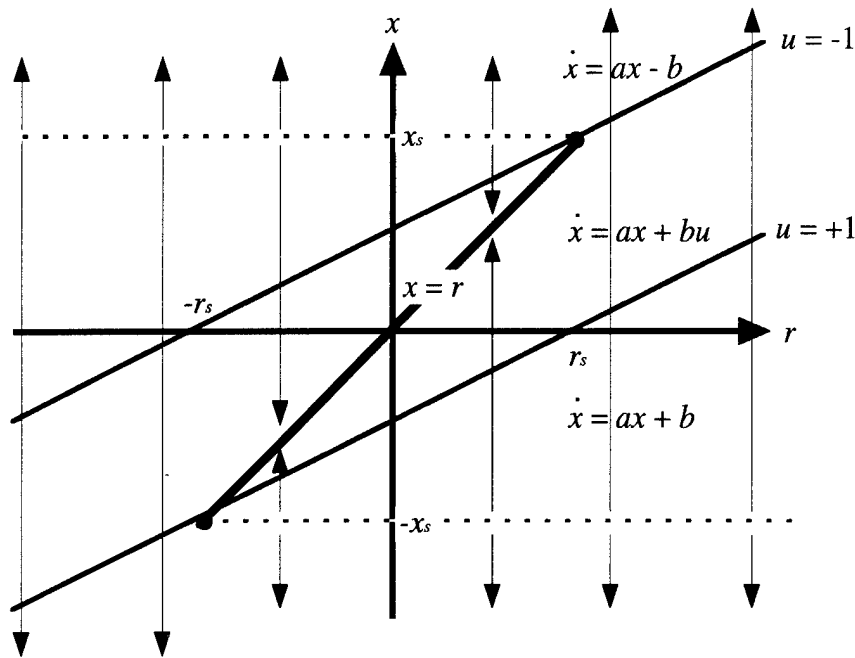


**Figure 5.3.** Stable and Unstable Equilibria ( $a > 0, b > 0, k_r > 0, k_x < 0$ )

assumed (without loss of generality) that  $k_x < 0, b > 0$ , and  $k_r > 0$ . Since unstable open-loop plants ( $a > 0$ ) are being considered, these assumptions are consistent with a stable closed-loop system which yields zero steady-state error. The sign of  $\dot{x}$  is indicated by arrows. It is apparent from Figure 5.3 that the closed-loop system has stable equilibrium points on  $int(X_s) = (-x_s, x_s)$ , viz.,  $x = r$ , and unstable equilibria at the endpoints  $x = \pm x_s$ . Thus, a successful saturation mitigation strategy (SMS) cannot allow  $x = \pm x_s$ . One could thus define some tolerance  $\epsilon > 0$ , and confine the state  $x$  to the smaller set  $[-x_s + \epsilon, x_s - \epsilon]$ . Is the problem then solved? Actually, no. As  $x$  approaches  $\pm x_s$  the amount of available, *stabilizing* control diminishes. Thus, as  $\epsilon$  becomes small, the system gets "sticky," with the worst case being getting stuck at  $x = \pm x_s$ . Whether or not  $|r| \leq r_s$  at any given point in time is of little consequence, but ensuring that  $x \in int(X_s)$  is crucial. Hence, confining  $v$  to

$V_f$  for all time is necessarily conservative from the tracking standpoint, since there exist  $[r, x]^T \notin V_f$  which can be included in the augmented state trajectory (AST), where:

1. The closed-loop system always operates linearly (constraints not encountered)
2. The AST is stable, and
3. The AST is recoverable

Now, due to the constraints on  $u$ , there exist values of  $r$  which cannot be tracked linearly. Since  $u$  depends linearly on  $r$ , the control constraints are readily transformed into constraints on  $r$ , viz.,

$$-\frac{1}{k_r}(1+k_x x) = r_{\min}(x) \leq r \leq r_{\max}(x) = \frac{1}{k_r}(1-k_x x) \quad (5.3)$$

Thus, if prior to the input to the system, the exogenous reference  $r$  is modified into an  $r'$  which always satisfies the inequality given by Eq. (5.3), the actuator saturation element becomes transparent, i.e., removing it from the physical system would have no effect. Specifically,  $r'$  is given by

$$r' = \begin{cases} r_{\min}(x), & r < r_{\min}(x) \\ r, & r_{\min}(x) \leq r \leq r_{\max}(x) \\ r_{\max}(x), & r > r_{\max}(x) \end{cases} \quad (5.4)$$

where  $r_{\min}(x)$  and  $r_{\max}(x)$  are given in Eq. (5.3).

This transformation of the constraints yields *saturated linear control* (the term "saturated linear control" is chosen because although linear, the control signal *appears* to be hard limited at the saturation values), which in this particular case provides no compensatory benefit in and of itself. Indeed, the block diagram shown in Figure 5.4, where the nonlinear block  $\mathcal{N}$  is as defined by Eq. (5.4), is input-output equivalent to the block diagram in Figure 5.1. Even so, there are some noncompensatory benefits of this transformation, namely, a linear system (from  $r'$  to  $x$ ) ensues, enabling the use of linear

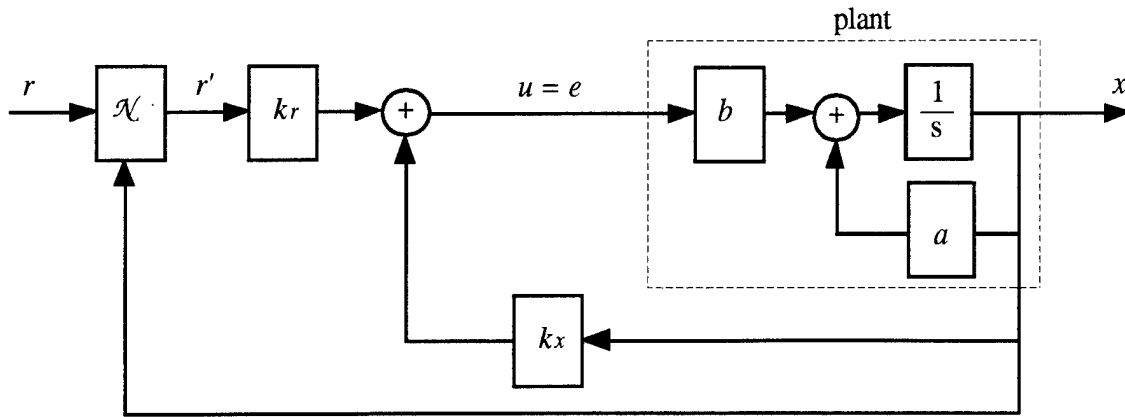


**Figure 5.4.** Transformed Closed-Loop System

analysis methods, saturation avoidance methods can be employed without tinkering inside the inner-most (plant stabilizing) control loop, and, moreover, provided that during the operation of the control system the nonlinear action  $\mathcal{N}$  does not cause  $r'$  to grow without bound when  $r$  is bounded, the system is guaranteed to be BIBO stable.

In the more general (and practical) case, where  $u$  is subject to some form of dynamics prior to the hard saturation, e.g., actuator dynamics are included, or a dynamic compensation element is used, e.g., integral action, a transformation of the constraints of this type does provide a compensatory benefit, viz., anti-windup, by maintaining consistency between the signals coming into and out of the saturation element. Thus, the element  $\mathcal{N}$  in the outer-loop in essence removes any dynamics from the inner-loop which are susceptible to windup when the control signal is saturated.

Hence, the control strategy entails a modification of  $r$  (to  $r'$ ) such that the input actually applied to the system is given by

$$u' = k_x x + k_r r'$$

where  $u'$  not only satisfies the control constraint (Eq. (5.3) is satisfied), but, and this is very important, also refrains from driving the state  $x$  too close to  $bnd(X_s)$ . This is accomplished, however, without otherwise restricting  $r'$  - specifically, the AST is not

restricted to  $V_r$ . The use of equivalent discrete-time models lends itself well to this strategy, since subsequent state values are readily determined. In fact, for the scalar case presented here, a one-step ahead constraint enforcement strategy can be employed which guarantees BIBO stability with a minimally conservative control signal.

The closed-loop system is thus given by

$$\begin{aligned}\dot{x} &= (a + bk_x)x + bk_r r' \\ &= a_{cl}x + bk_r r'\end{aligned}$$

Since perfect tracking should be achieved in steady state, it is clear that

$$bk_r = -a_{cl}$$

and thus

$$k_r = -\frac{a}{b} - k_x$$

Furthermore,  $x_s = r_s = b/a$ .

For example, let  $a = 1$ ,  $b = 2$ , and  $k_x = -6$ . Then  $k_r = 5.5$ , and  $x_s = r_s = 2$ . Also, let  $\epsilon = 0.1$  (the "anti-sticking" margin). First, consider the system responses to a pulse input of one second duration and with amplitude 2.4 as shown in Figure 5.5. A reference signal with magnitude greater than  $x_s$  has been purposely chosen, and thus it is impossible for the constrained system to track this signal with zero steady-state error. The unconstrained system tracks quite nicely, however, when the control constraint  $|u| \leq 1$  is enforced, the response diverges. Next, the constraint mitigation strategy just described is employed. It is implemented in discrete-time assuming a zero-order hold on the control signal  $u$  and a sample interval  $T = 0.01$  sec. That is, at each time step  $k$ ,  $r'$  is chosen such that  $|u'_k| \leq 1$  and  $x_{k+1} \in [-x_s + \epsilon, x_s - \epsilon]$ . Even when saturation mitigation is employed, it is impossible for the system to track this reference: The concept of static admissibility is dictated by the physical limitations imposed on the plant by the actuator constraints. Thus, the

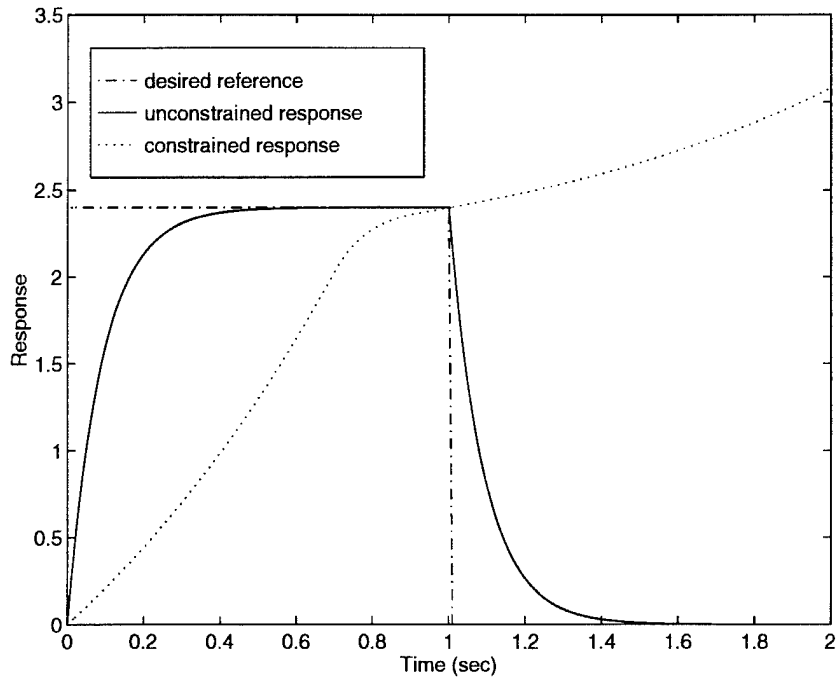


**Figure 5.5.** Unmitigated System Responses

performance should not be judged on how well the system tracks this reference, but how well the system tracks the nearest *feasible* reference. In this particular case ( $x_s = 2$ ,  $\epsilon = 0.1$ ), the feasible reference will never converge to a value greater than 1.9. The results (shown in Figure 5.6) are compared to Gilbert's reference governor implementation [19], which in essence restricts each  $[r_k, x_k]^T$  to remain inside the invariant set  $V_I$  (reduced accordingly by the parameter  $\epsilon$ ). The achieved improvement in tracking performance, although modest, is readily apparent (Note that the choice  $\epsilon = 0.1$  restricts the maximum output to 1.9 since  $x_s = 2.0$ ). For this simple case, not only is the tracking performance improved, but the computational burden is substantially reduced and global stability is not sacrificed. The main difference is that in the current approach,  $r' > r_s - \epsilon$  is allowed (see Figure 5.6). It should be noted however, that these results are specific to the scalar problem at hand. Indeed, Gilbert's discrete-time reference governor (DTRG) is quite

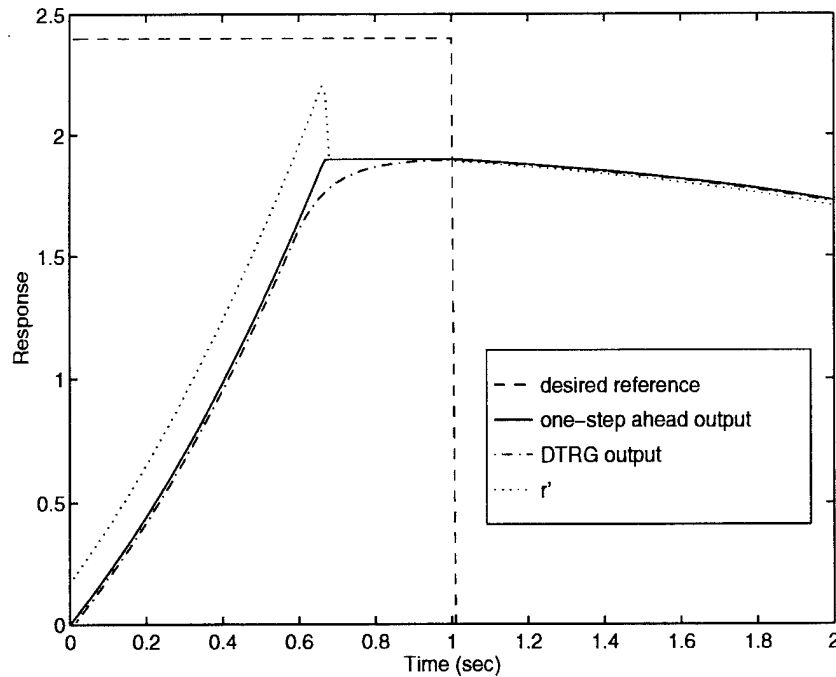


**Figure 5.6.** Scalar Example Results with Saturation Mitigation

admirable: The current method seeks to "squeeze out the last drop" of tracking performance - an issue not directly addressed by the DTRG. Thus, while BIBO stability is commendable, it is also obvious that attention needs to be given to tracking performance.

### 5.3 LQT with Saturation Effects Mitigation

Attention is now turned to the general case. Recall from Chapter 4 that the actuator displacements and actuator rates over the entire planning horizon can be written as a function of the current state  $\mathbf{x}_0$  and the predicted reference  $\mathbf{r}$  in the concise form

$$\begin{aligned}\boldsymbol{\delta} &= \mathbf{N}_x \mathbf{x}_0 + \mathbf{N}_r \mathbf{r} + \mathbf{n}_d d \\ \Delta_{\delta} &= \mathbf{P}_x \mathbf{x}_0 + \mathbf{P}_r \mathbf{r} + \mathbf{p}_d d\end{aligned}$$

where all of the coefficient matrices are constants and can be computed off-line. Additionally, the reference vector  $\mathbf{r}$  is parameterized as

$$\mathbf{r} = \mathbf{k}r_1 + \mathbf{h}$$

where  $\mathbf{k}$  is also a constant vector, but  $\mathbf{h}$  may depend on past reference values depending on the prediction method employed. Now, to characterize all possible amplitude and rate constraints over the planning horizon, let

$$\mathbf{f}_N = \begin{bmatrix} \mathbf{f}_\delta \\ \dots \\ \mathbf{f}_\Delta \end{bmatrix}, \quad \boldsymbol{\beta}_N = \begin{bmatrix} \boldsymbol{\beta}_\delta \\ \dots \\ \boldsymbol{\beta}_\Delta \end{bmatrix}, \quad \text{and} \quad \mathbf{g}_N = \begin{bmatrix} \mathbf{g}_\delta \\ \dots \\ \mathbf{g}_\Delta \end{bmatrix}$$

where

$$\mathbf{f}_\delta = \delta_{\min} \mathbf{1}_N - \mathbf{N}_x \mathbf{x}_0 - \mathbf{N}_r \mathbf{h} - \mathbf{n}_d d$$

$$\mathbf{f}_\Delta = T \dot{\delta}_{\min} \mathbf{1}_N - \mathbf{P}_x \mathbf{x}_0 - \mathbf{P}_r \mathbf{h} - \mathbf{p}_d d$$

$$\boldsymbol{\beta}_\delta = \mathbf{N}_r \mathbf{k}$$

$$\boldsymbol{\beta}_\Delta = \mathbf{P}_r \mathbf{k}$$

$$\mathbf{g}_\delta = \delta_{\max} \mathbf{1}_N - \mathbf{N}_x \mathbf{x}_0 - \mathbf{N}_r \mathbf{h} - \mathbf{n}_d d$$

and

$$\mathbf{g}_\Delta = T \dot{\delta}_{\max} \mathbf{1}_N - \mathbf{P}_x \mathbf{x}_0 - \mathbf{P}_r \mathbf{h} - \mathbf{p}_d d$$

The actuator constraints can then be written in terms of explicit constraints on the reference signal at time now  $r_1$  viz.,

$$\mathbf{f}_N \leq \boldsymbol{\beta}_N r_1 \leq \mathbf{g}_N \quad (5.5)$$

If a modified  $r_1'$  can be determined such that the constraint Eq. (5.5) is satisfied, then the solution is said to be *consistent*, and there exists a feasible reference vector  $\mathbf{r}' = \mathbf{k}r_1' + \mathbf{h}$  which can be optimally tracked with the LQT control law, without violating the actuator constraints. For the general case, however, there is no guarantee that such an  $r_1'$  exists. In this case, the solution is referred to as being *inconsistent*.

The vectors  $\delta$  and  $\Delta_\delta$  are based on the reference signal prediction. Since too much emphasis should not be placed on this prediction of the future, one may desire to account for only some of these constraints. In fact, simulation results have shown that even a

1-step ahead constraint mitigation strategy will yield greatly improved large signal tracking performance. Thus, define

$$\mathbf{f}_{\delta_n} = [\mathbf{I}_n \ \vdots \ \mathbf{0}_{n \times N-n}] \mathbf{f}_{\delta}$$

$$\mathbf{f}_{\Delta_n} = [\mathbf{I}_n \ \vdots \ \mathbf{0}_{n \times N-n}] \mathbf{f}_{\Delta}$$

$$\boldsymbol{\beta}_{\delta_n} = [\mathbf{I}_n \ \vdots \ \mathbf{0}_{n \times N-n}] \boldsymbol{\beta}_{\delta}$$

$$\boldsymbol{\beta}_{\Delta_n} = [\mathbf{I}_n \ \vdots \ \mathbf{0}_{n \times N-n}] \boldsymbol{\beta}_{\Delta}$$

$$\mathbf{g}_{\delta_n} = [\mathbf{I}_n \ \vdots \ \mathbf{0}_{n \times N-n}] \mathbf{g}_{\delta}$$

$$\mathbf{g}_{\Delta_n} = [\mathbf{I}_n \ \vdots \ \mathbf{0}_{n \times N-n}] \mathbf{g}_{\Delta}$$

and let

$$\mathbf{f}_n = \begin{bmatrix} \mathbf{f}_{\delta_n} \\ \vdots \\ \mathbf{f}_{\Delta_n} \end{bmatrix}, \quad \boldsymbol{\beta}_n = \begin{bmatrix} \boldsymbol{\beta}_{\delta_n} \\ \vdots \\ \boldsymbol{\beta}_{\Delta_n} \end{bmatrix}, \quad \text{and} \quad \mathbf{g}_n = \begin{bmatrix} \mathbf{g}_{\delta_n} \\ \vdots \\ \mathbf{g}_{\Delta_n} \end{bmatrix}$$

One must then be concerned only with satisfying the constraints

$$\mathbf{f}_n \leq \boldsymbol{\beta}_n r_1 \leq \mathbf{g}_n \tag{5.6}$$

This is referred to as *n-step ahead constraint mitigation*. The feasible reference value at time now  $r_1'$  is determined as follows. For each  $1 \leq i \leq 2n$ , if  $\beta_n(i) < 0$ , switch the values  $\mathbf{f}_n(i)$  and  $\mathbf{g}_n(i)$ . The physical interpretation of  $\beta_n(i) = 0$  or  $\beta_n(i)$  very small implies that  $r_1'$  can be infinite or very large. Under these circumstances, the constraints are not significant and need not be considered. Moreover, this situation implies that the actuator amplitude and rate are somewhat independent of the reference input, and hence, is an unlikely occurrence. Next, the vectors  $\mathbf{r}_{\min}$  and  $\mathbf{r}_{\max}$  are determined, where  $\mathbf{r}_{\min}(i) = \mathbf{f}_n(i)/\beta_n(i)$ , and  $\mathbf{r}_{\max}(i) = \mathbf{g}_n(i)/\beta_n(i)$ . Finally, bounds on  $r_1'$  are specified by

$$r_{1\min}' = \max_i [\mathbf{r}_{\min}(i)]$$

and



$$r'_{i_{\max}} = \min_i [r_{\max}(i)]$$

It is also possible to include additional constraints in this formulation, e.g., to account for multiple actuators and/or to enforce specific bounds on the remaining states. Thus, one would analogously define  $\mathbf{f}_x$ ,  $\beta_x$ , and  $\mathbf{g}_x$  vectors which could then be augmented onto the  $\mathbf{f}_n$ ,  $\beta_n$  and  $\mathbf{g}_n$  vectors respectively.

In the general case, any number of constraints  $n = 1, \dots, N$  can be enforced over the planning horizon. Then, for example, if one amplitude and one rate constraint are to be accounted for then  $\mathbf{f}_n$ ,  $\beta_n$ , and  $\mathbf{g}_n \in \mathbf{R}^2$ . Since the second through  $N$ -th components of  $\delta$  and  $\Delta_\delta$  represent predicted (future) system responses, it is not so critical that they be explicitly accounted for. Indeed, enforcement of all  $N$  constraints may prove to be unnecessarily conservative, bearing in mind that the exogenous reference signal is continuously changing. When high gain control laws and/or high-order polynomial extrapolations are employed, attempts to enforce a large number of these future constraints increases the likelihood that an inconsistent solution will occur. It is important to realize, however, that an inconsistent solution at a future time step does not necessarily imply a breakdown in the LQT control law. That is, although an inconsistent solution arises, the LQT inputs which actually reach the system, viz., the  $u_0$ 's, will not necessarily ever attempt to exceed the actuator constraints because of the inexact nature of a predictive control strategy.

Consider for the moment a 1-step ahead mitigation strategy. The appeal of this method lies in the availability of a relatively simple closed-form control solution which requires little on-line computation for constraint mitigation purposes. Since the first elements of  $\delta$  and  $\Delta_\delta$  represent actual system responses, it is clear that  $r'_i$  should be chosen such that it does not immediately induce a saturation. This does not preclude the state of

affairs from occurring in which the actuator rate and amplitude constraints can not be simultaneously satisfied. However, extensive simulation has shown that this method can be effective when reasonable inputs are applied to the system. Thus, a suitable prefilter, combined with an open-loop hard limiter on the pilot stick (as is employed in many operational aircraft today), and coupled with a properly tuned 1-step ahead LQT controller, can yield a rather robust closed-loop control system. Indeed, the large signal range of operation is greatly extended over that of the uncompensated system.

#### 5.4 Simulation Examples and Discussion

This section provides a representative sample of simulation examples which demonstrate the potential performance gains attainable with the LQT control method. Each example has been chosen in order to illustrate or clarify specific aspects of the problem. Additional simulation results can be found in the appendix.

The first example demonstrates the potential performance improvements of the LQT control method over a linear, small signal, regulator-based design. The LQT method is applied to the F-16 longitudinal plant model of Example 3.1, but where actuator amplitude and rate constraints have been included, viz.,

$$\begin{aligned} -0.37 &\leq \delta(t) \leq 0.37 \\ -1.0 &\leq \dot{\delta}(t) \leq 1.0 \end{aligned}$$

in rad and rad/sec respectively. In the discrete-time formulation with a sample interval  $T = 0.01$ , these constraints are represented by

$$\begin{aligned} -0.37 &\leq \delta_{k+1} \leq 0.37 \\ -0.01 &\leq \delta_{k+1} - \delta_k \leq 0.01, \quad k = 0, 1, \dots \end{aligned} \tag{5.7}$$

The LQ weights  $Q_I = 47$ ,  $Q_P = 0.29$ , and  $R = 0.91$  are chosen. A planning horizon  $N = 15$  (thus, the reference signal is predicted 0.15 sec into the future) is used with a poly-1 + poly-1 reference prediction strategy. The resultant LQT control law is explicitly given by

$$u_k = \mathbf{k}_x^T \mathbf{x}_k + \mathbf{k}_r^T [r_k \quad r_{k+1}]^T + k_r r'_{k+1}$$

where the precomputed and fixed gains  $\mathbf{k}_x^T = [0.2013 \quad 0.7317 \quad -0.5686 \quad -4.007]$ ,  $\mathbf{k}_r^T = [5.2366 \quad -5.6107]$ , and  $k_r = -0.4197$ . The pitch rate reference input is an aggressive 1 rad/sec pulse doublet, prefiltered by a second-order flying qualities prefilter with unity gain and (s-plane) poles  $s = -10 \pm j10$ . The unconstrained responses (i.e., the actuator constraints are not imposed) of both the LQT controlled system and the LQR based controller of Example 3.1 are compared in Figure 5.7a. Note that both control laws exhibit

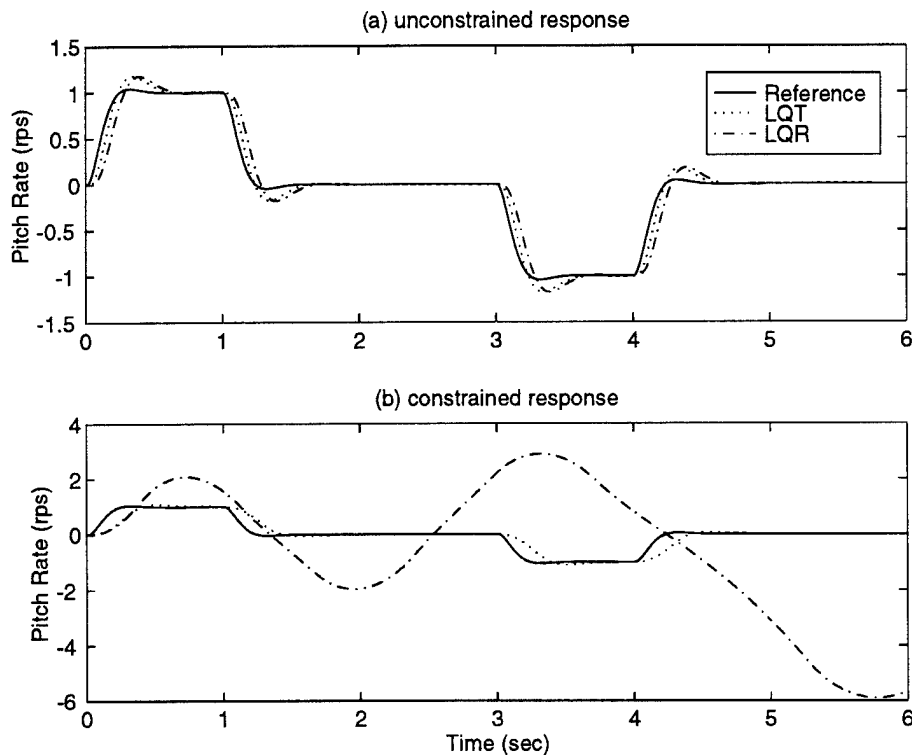


**Figure 5.7.** LQT/LQR Comparison

similar tracking performance. The LQT controller yields slightly improved tracking performance, and although not readily apparent from the plot, the LQT control law yields a lower actual cost over the entire simulation by approximately 50%. Next, the constrained responses are shown in Figure 5.7b. The advantage of the LQT constraint mitigation is

now apparent: The LQT controlled system's tracking performance, while unavoidably degraded somewhat due to the physical limitations of the actuator, does a nice job of tracking, while the simpler LQR controller does quite poorly. Note that if the LQT solution is employed, but without the saturation mitigation compensation, the constrained LQT response is similar to the hard constrained LQR response. The LQT constraint mitigation compensation has clearly extended the range of acceptable operation of the constrained system. The actuator activity for each of these controllers is shown in Figure 5.8. It

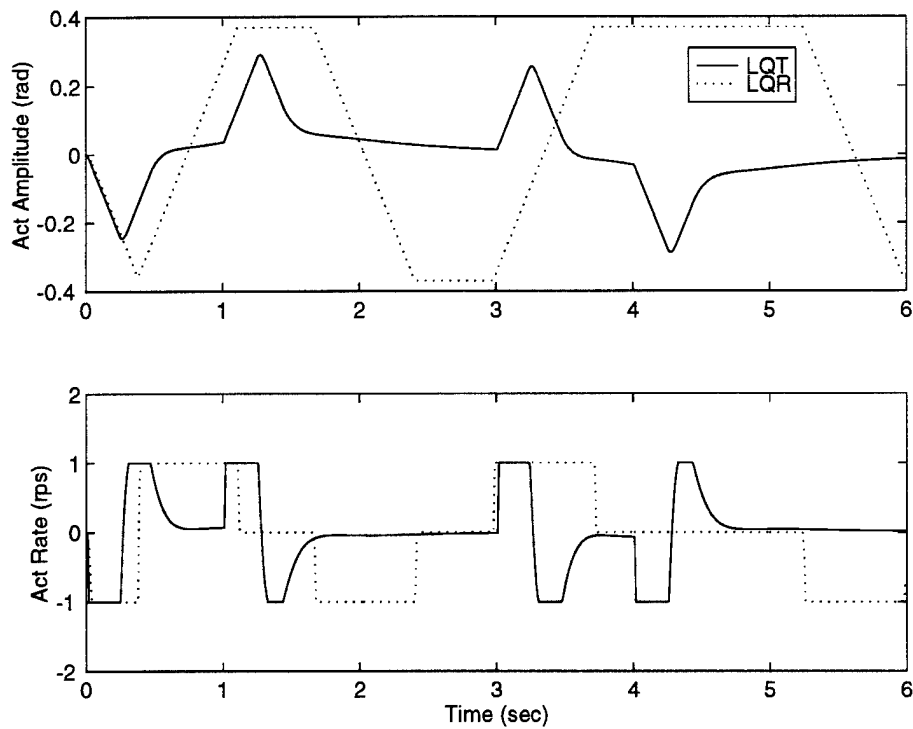


**Figure 5.8.** LQT/LQR Actuator Responses

should be noted that although both actuator rate responses appear to be hard limited, in the LQT case this appearance is due to the feasible reference value  $r_1'$  and is not the result of encountering the hard saturation. In fact, whether or not the hard constraints are even enforced in the LQT simulations makes no difference since the LQT controller does not generate actuator responses outside the linear range of operation.

In terms of small signal operation, the predictive reference information can be augmented into the closed-loop dynamics matrix, yielding the linear, closed-loop system equation

$$\xi_{k+1} = \mathbf{A}_{cl} \xi_k + \mathbf{b}_{cl} r_{k+1} \quad (5.8)$$

where in this particular case (poly-1 + poly-1 reference prediction)

$$\xi_k = \begin{bmatrix} \mathbf{x}_k \\ \vdots \\ r_k \end{bmatrix}$$

$$\mathbf{A}_{cl} = \begin{bmatrix} \mathbf{A} + \mathbf{b}\mathbf{k}_x & \mathbf{b}\mathbf{k}_r(1) \\ \mathbf{0}_{n \times 1} & 0 \end{bmatrix}$$

and

$$\mathbf{b}_{cl} = \begin{bmatrix} \mathbf{b}(\mathbf{k}_r(2) + k_{r'}) \\ 1 \end{bmatrix}$$

Now, given the formulation of Eq. (5.8), the system meets the requirements for the implementation of a discrete-time reference governor (DTRG). The application of the DTRG saturation mitigation strategy to this closed-loop LQT design (in lieu of performing the LQT saturation mitigation strategy) yields poor tracking as compared to the full LQT response - see Figure 5.9. The actuator response for both of these methods is shown in Figure 5.10.

This disparity between the LQT and LQT/DTRG approaches is greatly exacerbated when higher order reference signal prediction algorithms are employed. Consider for example a poly-2 + poly-2 reference prediction strategy, applied to the same problem using a planning horizon  $N = 30$ . The responses from the 1-step ahead LQT and the LQT/DTRG methods to a 0.5 rad step, prefiltered by a first-order filter with bandwidth of 10 rad/sec are compared in Figure 5.11. Thus, although the LQT/DTRG controller delivers BIBO stability, its tracking performance is substantially lacking.

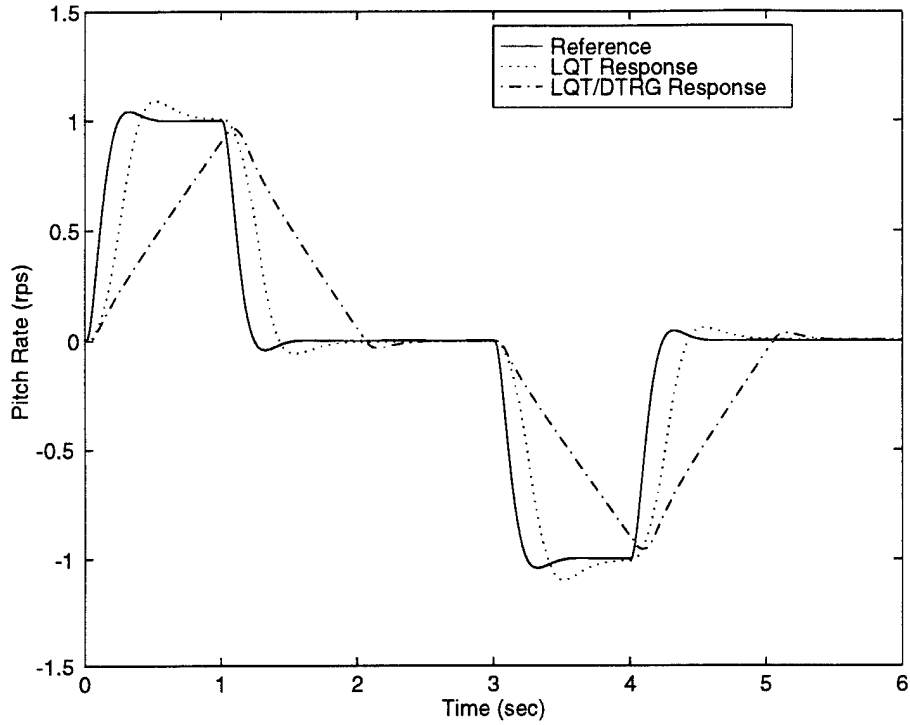


**Figure 5.9.** LQT vs LQT/DTRG with First-Order Prediction

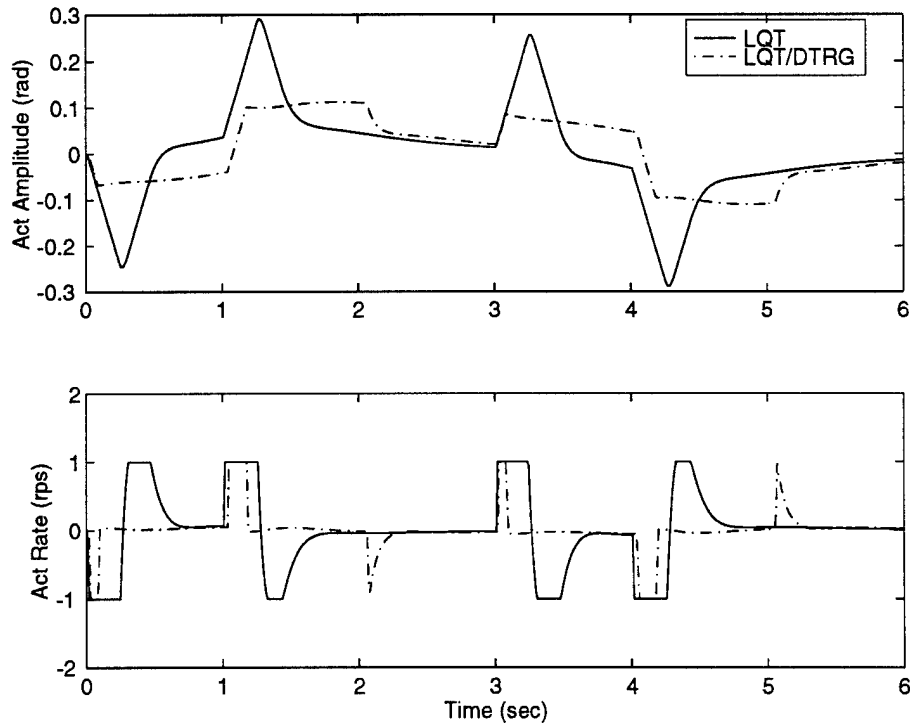


**Figure 5.10.** LQT and LQT/DTRG Actuator Response Comparisons

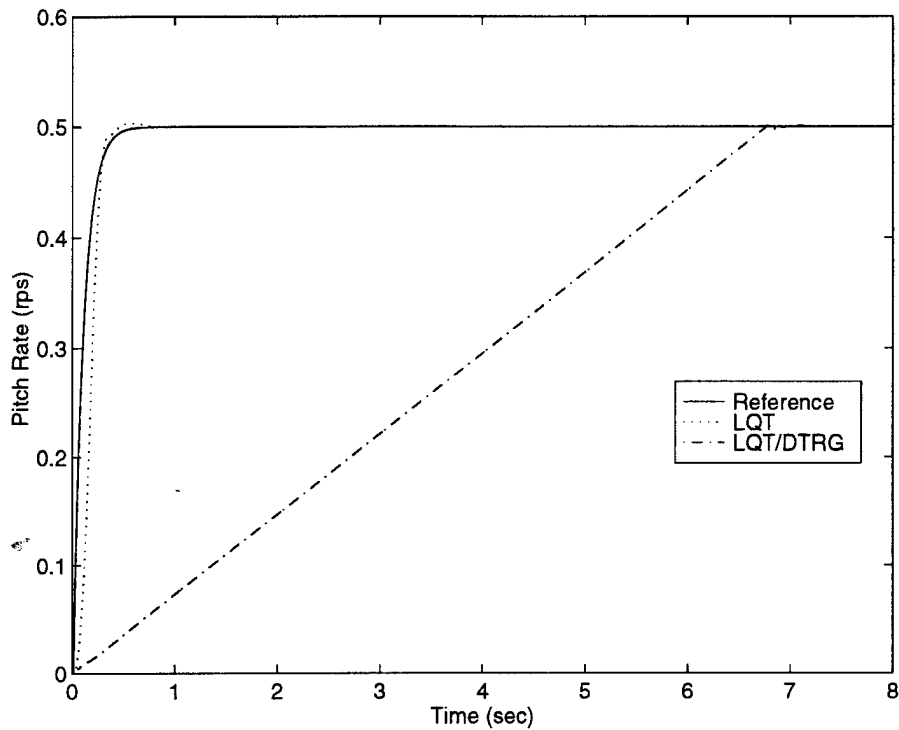


**Figure 5.11.** 1-Step LQT vs LQT/DTRG with Second Order Prediction

In all fairness, the DTRG performs much better when applied to a non-predictive, e.g., a simpler, LQR type inner-loop control law. Additionally, the LQT system response becomes more conservative when additional "future" actuator saturations are accounted for. When a predictive strategy such as this Poly-1 + Poly-1 strategy is employed, the LQT controlled system may become even more conservative than the LQR/DTRG system, because the effects of *potential* future constraints are being mitigated in the former. Figure 5.12 repeats the simulation of Figure 5.7, but compares the 1-step and 10-step LQT responses, to the LQR solution, but with the DTRG constraint mitigation. It is observed that now the 1-step LQT solution is less conservative than the LQR/DTRG solution, but the 10-step LQT solution is more conservative than the LQR/DTRG solution. It is apparent, however, that the consideration of the actuator constraints in the initial design phase is beneficial.

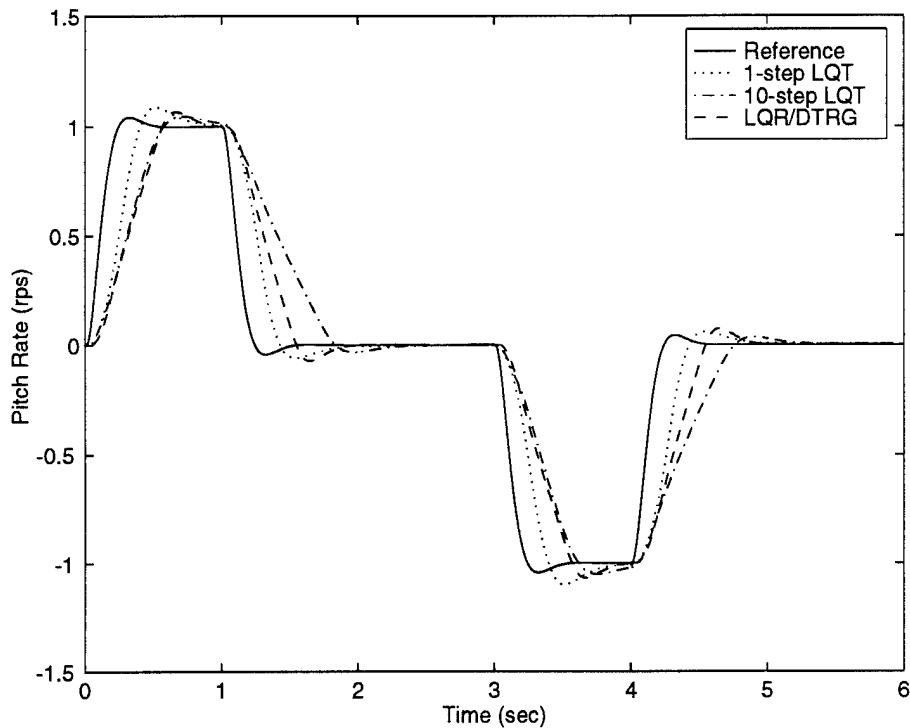


**Figure 5.12.** LQT 1-step, 10-step and LQR/DTRG Comparison

### 5.5 A Globally Bounded Output LQT Controller

The novel LQT nonlinear control method will yield a globally bounded output stable closed-loop control system under the following conditions:

1. A poly-0 + parallel (or equivalent) reference prediction strategy is employed,
2. Static admissibility is included in the feasibility criteria, and
3.  $n$ -step ahead constraint enforcement is employed, where  $n$  is *sufficiently large*.

That is, the controlled system output is then guaranteed to always be bounded, regardless of the reference input, whether bounded or unbounded, given to the constrained closed-loop system. This proposition holds because saturation avoidance and consistent (i.e., the constraints will not conflict with one another) solutions are guaranteed. Thus, the system is then always operating in the small signal regime and hence, linear, mode of operation, which is bounded-input bounded-output (BIBO) stable by design. Obviously, the overall



system will be BIBO stable provided that  $r'$  is bounded and saturations are not encountered. This fixed output bound is determined by the linear (closed-loop) system dynamics and the maximum *steady-state* system output which can be achieved without violating the actuator constraints. Moreover, only the amplitude constraints come into play with respect to these static admissibility concerns, since when the control surface is at its limit in steady-state, the actuator rates are obviously zero. Furthermore, such a stability guarantee necessarily entails a trade-off in tracking performance, since the system obviously will not be able to track any reference signals which exceed this bound.

In terms of constraint mitigation, this special case is very similar in concept to the DTRG. The basic idea entails at each time step ensuring that saturations will never occur, provided that the reference signal remains constant. By using a poly-0 prediction of the reference, the reference signal is indeed assumed constant over the planning horizon. The (small signal) closed-loop system is thus of the form

$$\mathbf{x}_{k+1} = \mathbf{A}_{cl}\mathbf{x}_k + \mathbf{b}_{cl}r_{k+1} \quad (5.9)$$

where

$$\mathbf{A}_{cl} = \mathbf{A} + \mathbf{b}\mathbf{k}_x^T$$

and

$$\mathbf{b}_{cl} = \mathbf{b}\mathbf{k}_{r'} + \boldsymbol{\gamma}$$

as described in Chapter 2. Now, since the linear (small signal) system is stable, a constant reference input  $r_o$  will cause the state vector to asymptotically approach some terminal quiescent state  $\mathbf{x}_{ss}$  given by

$$\mathbf{x}_{ss} = [\mathbf{I} - \mathbf{A}_{cl}]^{-1} \mathbf{b}_{cl}r_o$$

If  $\mathbf{x}_{ss}$  is such that the actuator (amplitude) constraints are not violated, i.e.,

$$\delta_{\min} \leq \mathbf{c}_{\delta}^T \mathbf{x}_{ss} \leq \delta_{\max}$$

then  $r_o$  is said to be statically admissible. One must then also ensure that no *transient saturations* occur. That is, no saturations occur in the resultant state trajectory during the transient between the initial and terminal states. If  $n$  is chosen sufficiently large, then the enforcement of Eq. (5.6) will ensure the avoidance of transient saturations. Eq. (5.6) could also be used to enforce static admissibility, but because of the asymptotic nature of the linear system response, this requires  $n \rightarrow \infty$ . An anti-sticking tolerance should be included to avoid the sticking phenomenon discussed in Section 5.2, which will also ensure the existence of a finite  $n$  which can preclude saturation in the steady-state. This is, in fact, the concept utilized by the DTRG. However, unless one is willing to sacrifice a substantial portion of the available control authority,  $n$  can still be quite large.

The required size of  $n$  (and thus, the on-line computational requirements) can be substantially reduced by breaking the enforcement of static admissibility and the avoidance of transient saturations into a two-stage process. Thus, Eq. (5.6) is used only to avoid transient saturation, while more direct means are employed to ensure static admissibility, viz., hard limiting of the feasible reference value. That is, the feasible reference value at time now  $r'_1$  is determined subject to both Eq. (5.6) and

$$r_{sa-} \leq r'_1 \leq r_{sa+} \quad (5.10)$$

where  $r_{sa-}$  and  $r_{sa+}$  are given by

$$r_{sa-} = \left\{ \mathbf{c}_\delta^T [\mathbf{I} - \mathbf{A}_{cl}]^{-1} \mathbf{b}_{cl} \right\}^{-1} (\delta_{\min} + tol) \quad (5.11)$$

and

$$r_{sa+} = \left\{ \mathbf{c}_\delta^T [\mathbf{I} - \mathbf{A}_{cl}]^{-1} \mathbf{b}_{cl} \right\}^{-1} (\delta_{\max} - tol) \quad (5.12)$$

where  $tol$  is the anti-sticking tolerance mentioned previously. When there are multiple control surfaces with constrained actuators, Eqs. (5.11) and (5.12) are written for each one with the most restrictive results being used in Eq. (5.10).

Thus, at each time step (in real-time),  $r_1'$  is determined in accordance with Eqs. (5.6) and (5.10). Now, with  $n$  sufficiently large, enforcement of Eq. (5.6) precludes any transient saturations from occurring, and since the reference input is further restricted to values which will not cause saturation in steady state, it is guaranteed that saturations will never occur provided that the feasible reference input is held constant. Thus, the necessary condition that a viable fallback is available at the subsequent time step, viz., maintaining the same feasible reference determined in the previous time step, is satisfied. Hence, the system always operates in the stable small signal mode described by Eq. (5.9). It is by now apparent that  $n$  "sufficiently large" implies that any potentially offensive transient characteristics of the actuator response have died out within  $n$  time steps. It is important to realize that when saturation is averted, the linear characteristics of the closed-loop system are well-behaved and highly predictable. Furthermore, the constrained closed-loop stable system output is bounded by the same bounds that the linear (unconstrained) system adheres to when the reference input is restricted to  $[r_{sa-}, r_{sa+}]$ .

For a more formal analysis, consider the linear system

$$\mathbf{x}_{k+1} = \mathbf{A}_{cl}\mathbf{x}_k + \mathbf{b}_{cl}r_{k+1}, \quad k = 0, 1, \dots \quad (5.13)$$

with actuator displacement

$$\delta_{k+1} = \mathbf{c}_\delta^T \mathbf{x}_{k+1}$$

and actuator rate

$$\Delta_{k+1} = \delta_{k+1} - \delta_k$$

and where  $\mathbf{A}_{cl}$  is asymptotically stable. Let the initial state at time  $k = 0$  be  $\mathbf{x}_0$ , and assume that

(i)  $|\delta_0| = |\mathbf{c}_\delta^T \mathbf{x}_0| < \delta_{\max}$ , and

(ii) There exists an  $r_1'$  such that

$$\text{a. } |\delta_{n+1}| = \left| \mathbf{c}_\delta^T \left[ \mathbf{A}_{cl}^{n+1} \mathbf{x}_0 + \sum_{m=0}^n \mathbf{A}_{cl}^m \mathbf{b}_{cl} r_1' \right] \right| \leq \delta_{\max}, \quad \forall n = 0, 1, \dots, \text{ and}$$

$$\text{b. } |\Delta_{n+1}| = \left| \mathbf{c}_\delta^T \left[ (\mathbf{A}_{cl} - \mathbf{I})^{n+1} \mathbf{x}_0 + \sum_{m=0}^n (\mathbf{A}_{cl} - \mathbf{I})^m \mathbf{b}_{cl} r_1' \right] \right| \leq \Delta_{\max}, \quad \forall n = 0, 1, \dots$$

Note that the condition (ii) is not overly restrictive. Indeed, an infinite number of small perturbation situations about the origin satisfy both (i) and (ii), and in addition, whenever (i) is satisfied and  $\mathbf{x}_0$  is an equilibrium state of the system, then (ii) is satisfied with an  $r_1'$  such that  $\mathbf{x}_0 = (\mathbf{I} - \mathbf{A}_{cl})^{-1} \mathbf{b}_{cl} r_1'$ . Thus, whenever the initial system is at rest, only condition (i) must be satisfied. In essence, these conditions simply require that the system not start at an initial state where it is impossible to avoid saturation, an obvious necessity.

Let  $r_{sa} > 0$  yield the steady state equilibrium

$$\mathbf{x}_{sa} = (\mathbf{I} - \mathbf{A}_{cl})^{-1} \mathbf{b}_{cl} r_{sa}$$

such that

$$|\delta_{sa}| = |\mathbf{c}_\delta^T \mathbf{x}_{sa}| = \delta_{\max}$$

Then, clearly, satisfaction of (i) implies that  $-r_{sa} \leq r_1' \leq r_{sa}$ . In order to guarantee that a feasible  $r_{k+1}'$  can be finitely determined at each time step  $k$ , feasible reference values are restricted to the interval  $R_{sa} = [\varepsilon_1 - r_{sa}, r_{sa} - \varepsilon_1]$ , where  $\varepsilon_1 > 0$  can be selected arbitrarily small, and specifically  $\varepsilon_1 \ll r_{sa}$ . For any  $r_1'$  in this interval, the steady-state actuator deflection magnitude

$$|\delta_{ss}| = \left| \lim_{n \rightarrow \infty} \delta_{n+1} \right|$$

lies inside the interval  $[\varepsilon_2 - \delta_{\max}, \delta_{\max} - \varepsilon_2]$ , where

$$\varepsilon_2 = \left| \mathbf{c}_\delta^T (\mathbf{I} - \mathbf{A}_{cl})^{-1} \mathbf{b}_{cl} \right| \varepsilon_1$$

Moreover, the actuator rate tends to zero in the steady state. Thus, by restricting  $r_1'$  to  $R_{sa}$ , saturation will not be a problem in steady state, and only transient saturations need to be addressed.

Now, since  $\mathbf{A}_{cl}$  is asymptotically stable, there exist finite "settling times"  $n_1 = n_1(\varepsilon_3)$  and  $n_2 = n_2(\varepsilon_4)$  such that

$$|\delta_{n+1}| \leq \delta_{\max} - \varepsilon_3, \quad \forall n \geq n_1$$

and

$$|\Delta_{n+1}| \leq \varepsilon_4, \quad \forall n \geq n_2$$

where  $0 < \varepsilon_3 < \varepsilon_2$ , and  $0 < \varepsilon_4 < \Delta_{\max}$ . Thus, over the finite interval  $n = 0, 1, \dots, n^* = \max(n_1, n_2)$  both  $|\delta_{n+1}|$  and  $|\Delta_{n+1}|$  achieve maximum values. If the pilot demanded reference  $r_1$  yields either

$$\max_{0 < n \leq n^*} |\delta_{n+1}| > \delta_{\max}$$

or

$$\max_{0 < n \leq n^*} |\Delta_{n+1}| > \Delta_{\max}$$

then a feasible reference value  $r_1'$  must be determined as described in Section 5.3, which ensures that  $|\delta_{n+1}| \leq \delta_{\max}$  and  $|\Delta_{n+1}| \leq \Delta_{\max}$  for all  $n = 0, \dots, n^*$ . Otherwise,  $r_1' = r_1$ . This  $r_1'$  is guaranteed to exist by condition (ii). Thus,  $r_{k+1}'$  is determined and used to drive the system yielding the updated state  $\mathbf{x}_1 = \mathbf{x}_1(r_1')$  according to the stable, linear system dynamics. At the subsequent step,  $k = 1$ , the process is repeated, where conditions (i) and (ii) become

$$(iii) \quad |\delta_1| = |\mathbf{c}_\delta^T \mathbf{x}_1| < \delta_{\max}, \quad \text{and}$$

(iv) There exists an  $r_2'$  such that

$$\text{a. } |\delta_{n+1}| = \left| \mathbf{c}_\delta^T \left[ \mathbf{A}_{cl}^{n+1} \mathbf{x}_1 + \sum_{m=0}^n \mathbf{A}_{cl}^m \mathbf{b}_{cl} r_2' \right] \right| \leq \delta_{\max}, \quad \forall n = 0, 1, \dots, \text{ and}$$

$$\text{b. } |\Delta_{n+1}| = \left| \mathbf{c}_\delta^T \left[ (\mathbf{A}_{cl} - \mathbf{I})^{n+1} \mathbf{x}_1 + \sum_{m=0}^n (\mathbf{A}_{cl} - \mathbf{I})^m \mathbf{b}_{cl} r_2' \right] \right| \leq \Delta_{\max}, \quad \forall n = 0, 1, \dots$$

Condition (iii) is satisfied because of condition (ii)a, specifically at  $n = 0$ . Condition (iv) is satisfied because of condition (ii), viz.,  $r_2' = r_1'$  is a feasible reference value (according to condition (ii) for  $n \geq 1$ ), and hence, a feasible reference is guaranteed to exist. Generally,  $r_2' = r_1'$  will not be the only viable reference value. Ideally, the pilot demanded reference is acceptable, i.e.,  $r_2' = r_2$ . When this is not the case,  $r_2'$  is chosen such that  $|r_2 - r_2'|$  is minimized and conditions (iii) and (iv) are satisfied, as described in Section 5.3. At the next time step  $k = 2$  the predetermined existence of  $r_2'$  guarantees that the analogous set of required conditions can be satisfied and thus the existence of  $r_3'$  for the same reasons that  $r_1'$  guarantees the existence of  $r_2'$  as just described. Clearly, this is true for all subsequent time steps: The existence of  $r_{k+1}'$  guarantees the existence of a feasible  $r_{k+2}'$ . Thus, the following facts concerning the system Eq. (5.13) subject to the hard saturation constraints

$$|\delta_{k+1}| \leq \delta_{\max}, \quad \forall k = 0, 1, 2, \dots$$

and

$$|\Delta_{k+1}| \leq \Delta_{\max}, \quad \forall k = 0, 1, 2, \dots$$

are ascertained:

1. The system will never attempt to exceed the hard actuator constraints.
2. The system behavior is always determined by the linear stable difference Eq. (5.13)
3. The system state never attains any value that cannot be attained by the unconstrained linear system, where each stimulus  $r_{k+1} \in R_{sa}$ .

Hence, the constrained system is guaranteed to be bounded output stable.

Consider once again the F-16 longitudinal plant model of Example 3.1, subject to the actuator constraints of Eq. (5.7). The global stability properties of the LQT control design using a poly-0 + poly-0 reference prediction strategy are demonstrated. The planning horizon is  $N = 60$ , and the LQ weights are the same as chosen previously. Approximate requirements for the constraint enforcement horizon  $n$  can be quickly determined from an examination of the quantities of interest in the closed-loop system's unconstrained step response, as shown in Figure 5.13. A good rule of thumb is twice the number of time

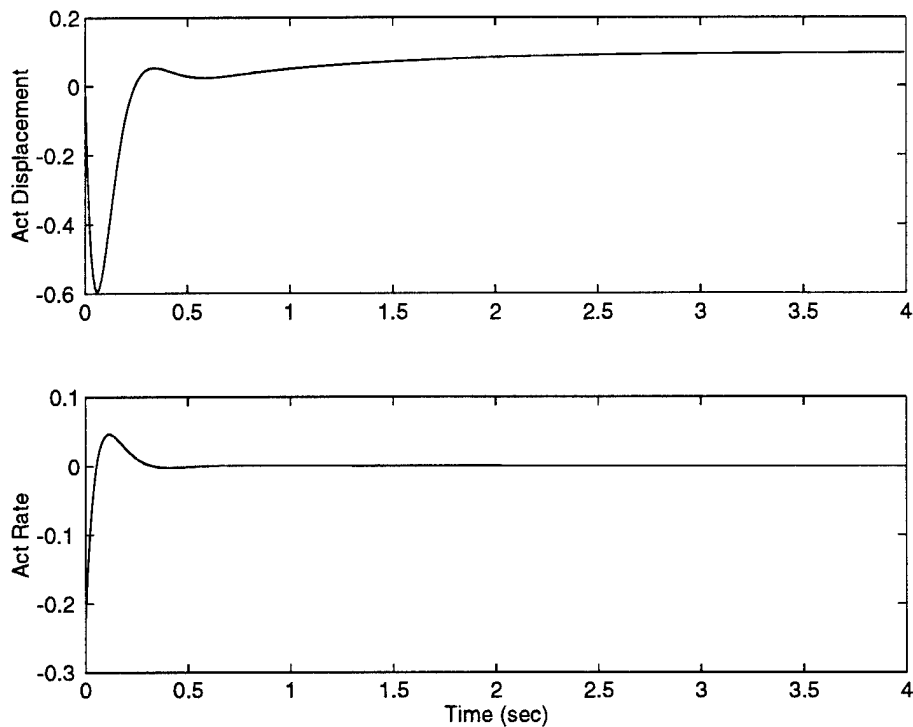


**Figure 5.13.** Unconstrained Actuator Step Responses

steps to the latest maximum peak value in all the constrained quantities. In this case, the largest peak in actuator displacement occurs at approximately time step 6, and the worst peak in rate is at time step 1, but with another potentially offensive peak at approximately time step 11. Thus,  $n = 15$  is chosen. Simulation results verify that this value of  $n$  is sufficient. The step response to a very high amplitude 4 rad/sec pitch rate step command

using an anti-sticking tolerance of 0.5 rad is shown in Figure 5.14. For this particular example, static admissibility requires that  $|r| \leq 3.7935$ , and the step input is purposely chosen at a larger value.

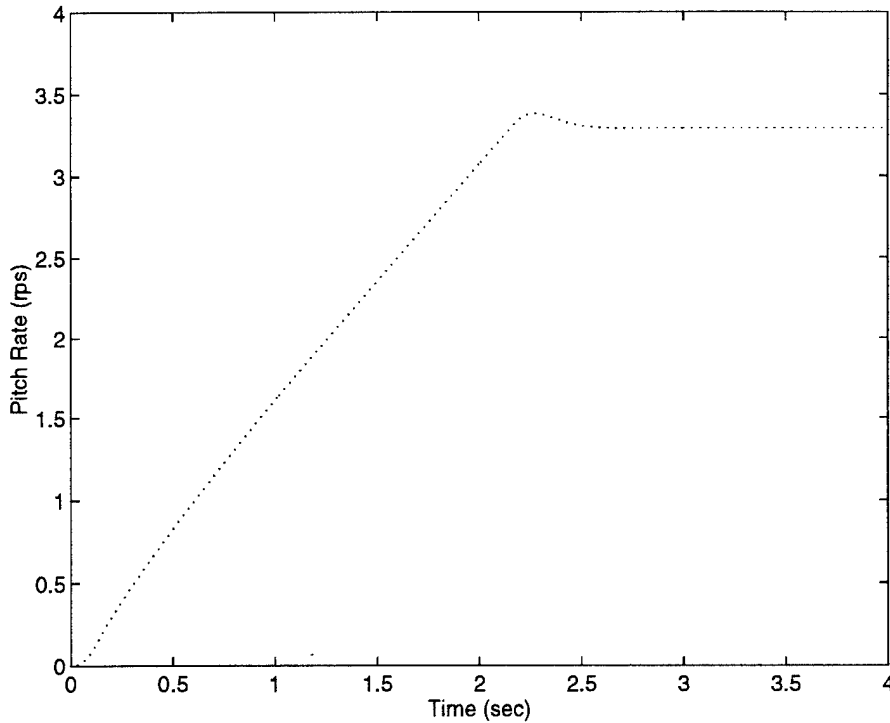


**Figure 5.14.** High Amplitude Step with  $tol = 0.5$

The importance of the anti-sticking tolerance is clearly illustrated in Figure 5.15. When zero tolerance is enforced, the system becomes stuck with the actuator amplitude at its limit. Note that this situation is preferable to the unmitigated system. Indeed, since the open-loop plant is unstable, having the actuator hard saturated would result in a departure. This state of affairs is, nonetheless highly undesirable. As the tolerance is increased the system becomes less sticky, where the phenomenon is basically gone for  $tol = 0.5$ , as evidenced by the fact that the "downward" response is approximately as fast as the "upward" response.



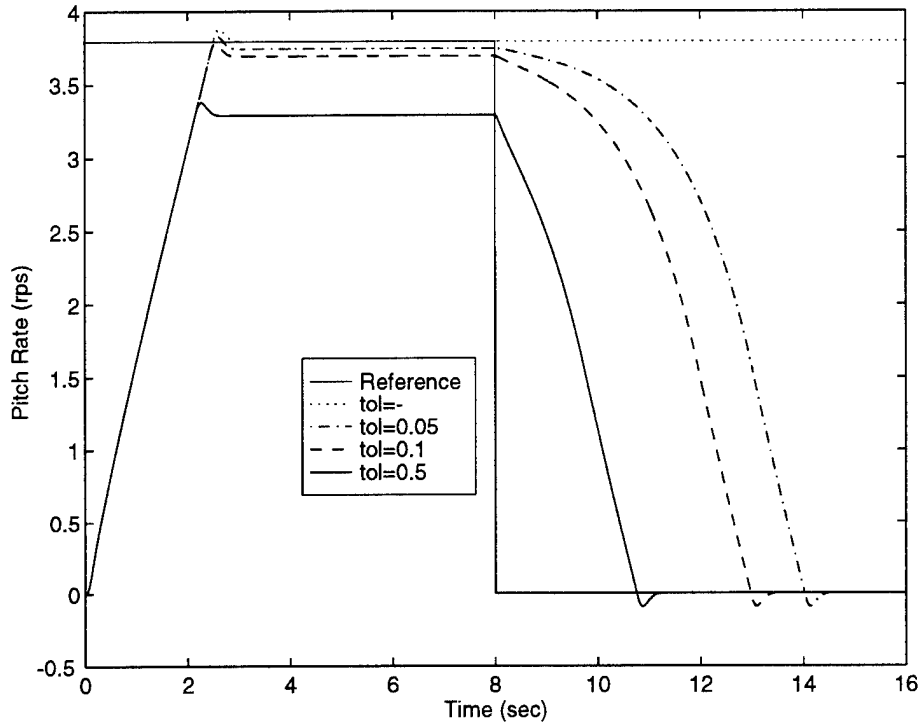


**Figure 5.15.** The Sticking Phenomenon

It has also been observed through simulation, that enforcing artificial bounds on the remaining states can be an effective method to ensure static admissibility. Although one would expect  $n$  to have to be quite large, a relatively modest value  $n = 15$  works quite well here. The procedure here is to enforce artificial constraints on the remaining states, viz.,  $\alpha$  and  $q$ , at levels which correspond to  $r_{ss}$  less the desired tolerance, in lieu of enforcing the hard constraint on  $r_1'$ . The system response to the same input used in Figure 5.14, but using this strategy, is shown in Figure 5.16. The response is similar, but lacks the slight overshoot which featured in Figure 5.14.

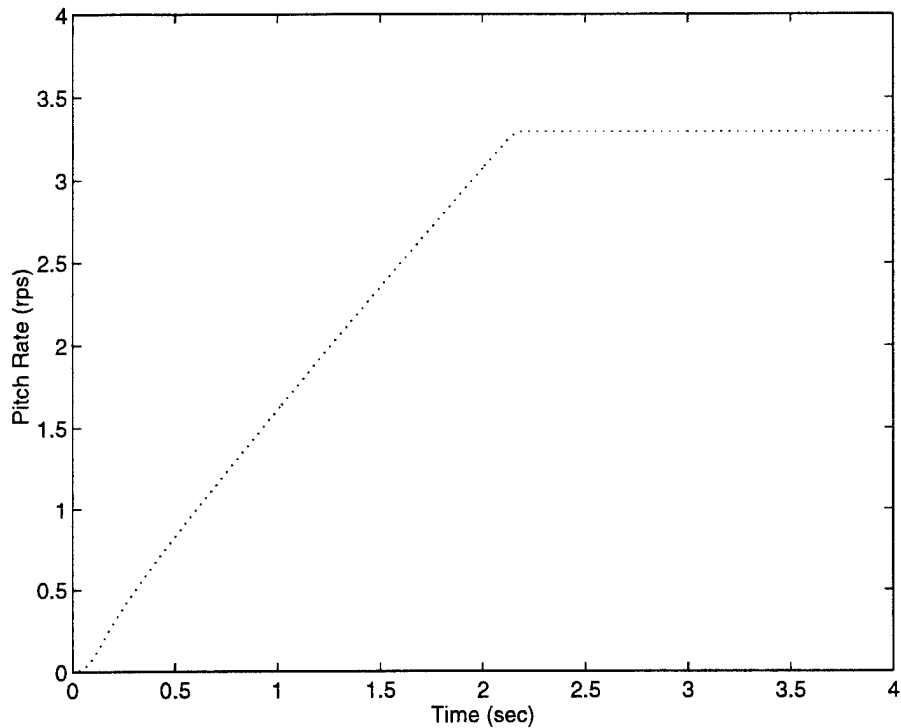


**Figure 5.16.** High Amplitude Step with Artificial State Bounds

## 5.6 Summary

The LQT control concept entails the following. First, the pilot's reference signal is predicted into the future over the planning horizon, and parameterized in terms of its present value. Next, an expression for the optimal control solution over the planning horizon is obtained in terms of this reference signal. Subsequently, a modified feasible reference value is determined which can be optimally tracked with this control law over the planning horizon without violating the actuator constraints. The term *feasible* is determined by the saturation effects mitigation strategy selected. That is, feasibility may imply that hard saturation will not occur anywhere from 1 to N-steps ahead, or hard saturation will only be avoided at time step 1, or, e.g., static admissibility is enforced. The resultant nonlinear control solution is a closed-form, constant gain feedback solution in the state, current and possibly previous reference values, and this present feasible reference.

This control law is easily implementable. It has been observed that emphasis on the potential future saturations is not necessary, and may lead to overly conservative responses. It has also been shown that a 1-step ahead constraint enforcement strategy yields acceptable performance.

The LQT controller whose synthesis has been outlined above does not come with any guarantees regarding BIBO stability or the existence of consistent solutions, but extensive simulation has shown that a properly tuned LQT controller can yield greatly improved large signal performance, prevent saturation induced departures experienced by small signal design methods, and substantially increase the acceptable range of operation for a constrained system.

An adaptation of the general LQT concept which utilizes a zero-order reference signal prediction strategy, and in which the feasible reference is confined to statically admissible values, has been shown to yield a globally bounded output stable control system. This method while similar to the DTRG concept in terms of constraint mitigation, yields somewhat improved tracking performance. Finally, by separating the transient and steady-state saturation issues and breaking the constraint mitigation process into two stages, a lower on-line computational burden is achieved, as compared to a brute force search for the maximal invariant set.

## *VI. Conclusion*

### *6.1 Overview*

Manual tracking control in the presence of constrained dynamic actuators is indeed a rich research area. It has been demonstrated that even the simplest tracking control problem is rather complex. Research which places a high degree of emphasis on the tracking aspect of the problem, while at the same time gives attention to the mitigation of the impact of actuator rate and amplitude constraints, and particularly for the challenging case of open-loop unstable plants, is warranted. Section 6.2 outlines the accomplishments of this research and the contributions to the literature, followed by an overview of the LQT design process and the resultant control law. Specific conclusions resulting from this research are listed in Section 6.3, and recommendations for future research are listed in Section 6.4.

### *6.2 Contributions & Accomplishments*

Aggressive tracking performance and the mitigation of actuator hard saturation effects are directly conflicting objectives. While a number of robust and high gain tracking control paradigms exist in the literature, the failure to explicitly address this conflict precludes the practical implementability of these powerful methodologies. Thus, the often lamented "disparity between theory and practice" arises. In this dissertation the novel time-domain tracking control approach LQT, which uses an on-line optimization strategy, that directly addresses both rate and displacement saturation is developed. The LQT control methodology, by acknowledging the hard actuator constraints upfront, makes it possible to concisely address both aggressive tracking and saturation effect mitigation objectives

simultaneously. Thus, this research provides a stepping stone toward closing the gap between the high gain theoretical control paradigms and those actually implemented in industry.

Because actuator rate saturations have been known to contribute to the onset of pilot induced oscillations, the LQT approach also implicitly addresses the nonlinear PIO problem. Simulations have demonstrated that the "large signal" performance of a constrained system is greatly enhanced over that of a small signal design when the LQT methodology is employed. Thus, the acceptable range of operation of a dynamic FCS can be extended by the LQT control method. Moreover, since the hard saturation effects are effectively mitigated, the likelihood of encountering a PIO situation is greatly reduced.

The development of computationally inexpensive reference signal prediction strategies affords a practical implementation of the optimal tracking control paradigm in a manual flight control context, viz., real-time tracking of an exogenous, unknown ahead of time dynamic reference signal. Thus, one is not forced to manipulate the regulation paradigm to fit the manual control problem. The causal, closed-form, state feedback LQT control law yields constant feedback gains which can be computed off-line, and thus minimal on-line computation is required. Moreover, simple, one-step ahead constraint mitigation strategies have been demonstrated to prevent unstable responses to inputs which cause unmitigated small signal control designs to diverge. Hence, the LQT control methodology is readily implementable in real-time.

A special case of LQT control, in which a zero-order reference prediction strategy is employed, and static admissibility issues are addressed, has been shown to yield a globally (with respect to the reference input) bounded output closed-loop control system. While necessarily requiring a relaxation of the tracking performance expectations, and additional computational burden, this approach is a viable option when mathematical stability guarantees are desired. The trade-offs between tracking performance, stability, and computational requirements have been addressed.

The constraint mitigation strategy which has been presented can be used not only to mitigate the effects of hard actuator constraints, but can also be used to impose "soft constraints" on the state vector. That is, artificial bounds may be imposed on other critical states to prevent the system from realizing undesirable states. For example, one may desire to confine an aircraft's angle of attack to a predetermined range in which the aircraft's performance is known to be well behaved.

Implementation of the LQT control methodology consists of:

1. Selecting a reference prediction strategy, where low order polynomial extrapolation for stage one, and low order polynomial interpolation or the parallel approach for stage two are recommended.
2. Tuning the linear controller to obtain desired small signal performance, i.e., select the LQ weights  $Q_r$ ,  $Q_p$  and  $R$ , and the planning horizon  $N$ .
3. Assess the impact of the constraints with this small signal controller.
4. Establish an acceptable feasibility criteria, e.g., employ an  $n$ -step ahead constraint mitigation strategy, enforce static admissibility, and/or impose "soft" constraints on the state vector.

The result is a computationally inexpensive, causal, closed-form and in real-time implementable solution to the constrained tracking problem. Specifically, the solution is given by an explicit control law of the form

$$u_k = \mathbf{k}_x^T \mathbf{x}_k + k_r r'_{k+1} + \phi_k + k_d d \quad (6.1)$$

where  $\phi_k$  is of the general form

$$\phi_k = \mathbf{k}_r^T [r_{k+1-p}, \dots, r_{k+1}]^T + \mathbf{k}_{r^*}^T [r_{k+2-p}^*, \dots, r_k^*]^T$$

and where the gain vectors  $\mathbf{k}_x$ ,  $\mathbf{k}_r$ ,  $\mathbf{k}_{r^*}$ , and the gains  $k_r$ , and  $k_d$  are constants which depend only on the optimization horizon  $N$ , the plant parameters  $\mathbf{A}$ ,  $\mathbf{b}$ ,  $\mathbf{c}$ ,  $\gamma_1$ ,  $\gamma_2$  and the LQ weights  $Q$ ,  $Q_p$ , and  $R$ , and therefore can be computed off-line. Thus, the on-line computational requirements for the linear LQT control law are independent of the optimization horizon  $N$ .  $\mathbf{x}_k$  is the current state,  $r_j$ ,  $j = k+1, k, \dots, k+1-p$  are the present and past pilot's commands  $r'_{k+1}$  is the current feasible reference, and the  $r_j^*$ ,  $j = k, k-1, \dots, k+2-p'$ , are the previous feasible (and therefore, applied to the control system and known) reference signals, and  $d$  is the known constant disturbance. Thus, the constrained *Linear Quadratic Tracking* (LQT) solution is expressed as a fixed gain controller which operates on the current values of the state, reference input, and feasible reference,  $p$  previous values of the pilot desired reference, and  $p'-1$  previous values of the (actually input) feasible reference. Note however that this control is only linear in appearance, for in the case of large inputs or strong deviations from trim the feasible reference signal  $r'_{k+1}$  is nonlinearly determined as a function of the current state, the present and possibly past reference values.

When actuator saturation is not encountered, as in small signal operation, the signals  $r^*$  and  $r'$  are simply the pilot input  $r$ , and full linear action is realized. Thus, when the actuator saturation limits are not infringed, the control  $u_k$  is linear in  $\mathbf{x}_k$ ,  $r_{k+1-p}, \dots, r_{k+1}$ , and  $d$ , and Eq. (6.1) can be written

$$u_k = \mathbf{k}_x^T \mathbf{x}_k + \mathbf{k}_R^T [r_{k+1-p}, \dots, r_{k+1}]^T + k_d d$$

with

$$\mathbf{k}_R^T = \mathbf{k}_r^T + [0 \mid \mathbf{k}_{r^*}^T \mid k_r]$$

Now, the inclusion of the reference signal past values introduces additional dynamics and causes an augmentation of the closed-loop system, yielding  $p$  additional states. In the

linear case, however, the only effect on the closed-loop system lies in the number and placement of the closed-loop zeros, as the additional  $p$  poles will always be at  $s = -\infty$ .

In the constrained case, and has been alluded to above, the control law is nonlinear due to the nonlinear calculation of  $r'$ , viz.,

$$u_k = \mathbf{k}_x^T \mathbf{x}_k + \mathbf{k}_r^T [r_{k+1-p}, \dots, r_{k+1}]^T + \mathbf{k}_{r^*}^T [r_{k+2-p}^*, \dots, r_k^*]^T + k_d d + k_{r'} f(\mathbf{x}_k, r_{k+1-p}, \dots, r_{k+1}, r_{k+2-p}^*, \dots, r_k^*, d) \quad (6.2)$$

Moreover, the nonlinear function  $f(\mathbf{0}, r_{k+1-p}, \dots, r_k, 0, r_{k+2-p}^*, \dots, r_k^*, 0) \neq 0$ . Note however that the nonlinearity  $f$  is piecewise linear in its arguments. The dependence of the nonlinear component  $f$  of Eq. (6.2) on not only previous (closed-loop system) input values, but also on previous state values (via the  $r_{k+2-p}^*, \dots, r_k^*$ ) augments the system, for  $r_{k+1}^* = f_{r^*}(\mathbf{x}_k, r_{k+1-p}, \dots, r_{k+1}, r_{k+2-p}^*, \dots, r_k^*, d)$  and will clearly affect the closed-loop poles.

The LQT optimization-based approach to manual tracking control includes actuator dynamics and accounts for both rate and displacement actuator (not control) constraints, addresses the dynamic and transient nature of the manual tracking problem, has no inherent requirement for stability of the open-loop plant, and employs full state feedback. Furthermore, the resulting piecewise linear control law is computationally inexpensive, does not require the use of on-line numerical search/optimization routines, is easily implementable in real-time, and small signal performance is maintained. At the same time, good responses to large exogenous (pilot) commands are obtained. In the case of a non-varying certain plant, the optimization horizon  $N$  can be chosen arbitrarily large without affecting the on-line computational requirements, as this information is embedded in the constant gains  $\mathbf{k}_x$ ,  $\mathbf{k}_r$ ,  $\mathbf{k}_{r^*}$  and  $k_{r'}$ . For the case of uncertain and/or varying plants, it may be possible to combine this control strategy with an on-line system identification algorithm, in which case it would be desirable to keep  $N$  small, since these gains would have to be reevaluated on-line.



Finally, in the context of manual flight control an additional benefit of the LQT tracking control paradigm is in the handling qualities arena, for the proposed saturation mitigating controller will tend to delay or preclude the onset of nonlinear, viz., actuator saturation caused, PIO's.

### *6.3 Research Conclusions*

Based on this research, the following specific conclusions are drawn:

1. Predictive tracking control strategies can yield better tracking performance over comparable regulator based trackers.

2. The use of receding horizon control, combined with short term reference signal predictions and optimal tracking control algorithms is a viable real-time manual tracking control strategy.

3. The transformation of actuator constraints into constraints on the reference signal is an effective anti-windup strategy.

4. The parameterization of the predicted reference vector in it's current value, is highly useful to develop extremely cost effective constraint mitigation strategies.

5. Simple, one-step ahead constraint mitigation strategies can yield significant performance improvements.

6. Linear system modeling tools cannot be indiscriminately applied to linear system models subjected to hard saturation constraints.

#### *Specifically concerning open-loop unstable plants:*

7. Anti-windup is important, but does not adequately address the actuator saturation problem when the open-loop plant is unstable.

8. Static admissibility is an important issue, but temporary excursions of the reference signal outside the statically admissible range are not necessarily a problem: It is static admissibility of the state which is critical, as opposed to static admissibility of the reference signal.

9. Enforcing static admissibility of the reference signal is an effective and efficient method which can be used to obtain stability guarantees.

10. The situation where the closed-loop system attains an equilibrium at the maximum statically admissible value should be avoided, as this is generally a non-recoverable situation.

11. The goal of obtaining stability guarantees necessarily entails significant compromises in tracking performance.

#### *6.4 Recommendations*

The following areas are recommended for future research:

1. Perform a complete MIMO extension of the LQT control methodology. That is, develop the optimal control tracking solution for a multiple reference signal situation (e.g., longitudinal and lateral aircraft control), and apply the existing LQT constraint mitigation techniques. This will require attention being given to the directionality of the control signal issues.

2. Combine the receding horizon LQT control paradigm with on-line system identification to achieve full envelope adaptive flight control.

3. Investigate the on-line adaptation of the LQ weighting coefficients in the inner-loop linear controller to reduce actuator stress (perhaps using a fuzzy logic approach), and possibly including an actuator rate penalty in the performance functional. Although this would entail a significant increase in the on-line computational workload, it may prove to

be an efficient way of implementing “inner-loop” techniques with minimal concern regarding destabilization of the inner (i.e., stabilizing) control loop.

4. Investigate the application of more sophisticated extrapolation methods to the LQT methodology.

5. Use man-in-the loop paper pilot modeling techniques to investigate and characterize the relationships between PIO's and actuator saturation.

## *Appendix: Additional Simulation Results*

This appendix contains selected simulation results for several examples in order to demonstrate some of the trends associated with the various parameters in the reference signal prediction strategies. While the LQT controller's parameters using each prediction strategy can be tuned to achieve acceptable optimal performance of the overall LQT predictor/controller, "good optimal tuning" is not always performed for each set of predictor parameters so that the effects specific to the particular predictor parameter being modified is more clear. Thus, many of these results represent "poorly tuned" controllers and do not represent the best achievable performance of the LQT method utilizing the given reference signal prediction strategy. The inclusion of simulation results with all possible parameter variations is not feasible, and thus only a representative sample is included.

The first set of plots demonstrates the effects of the planning horizon length  $N$  for selected values of  $p$  and  $p'$  using the poly- $p$  + poly- $p'$  reference signal prediction strategy. In each of these plots, Figures A.1 through A.6, The LQ weights are  $Q_l = 47$ ,  $Q_p = 0.29$ , and  $R = 0.91$ . The plant is the F-16 model used throughout the dissertation, and the reference is a 1.0 rad/sec pulse doublet input prefiltered with a critically damped second-order filter. Generally, an increase in the planning horizon  $N$  corresponds to a higher state feedback gain, and tighter tracking ensues. However, there are limits to this trend. This occurs when the LQT state feedback gain is approximately equal to the analogous LQR state feedback gain. If the tracking performance is not satisfactory at the maximum length planning horizon, then one must turn to the LQ weighting coefficients to improve tracking performance.

Next, several unconstrained examples are provided (Figures A.7 through A.10) where the poly- $p$  + asymptotic convergence reference prediction strategy is employed. The plant

model and reference input signal is the same as in the previous set of plots. In this case, the LQ weighting coefficients  $Q_I = 47$ ,  $Q_P = 29$ , and  $R = 0.91$  are used. In Figure A.7 the effects of the planning horizon are examined, while in Figures A.8 through A.10, the asymptotic convergence coefficient  $k_a$  is varied.

Finally, constrained system responses are demonstrated in Figures A.11 through A.16. The same F-16 plant model is used, but actuator displacement and rate constraints of  $\pm 0.37$  rad and  $\pm 1.0$  rad/sec, respectively, are included. In each case, the reference signal doublet is scaled to 0.5, 1.0 and 2.0 rad/sec and the normalized responses are overlaid on a single plot for each method. It should be noted that each of these magnitudes represents an extremely aggressive input for the given plant. These overly large magnitudes are chosen for demonstrative purposes only. The actuator activity is also provided in each case, and it is obvious that these simulations induce a considerable amount of stress on the actuators. The parameter values used in these simulations are provided in Table A.1.

**Table A.1** Constrained Simulation Parameters

Figure	$Q_I$	$Q_P$	$R$	$N$	$p$	$p'$	$k_a$
A.11	47.0	29.0	22.75	15	2	2	-
A.12	47.0	29.0	22.75	15	2	2	-
A.13	47.0	29.0	0.91	10	2	-	0.8
A.14	47.0	29.0	0.91	10	2	-	0.8
A.15	47.0	29.0	22.75	15	2	-	-
A.16	47.0	29.0	22.75	15	2	-	-

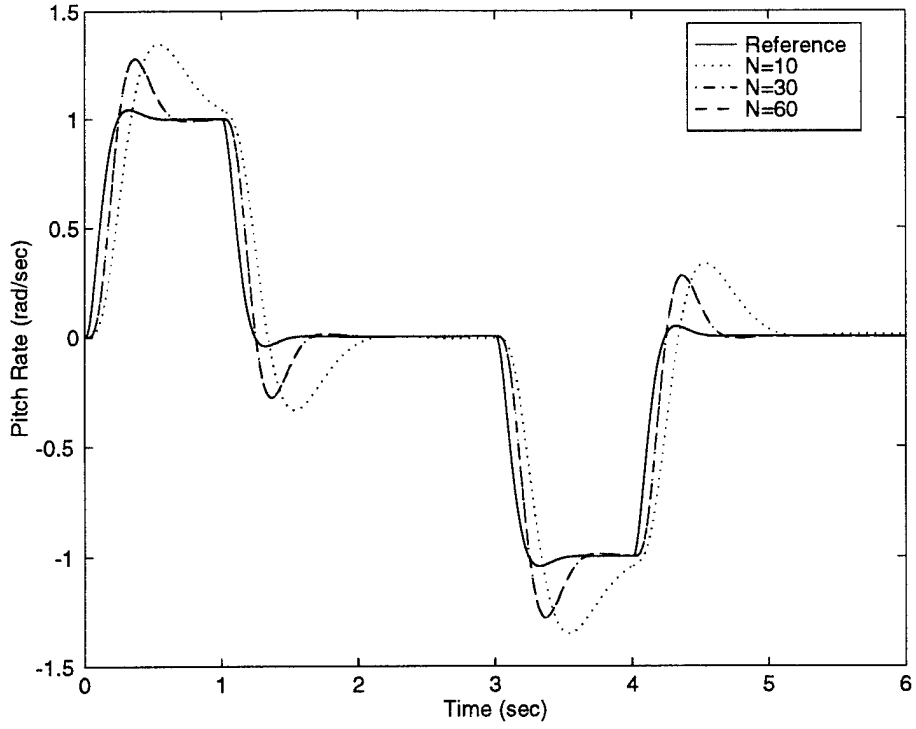


**Figure A.1.** Unconstrained Poly-0 + Poly-0 vs.  $N$

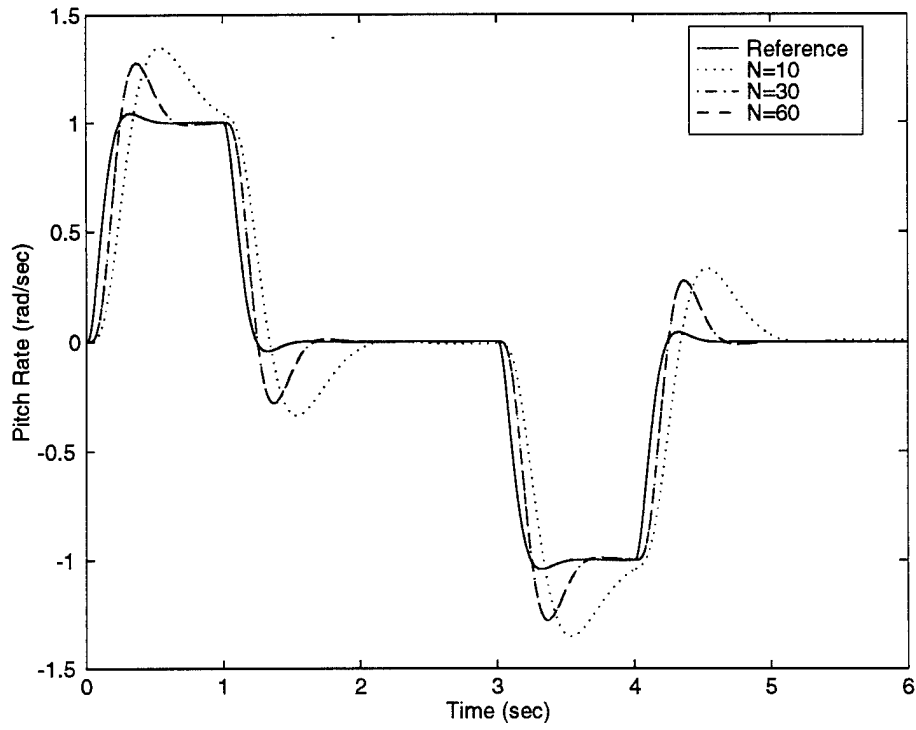


**Figure A.2.** Unconstrained Poly-0 + Poly-1 vs.  $N$

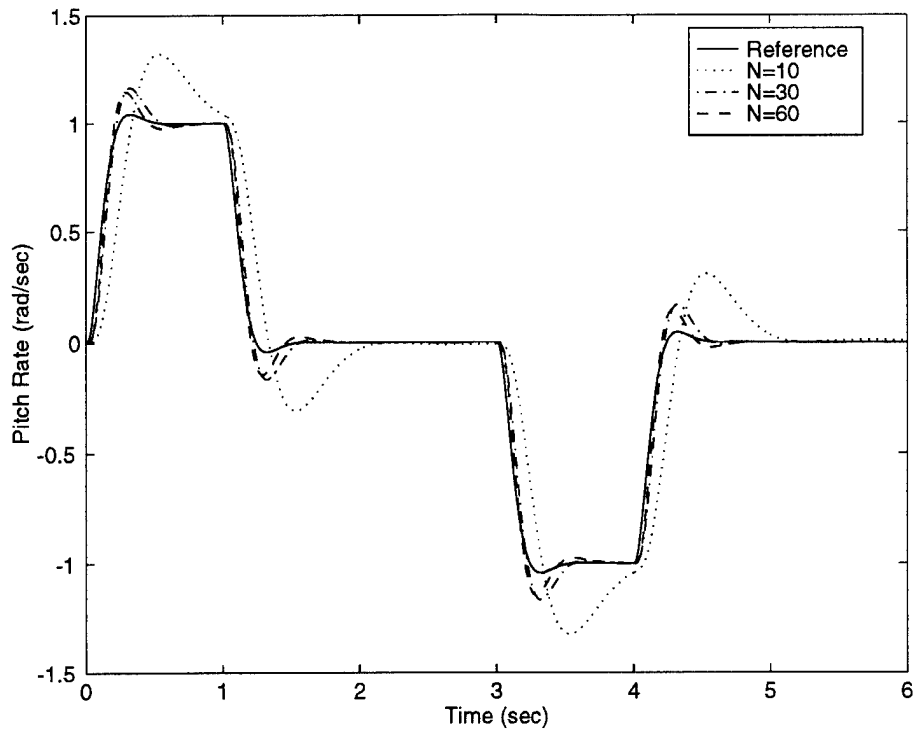


**Figure A.3.** Unconstrained Poly-0 + Poly-2 vs.  $N$

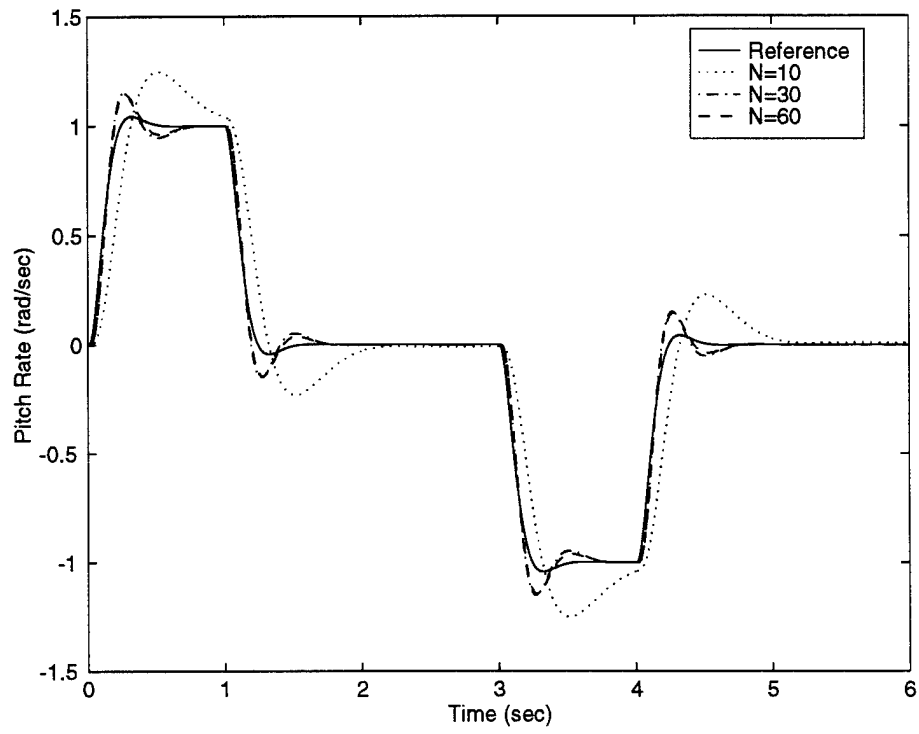


**Figure A.4.** Unconstrained Poly-1 + Poly-1 vs.  $N$

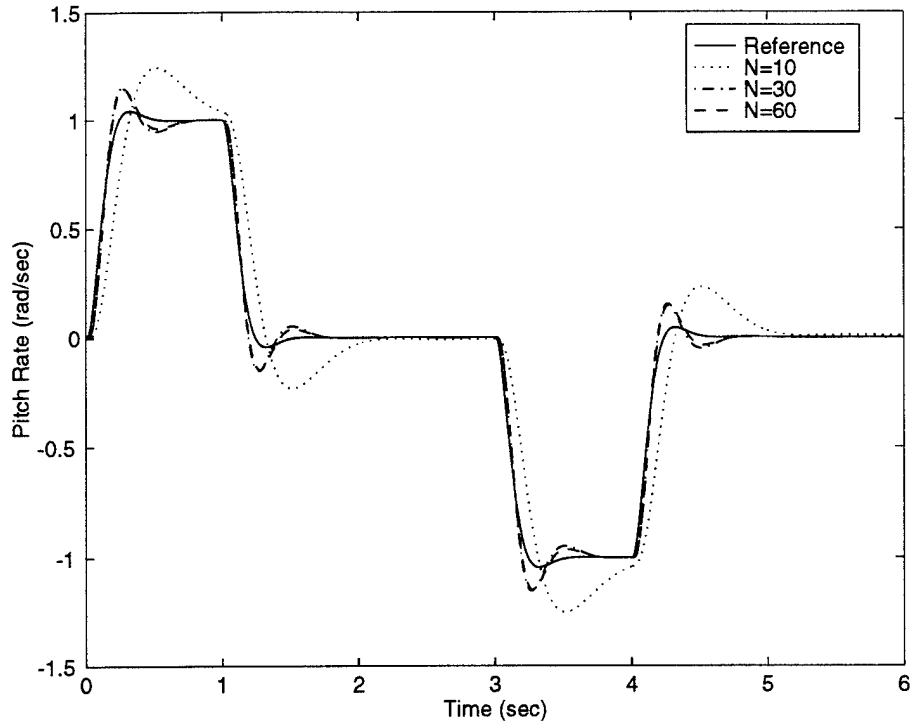


**Figure A.5.** Unconstrained Poly-1 + Poly-2 vs.  $N$

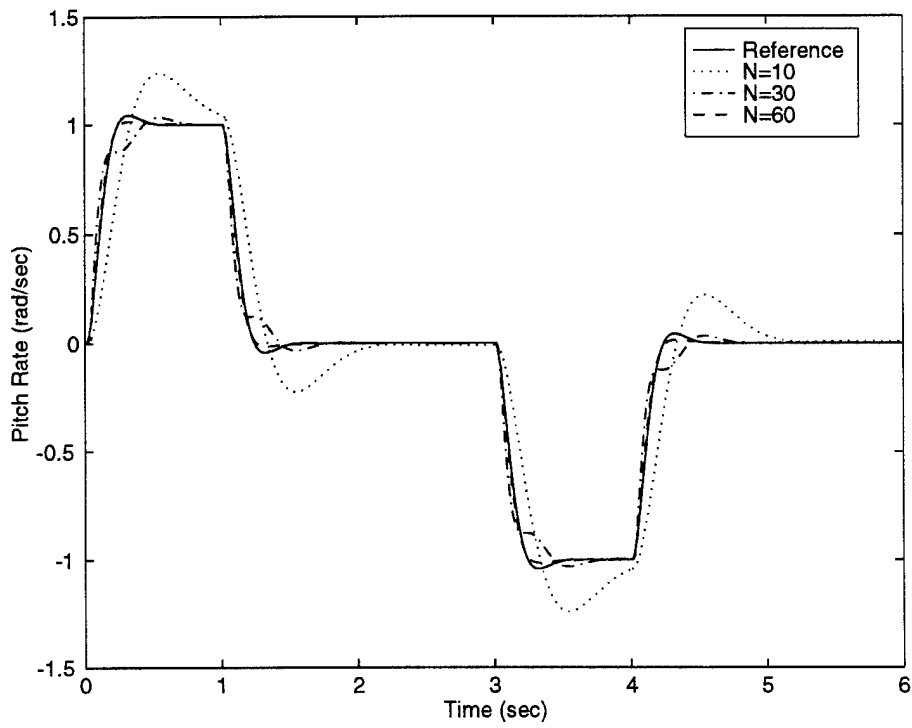


**Figure A.6.** Unconstrained Poly-2 + Poly-2 vs.  $N$



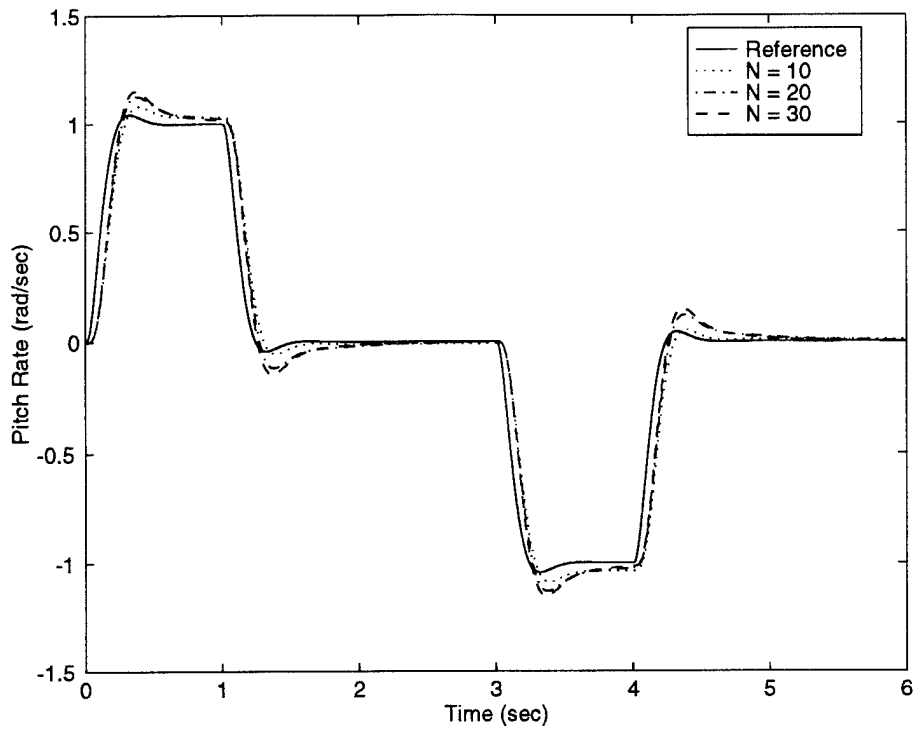


**Figure A.7.** Unconstrained Poly-0 + AC vs.  $N$ ,  $k_a = 0.4$

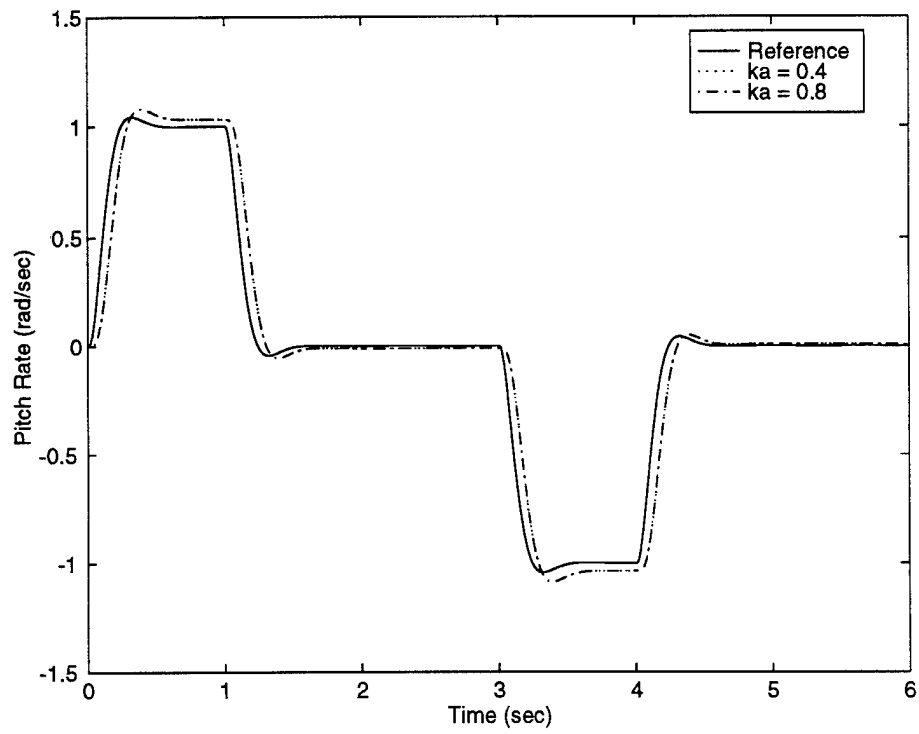


**Figure A.8.** Unconstrained Poly-0 + AC vs.  $k_a$ ,  $N = 10$

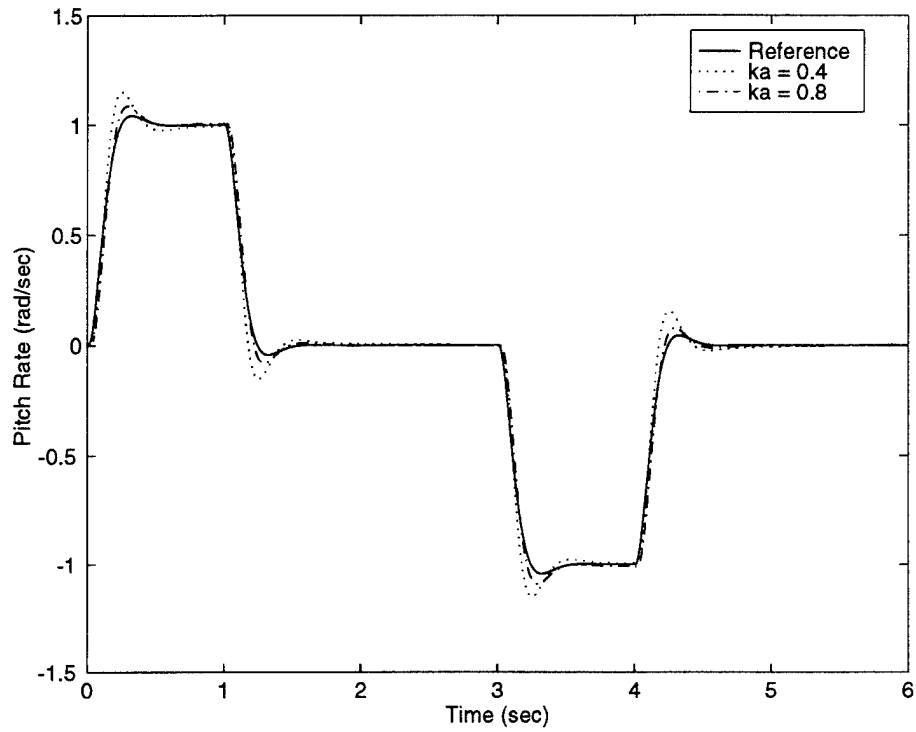


**Figure A.9.** Unconstrained Poly-1 + AC vs.  $k_a$ ,  $N = 10$

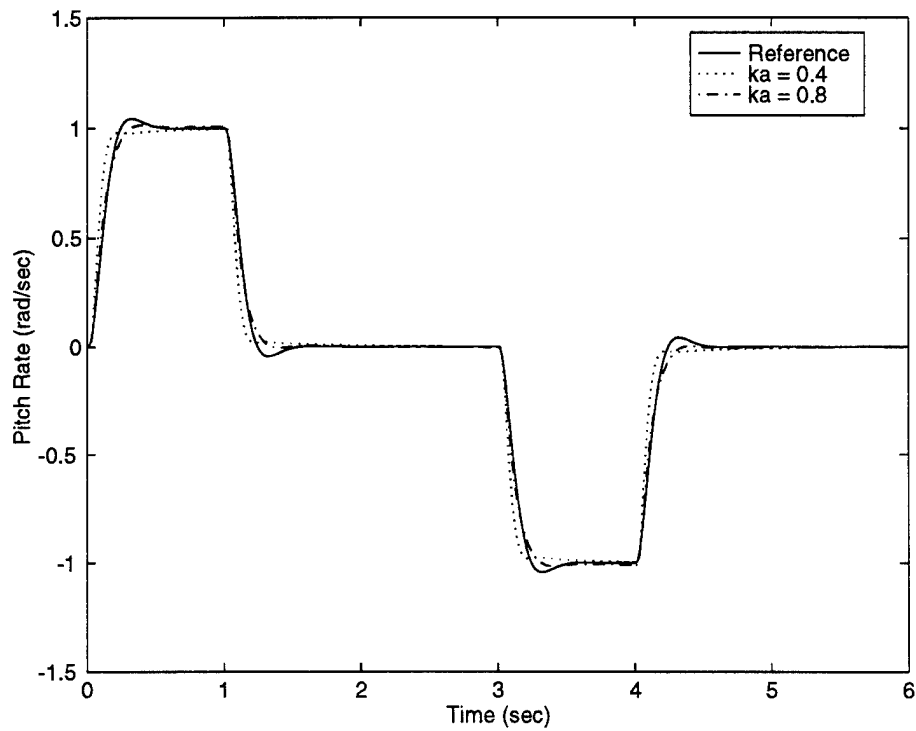


**Figure A.10.** Unconstrained Poly-2 + AC vs.  $k_a$ ,  $N = 10$

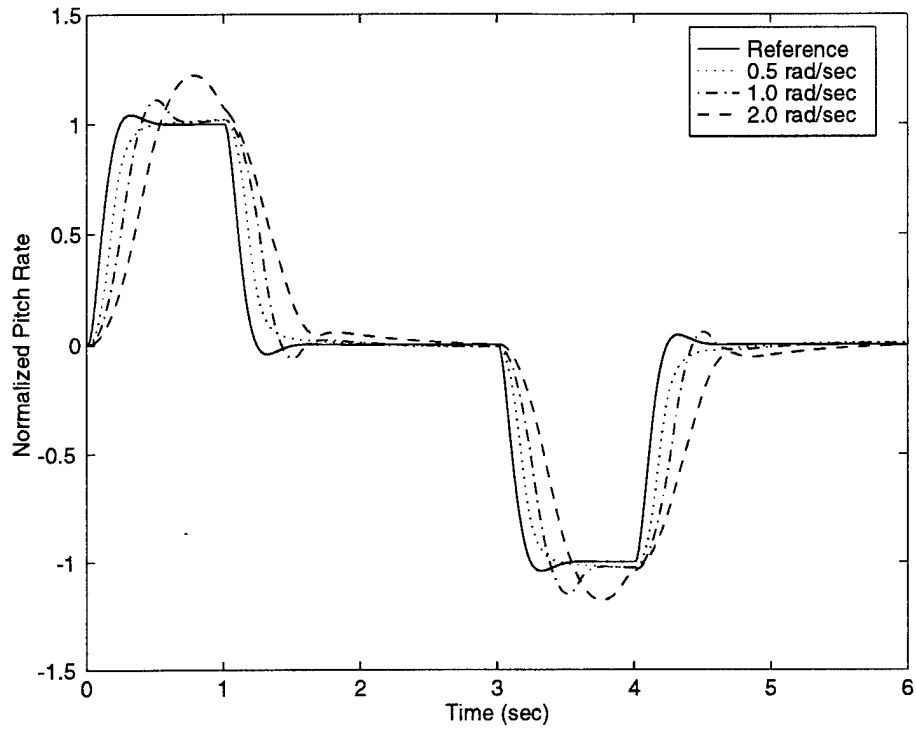


**Figure A.11.** Constrained Poly-2 + Poly-2,  $N = 15$

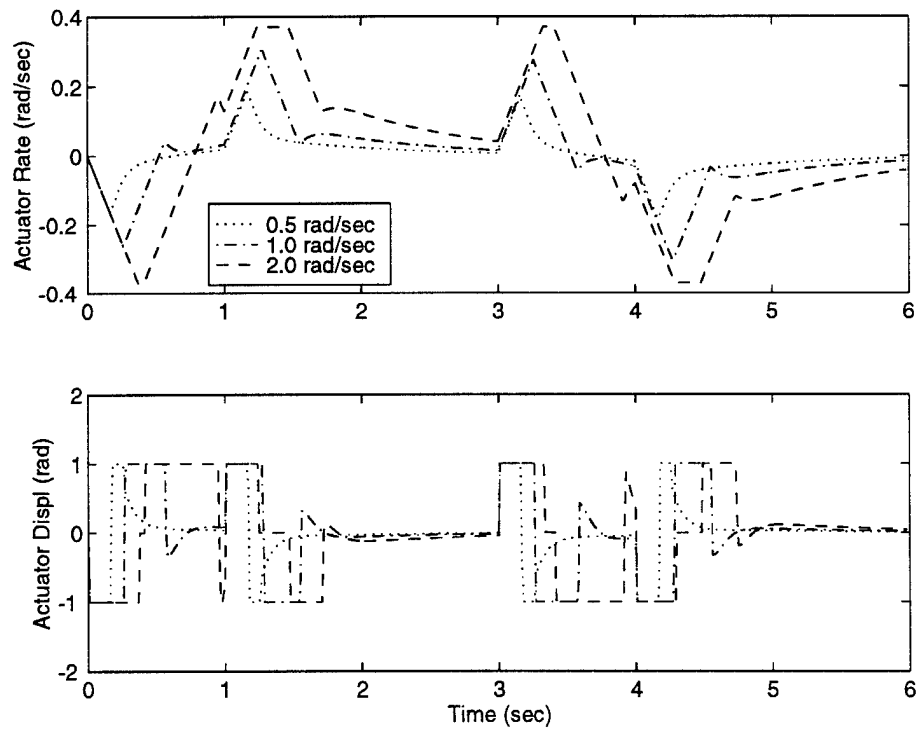


**Figure A.12.** Constrained Poly-2 + Poly-2 Actuator Activity

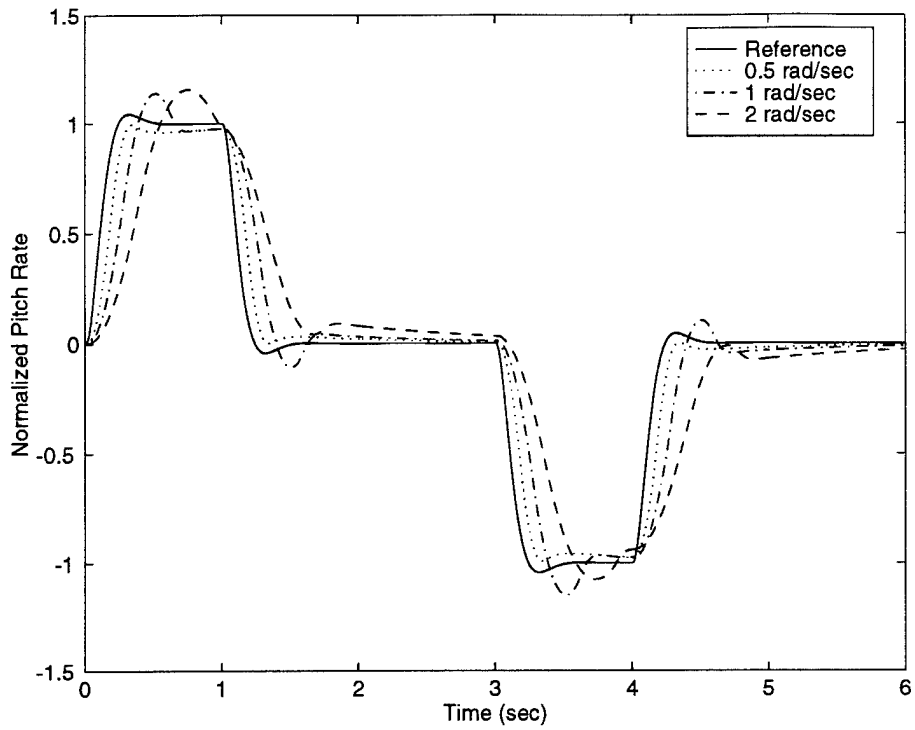


**Figure A.13.** Constrained Poly-2 + AC

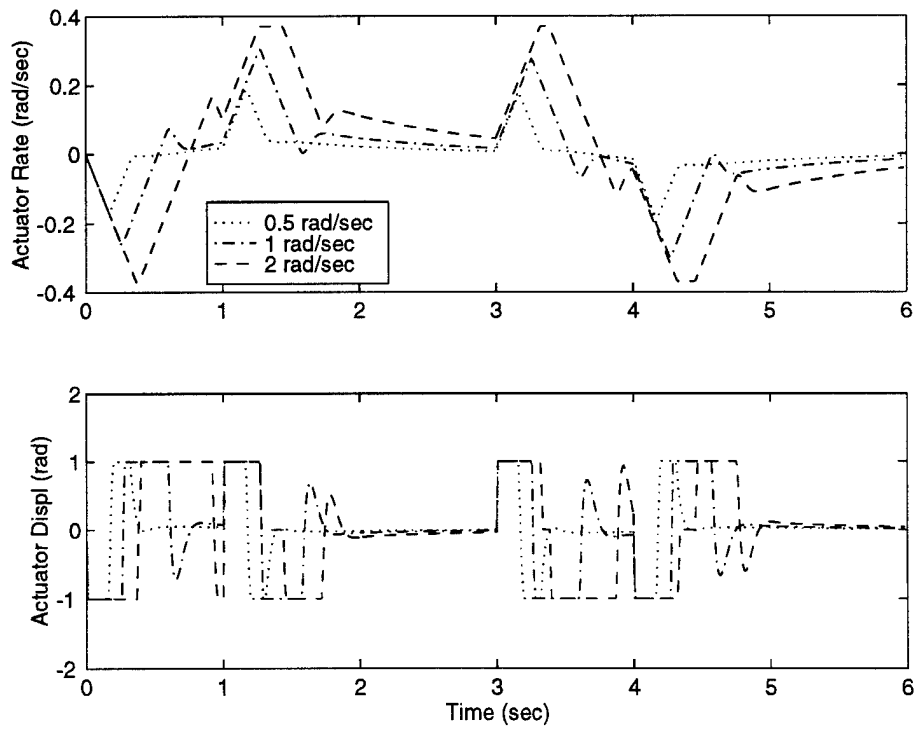


**Figure A.14.** Constrained Poly-2 + AC Actuator Activity

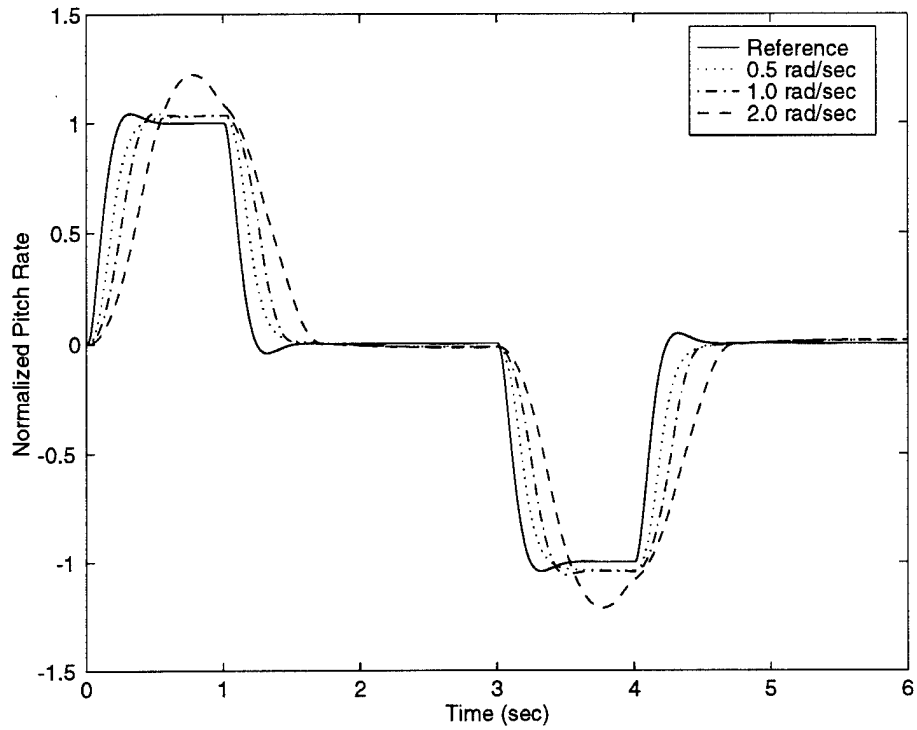


**Figure A.15.** Constrained Poly-2 + Parallel Response

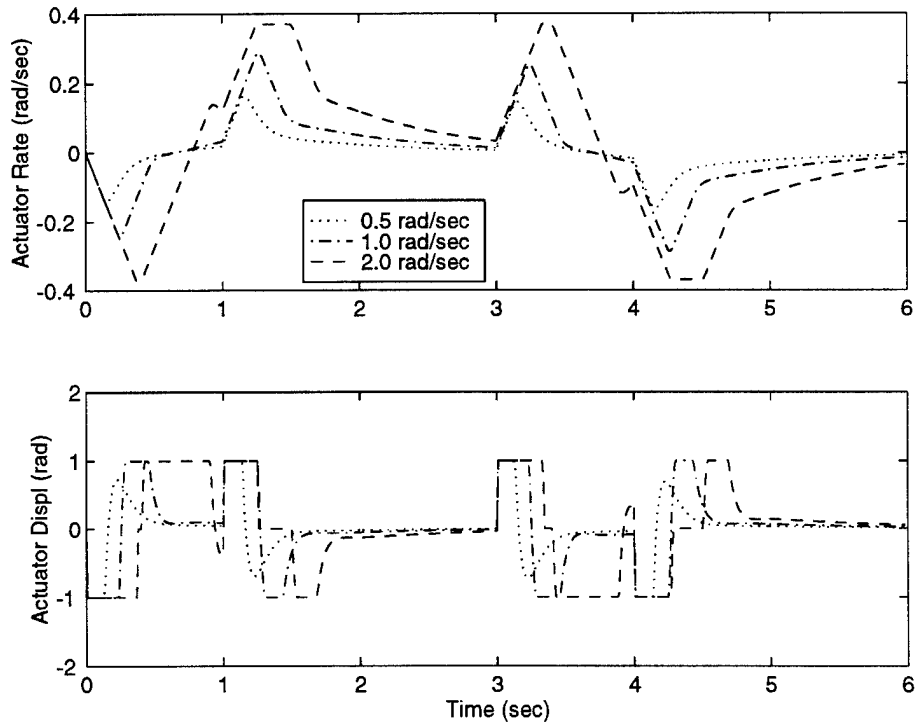


**Figure A.16.** Constrained Poly-2 + Parallel Actuator Activity

## *Bibliography*

1. Anon., "Why the Grippen crashed," *Aerospace America*, p. 11, Feb. 1994.
2. Anon., "SAAB seeks patent for control software," *Aviation Week and Space Technology*, 1995.
3. Åström, K.J. and L. Rundquist, "Integrator windup and how to avoid it," *Proceedings of the 1989 American Control Conference*, 2: 1693-8, (1989).
4. Åström, K.J. and B. Wittenmark, *Computer Controlled Systems: Theory and Design*. Englewood Cliffs, NJ: Prentice-Hall, 1984,1990.
5. Athans, M. and P.L. Falb, *Optimal Control: An Introduction to the Theory and Its Applications*, McGraw Hill, New York,1966.
6. Baheti, R.S., "Simple anti-windup controllers," *Proceedings of the 1989 American Control Conference*, 2: 1684-6, (1989).
7. Benzaouia, A. and C. Burgat, "Regulator problem for linear discrete-time systems with non-symmetrical constrained control," *International Journal of Control*, 48: 2441-2451, (1988).
8. Bernstein, D.S., "Optimal nonlinear, but continuous, feedback control of systems with saturating actuators," *Proceedings of the 32nd Conference on Decision and Control*: 2533-2537, (1993).
9. Blackwell, C.C., "Actuator saturation and control system performance," *Proceedings of the 1993 American Control Conference*, 3: 2420-1, (1993).

10. Campo, P.J., M. Morari, and C.N. Nett, "Multivariable antiwindup and bumpless transfer: a general theory," *Proceedings of the 1989 American Control Conference*, 2: 1706-11, (1989).
11. Campo, P.J. and M. Morari, "Robust Control of Processes Subject to Saturation Nonlinearities," *Computers chem Engng*, 14: 343-358.
12. Chandler, P.R., M.J. Mears, and M. Pachter, "A hybrid LQR/LP approach for addressing actuator saturation in feedback control," *Proceedings of the 1994 Conference on Decision and Control*: 3860-3867, (1994).
13. D'Azzo, J.J. and C.H. Houpis, *Linear Control System Analysis and Design*, McGraw-Hill Inc., 3rd Ed., New York, 1988.
14. Dornheim, M.A., "Report pinpoints factors leading to YF-22 crash," *Aviation Week and Space Technology*, pp. 53-54, Nov. 9, 1992.
15. Doyle, J.C., R.S. Smith, and D.F. Enns, "Control of Plants with Input Saturation Nonlinearities," *Proceedings of the 1987 American Control Conference*: 1034-1039, (1987).
16. Frankena, J.F. and R. Sivan, "A nonlinear optimal control law for linear systems," *International Journal of Control*, 30: 159-178, (1979).
17. Garcia, C.E., D.M. Prett, and M Morari, "Model predictive control: theory and practice," *Automatica*, 25: 335-348, (1989).
18. Gilbert, E.G. and K.T. Tan, "Linear Systems with State and Control Constraints: The Theory and Application of Maximal Output Admissible Sets," *IEEE Transactions on Automatic Control*, AC-36: 1008-1020, (1991).

19. Gilbert, E.G., Ilya Kolmanovsky and K.T. Tan, "Nonlinear Control of Discrete-time Linear Systems with State and Control Constraints: A Reference Governor with Global Convergence Properties," *Proceedings of the 33rd Conference on Decision and Control*: 144-149.
20. Glattfelder, A.H. and W. Schaufelberger, "Stability Analysis of Single Loop Control Systems with Saturation and Antireset-Windup Circuits," *IEEE Transactions on Automatic Control*, AC-28: No 12, (1983).
21. Gutman, P.O. and P. Hergander, "A New Design of Constrained Controllers for Linear Systems," *IEEE Transactions on Automatic Control*, AC-30: No 1, (1985).
22. Gyugyi, P.J. and G. Franklin, "Multivariable integral control with input constraints," *Proceedings of the 32nd IEEE Conference on Decision and Control*, 3: 2505-10, (1993).
23. Hanus, R., M. Kinnaert, and J.L. Henrotte, "Conditioning technique, a general antiwindup and bumpless transfer method," *Automatica*, 23: 729-739, (1987).
24. Hess, R.A. and S.A. Snell, "Flight control design with actuator saturation: SISO systems with unstable plants," *AIAA 95-0336, 33rd Aerospace Sciences Meeting and Exhibit*, (January 1995).
25. Horowitz, I. A synthesis theory for a class of saturating systems, *International Journal of Control*, 38: 169-187, (1983).
26. Horowitz, I. "Feedback systems with rate and amplitude limiting," *International Journal of Control*, 40: 1215-1229, (1984).
27. Horowitz, I. and Y.K. Liao. "Quantitative non-linear compensation design for saturating unstable uncertain plants," *International Journal of Control*, 44: 1137-1146, (1986).



28. Kapasouris, P. and M. Athans, "Control systems with rate and magnitude saturation for neutrally stable open-loop systems," *Proceedings of the 29th Conference on Decision and Control*, 6: 3404-9, (1990).
29. Kapasouris, P., M. Athans, and G. Stein "Design of Feedback Control Systems for Stable Plants with Saturating Actuators," *Proceedings of the 27th Conference on Decision and Control*: 469-479, (December 1988).
30. Kapasouris, P. and M. Athans, "Multivariable Control Systems with Saturating Actuators Antireset Windup Strategies," *Proceedings of the 1985 American Control Conference*: 1579-1584, (1985).
31. Karason, S.P. and A.M. Annaswamy, "Adaptive Control in the presence of input constraints," *Proceedings of the 1993 American Control Conference, part 2*: 1370-1374, (1993).
32. Kirk, D.E., *Optimal control theory; an introduction*, Prentice-Hall, Englewood Cliffs, NJ, 1970.
33. Kosut, R.L., "Design of linear systems with saturating linear control and bounded states," *IEEE Transactions on Automatic Control*, AC-28: 121-124, (1983).
34. Krikelis, N.J. and S.K. Barkas, "Design of tracking systems subject to actuator saturation and integrator windup," *International Journal of Control*, 39: 667-683, (1984).
35. Krikelis, N.J., "State feedback integral control with 'intelligent' integrators," *International Journal of Control*, 32: 465-473, (1980).
36. Liao, Y.K. and I. Horowitz. "Unstable uncertain plants with rate and amplitude saturations," *International Journal of Control*, 44: 1147-1159 (1986).

37. Lin S-F. and N-W. Lu. "Adaptive control system for a plant with input amplitude constraints and bounded external disturbances," *Proceedings of the 1993 American Control Conference*: 2207-2211, (1993).
38. Liu, W., Y. Chitour, and E. Sontag. "Remarks on finite gain stabilizability of linear systems subject to input saturation," *Proceedings of the 32nd IEEE Conference on Decision and Control*, 2: 1808-1813, (1993).
39. Luenberger, D.G., *Optimization by vector space methods*. New York: John Wiley & Sons, Inc., 1969.
40. Marcopoli, V.R., and S.M. Phillips, "Performance evaluation of a MIMO control system with limited actuators," *Proceedings of the 1993 American Control Conference*: 2800-2801, (1993).
41. Marquez, H.J. and C.P. Diduch, "On design tradeoffs in feedback systems in the presence of input constraints," *Proceedings of the 1992 American Control Conference*, 4: 2895-2899, (1992).
42. Maybeck, P.S., *Stochastic Models, Estimation, and Control*, Vol. 3, Academic Press, New York, 1982.
43. Middleton, R.H., G.C. Goodwin, D.J. Hill, and D.Q. Mayne, "Design issues in adaptive control," *IEEE Transactions on Automatic Control*, AC-33: 50-58, (1988).
44. Moussas, C. and G. Bitsoris, "Adaptive constrained control subject to both input-amplitude and input-velocity constraints," *Proceedings of the IEEE International Conference on Systems, Man and Cybernetics*, 4: 601-606, (1993).
45. Newman, W.S., "Robust near time-optimal control," *IEEE Transactions on Automatic Control*, 35: 841-4, (1990).

46. Pachter, M., et al, "Control Reconfiguration with actuator rate saturation," *Proceedings of the 1995 American Control Conference*: 3495-3499, (1995).
47. Patwardhan, A.A., J.B. Rawlings and T.F. Edgar, "Model Predictive Control of nonlinear processes in the presence of constraints," *Nonlinear Control Systems Design*, Selected Papers from the IFAC, June 14-16 1989, Ed: A Isidori, (1990).
48. Payne, A.N. "Adaptive one-step-ahead control subject to an input-amplitude constraint," *International Journal of Control*, 43: 1257-1269, (1986).
49. Powers, B.G., "Space Shuttle Longitudinal landing flying qualities," *Journal of Guidance, Control, and Dynamics*, 9: 566-572, (1986).
50. Rodriguez, A.A. and Y. Wang, "Saturation Prevention Strategies For An Unstable Bank-To-Turn (BTT) Missile: Full Information," Dept of EE, Arizona State U, CSSE, Tempe, Az 85287-7606.
51. Ryan, E.P., "Optimal feedback control of saturating systems," *International Journal of Control*, 35: 521-34, (1982).
52. Safanov, M.G. and M. Athans, "A Multiloop Generalization of the Circle Stability Criterion for Stability," *IEEE Transactions on Automatic Control*, AC-26: 415-422, (1981).
53. Sontag, E.D. and H.J. Sussman, "Nonlinear output feedback design for linear systems with saturating controls," *Proceedings of the Conference on Decision and Control*: 3414-3416, (1990).
54. Ting, Y., S. Tosunoglu, and R. Freeman, "Actuator saturation avoidance for fault-tolerant robots," *Proceedings of the IEEE Conference on Decision and Control*, 3: 2125-2130, (1993).
55. Tsiroki, A.G. and M. Morari, "Controller design with actuator constraints," *Proceedings of the Conference on Decision and Control*: 2623-2628, (1992).

56. Vassilaki, M., J.C. Hennes, and G. Bitsoris. "Feedback control of linear discrete-time systems under state and control constraints," *International Journal of Control*, 47: 1727-1735, (1988).
57. Walgama, K.S. and J. Sternby, "On the convergence properties of adaptive pole placement controllers with antiwindup compensators," *IEEE Transactions on Automatic Control*, 38: 128-32, (1993).
58. Walgama, K.S. and J. Sternby, "Inherent observer property in a class of anti-windup compensators," *International Journal of Control*, 52: 705-24, (1990).
59. Yang, S-S. and S-K. Hong, "Analysis on a saturating system with an intelligent limiter," *Proceedings of the 1989 American Control Conference*: 1699-1705, (1989).
60. Zhang, C. and R.J. Evans, "Continuous Direct Adaptive Control with Saturation Input Constraint," *IEEE Transactions on Automatic Control*, 39: 1718-1722, (1994).
61. Zhang, C., "Discrete time saturation constrained adaptive pole assignment control," *IEEE Transactions on Automatic Control*, 38: 1250-1254, (1993).
62. Zhang, C. and R.J. Evans, "Adaptive pole assignment subject to saturation constraints," *International Journal of Control*, 46: 1391-1398, (1987).
63. Zhang, C. and R.J. Evans, "Amplitude constrained adaptive control," *International Journal of Control*, 46: 53-64, (1987).

## *Vita*

Russel B. Miller [REDACTED]. He graduated from Alamogordo Senior High School, Alamogordo, New Mexico in 1980. He and his wife Linda, were married in 1981, the same year he enlisted in the United States Air Force. His preliminary undergraduate work was accomplished at the University of South Carolina-Sumter, Sumter, South Carolina. After selection for the Airman's Education and Commissioning Program in 1986, he attended New Mexico State University, Las Cruces, New Mexico, where he received his B.S.E.E. in 1989. Upon completion of Officer Training School at Lackland Air Force Base, Texas, as a distinguished graduate, he was commissioned a second lieutenant in 1989. He was subsequently assigned to the Air Force Institute of Technology, receiving his M.S.E.E. in 1990. He was then assigned to the National Air Intelligence Center, Wright-Patterson AFB, OH where he served as an Aerodynamic Missile Guidance and Control Systems Engineer until re-entering the Air Force Institute of Technology as a Ph.D. candidate in 1993. Upon graduation, he will be assigned to the Air Force Information Warfare Center, Kelly AFB, Texas.

Permanent Address: [REDACTED]  
[REDACTED]

# REPORT DOCUMENTATION PAGE

Form Approved  
OMB No. 0704-0188

Public reporting burden for this collection of information is estimated to average 1 hour per response, including the time for reviewing instructions, searching existing data sources, gathering and maintaining the data needed, and completing and reviewing the collection of information. Send comments regarding this burden estimate or any other aspect of this collection of information, including suggestions for reducing this burden, to Washington Headquarters Services, Directorate for Information Operations and Reports, 1215 Jefferson Davis Highway, Suite 1204, Arlington, VA 22202-4302, and to the Office of Management and Budget, Paperwork Reduction Project (0704-0188), Washington, DC 20503.

1. AGENCY USE ONLY (Leave blank)		2. REPORT DATE <b>January 1997</b>	3. REPORT TYPE AND DATES COVERED <b>Dissertation</b>	
4. TITLE AND SUBTITLE  <b>Manual Tracking Flight Control with Amplitude and Rate Constrained Dynamic Actuators</b>			5. FUNDING NUMBERS	
6. AUTHOR(S)  <b>Russel B. Miller Capt, USAF</b>			8. PERFORMING ORGANIZATION REPORT NUMBER  <b>AFIT/DS/ENG/96-15</b>	
7. PERFORMING ORGANIZATION NAME(S) AND ADDRESS(ES)  <b>Air Force Institute of Technology Wright-Patterson AFB, OH 45433-6583</b>				
9. SPONSORING / MONITORING AGENCY NAME(S) AND ADDRESS(ES)  <b>Mr. Duane Ruburtus WL/FIGS 2218 Eighth St. Suite 11 WPAFB, OH 45433-7521</b>			10. SPONSORING / MONITORING AGENCY REPORT NUMBER	
11. SUPPLEMENTARY NOTES				
12a. DISTRIBUTION / AVAILABILITY STATEMENT  <b>Approved for public release; distribution unlimited</b>			12b. DISTRIBUTION CODE	
13. ABSTRACT (Maximum 200 words) <p>A new control methodology for manual flight control, viz., real-time tracking control, is developed. Amplitude and rate constrained dynamic actuators are considered. Optimal tracking control is made possible by the use of unique reference signal prediction strategies which extrapolate the reference signal over the optimization horizon. A receding horizon, linear-quadratic inner-loop controller is employed in conjunction with an outer-loop nonlinear element. The constraint effects mitigation strategy is to optimally track a modified reference signal which yields feasible actuator commands over the optimization horizon when the pilot demanded reference is too aggressive to be tracked by the inner-loop optimal control law. A discrete-time implementation yields computationally inexpensive, closed-form solutions which are implementable in real-time and which afford the optimal tracking of an exogenous, unknown a priori reference signal. The developed control algorithm is applied to an open-loop unstable aircraft model, with attention being given to the trade-offs associated with the conflicting objectives of aggressive tracking and saturation avoidance. One-step ahead constraint mitigation is shown to provide substantial improvement in the constrained system response, while slightly more complicated constraint mitigation strategies yield stronger stability properties.</p>				
14. SUBJECT TERMS <b>Control systems, tracking control, actuator saturation, nonlinear control, amplitude saturation, rate saturation, actuator constraints, optimal control, receding horizon control, predictive control, flight control</b>			15. NUMBER OF PAGES <b>146</b>	
17. SECURITY CLASSIFICATION OF REPORT <b>Unclassified</b>			16. PRICE CODE	
			20. LIMITATION OF ABSTRACT <b>UL</b>	
18. SECURITY CLASSIFICATION OF THIS PAGE <b>Unclassified</b>		19. SECURITY CLASSIFICATION OF ABSTRACT <b>Unclassified</b>		